



**UNIFORMED SERVICES UNIVERSITY OF THE HEALTH SCIENCES
F. EDWARD HÉBERT SCHOOL OF MEDICINE
4301 JONES BRIDGE ROAD
BETHESDA, MARYLAND 20814-4799**



March 7, 2007

**BIOMEDICAL
GRADUATE PROGRAMS**

Ph.D. Degrees

APPROVAL SHEET

- Interdisciplinary
- Emerging Infectious Diseases
- Molecular & Cell Biology
- Neuroscience

Title of Dissertation: "The Central Role of the Matrix Protein in Nipah Virus Assembly and Morphogenesis"

- Departmental
- Clinical Psychology
- Environmental Health Sciences
- Medical Psychology
- Medical Zoology
- Pathology

Name of Candidate: Jared Patch
Doctor of Philosophy Degree
23 March 2007

Dissertation and Abstract Approved:

Doctor of Public Health (Dr.P.H.)

Physician Scientist (MD/Ph.D.)

Master of Science Degrees

- Molecular & Cell Biology
- Public Health

Masters Degrees

- Comparative Medicine
- Military Medical History
- Public Health
- Tropical Medicine & Hygiene

Graduate Education Office

Dr. Eleanor S. Metcalf, Associate Dean
Janet Anastasi, Program Coordinator
Tanice Acevedo, Education Technician

Web Site

www.usuhs.mil/geo/gradpgm_index.html

E-mail Address

graduateprogram@usuhs.mil

Phone Numbers

Commercial: 301-295-9474
Toll Free: 800-772-1747
DSN: 295-9474
FAX: 301-295-6772

CAPT Gerald Quinnan, USPHS
Department of Preventive Medicine & Biometrics
Committee Chairperson

4/10/07
Date

Christopher Broder, Ph.D.
Department of Microbiology & Immunology
Committee Member

3-23-07
Date

Eleanor Metcalf, Ph.D.
Department of Microbiology & Immunology
Committee Member

3-23-07
Date

Chou-Zen Giam, Ph.D.
Department of Microbiology & Immunology
Committee Member

3-23-07
Date

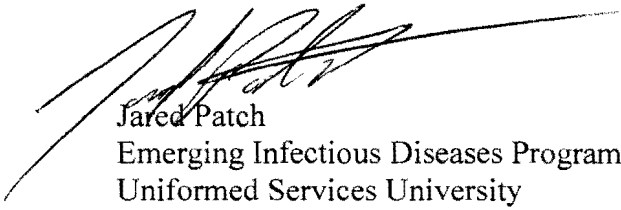
Dimitr Dimitrov, Ph.D.
National Cancer Institute
Committee Member

3/23/07
Date

The author hereby certifies that the use of any copyrighted material in the thesis manuscript entitled:

"The Central Role of the Matrix Protein in Nipah Virus Assembly and Morphogenesis"

is appropriately acknowledged and, beyond brief excerpts, is with the permission of the copyright owner.



Jared Patch
Emerging Infectious Diseases Program
Uniformed Services University

ABSTRACT

The Central Role of the Matrix Protein in Nipah Virus Assembly and Morphogenesis

Jared Renford Patch, Ph.D. 2007

Thesis supervisor: Dr. Christopher C. Broder, Professor and Director, Emerging Infectious Diseases Graduate Program

Nipah virus (NiV) is an emerging paramyxovirus distinguished by its ability to cause fatal disease in both animal and human hosts. Together with Hendra virus (HeV), they comprise the genus *Henipavirus* in the *Paramyxoviridae* family. NiV and HeV are restricted to Biosafety Level-4 (BSL-4) containment and this has hampered progress towards examining the details of their replication and morphogenesis mechanisms. Here, recombinant gene expression systems to study NiV particle assembly and budding through the formation of virus-like particles (VLPs) have been established to circumvent these obstacles. When expressed by recombinant Modified Vaccinia virus Ankara (rMVA) or by plasmid vector transfection, individual NiV matrix (M), fusion (F) and attachment (G) proteins were released into cell culture supernatants in a membrane-associated state as determined by sucrose density gradient flotation and immunoprecipitation analysis. However, co-expression of F and G along with M revealed a shift in their distribution across the gradient, indicating association with M in VLPs. Protein release was also altered depending on the context of viral proteins being expressed, with F, G and nucleocapsid (N) protein reducing the overall release of M, and

N release completely dependent on the co-expression of M. Immunoelectron microscopy and density analysis revealed VLPs that were structurally similar to authentic virus. Differences in the budding dynamics of NiV proteins were noted between rMVA and plasmid-based strategies. Mutational analysis of M revealed a sequence (YPLGVG) that was required for budding. Replacement of the known Ebola VP40 late budding domain (L-domain) with the NiV M sequence resulted in restoration of VP40 budding, and immunofluorescent microscopy revealed cells morphologically similar to those expressing wild-type VP40. Taken together, these results indicate that NiV M, F, and G each possess some ability to bud from expressing cells, and that co-expression of these viral proteins results in a more organized budding process with M playing a central role. Additionally, NiV M contains a sequence that is important for budding and appears to serve as an L-domain. These findings further our understanding of paramyxovirus particle assembly in general and could help facilitate the development of a novel vaccine approach for henipaviruses.

**THE CENTRAL ROLE OF THE MATRIX PROTEIN
IN NIPAH VIRUS ASSEMBLY AND
MORPHOGENESIS**

By

Jared Renford Patch

**Dissertation submitted to the Faculty of the
Emerging Infectious Disease Program of the Uniformed
Services University of the Health Sciences**

F. Edward Hebert School of Medicine

**In partial fulfillment of the requirements for the degree of
Doctor of Philosophy 2007**

Preface

Portions of this manuscript have been published as:

Patch, J.R., Crameri, G., Wang, L.F., Eaton, B.T., Broder, C.C. 2007. Quantitative analysis of Nipah virus proteins released as virus-like particles reveals central role for the matrix protein. *Virology Journal* **4**:1.

All Ebola VP40 experiments were performed in collaboration with Drs. Ziyang Han and Ronald Harty (University of Pennsylvania), and are included with permission.

Dedication

I wish to express my appreciation to the faculty of the Emerging Infectious Disease Program and to Uniformed Services University of the Health Sciences and associated staff for providing me this educational opportunity. In particular, I thank Dr. Lee Metcalf for opening the door to acceptance to the program and to Dr. Christopher Broder for his support and mentoring, as well as my dissertation committee members for their support.

I also thank Katharine Bossart, Kimberly Bishop, Andrew Hickey, Dimple Khetawat, as well as the rest of the members of the Broder lab for their friendship and help, and Yan-Ru Feng and Lemin Wang for making research easier.

Finally I thank Darcy and Madison for their love, support and patience, as well as my parents and in-laws for their love and support.

Table of Contents

List of Figures	viii
List of Tables	x
Chapter 1	1
Introduction.....	1
General Features of Paramyxoviruses	3
Paramyxovirus Assembly	11
Late Budding Domains	13
Henipavirus Biology	17
Hypothesis.....	22
Chapter 2	24
Methods.....	24
Chapter 3	39
Quantitative analysis of <i>Nipah virus</i> proteins released as virus-like particles reveals central role for the matrix protein.....	39
Introduction.....	39
Results.....	40
Discussion.....	60
Chapter 4	67
Mutational analysis of <i>Nipah virus</i> matrix protein reveals a domain required for budding	67
Introduction.....	67

Results.....	68
Discussion.....	96
Chapter 5.....	104
Discussion.....	104
Cytoskeletal Proteins	105
Lipid Rafts	107
Persistent Infection.....	108
Limitations and Future Directions	111
Chapter 6.....	112
Bibliography	112

List of Figures

Figure 1. Representation of Henipavirus genome organization.....	6
Figure 2. Representation of Late (L)-domain interaction with multivesicular body (MVB) proteins	15
Figure 3. MVA expression of NiV structural proteins results in protein release.....	41
Figure 4. Quantified release of MVA-expressed NiV structural proteins.....	44
Figure 5. NiV structural proteins are released in the absence of MVA.....	47
Figure 6. Comparison of NiV M release with SV5 M and kinetics of NiV M release.....	51
Figure 7. Immunoelectron microscopy shows particles consistent in size and morphology with authentic NiV virions.....	54
Figure 8. Sucrose gradient density analysis of NiV VLPs.....	58
Figure 9. NiV M release is insensitive to VPS4A inhibition.....	69
Figure 10. NiV M release is insensitive to VPS4B inhibition.....	72
Figure 11. NiV M release is insensitive to proteasome inhibition and AIP1/Alix over-expression.....	74
Figure 12. NiV and SV5 M protein chimeras are not released.....	78
Figure 13. Alignment of the NiV and HeV M proteins.....	81
Figure 14. NiV M protein N-terminus is dispensable for budding.....	84
Figure 15. The N-terminus of HeV M confers a decrease in release.....	86
Figure 16. Site-directed proline mutagenesis.....	89
Figure 17. NiV M sequence required for budding and possible late domain element.....	91

Figure 18. NiV late domain can rescue Ebola VP40 budding.....94

Figure 19. Alignment of mutations in Measles virus M.....109

List of Tables

Table 1. Overview of <i>Mononegavirales</i> and Paramyxovirus Taxonomy.....	4
-----------------------------------------------------------------------------	---

Chapter 1

Introduction

Nipah virus (NiV) is a newly recognized, emerging paramyxovirus capable of causing lethal infections in a number of mammalian species including humans (25). Together, with *Hendra virus* (HeV), they are members of the recently created *Henipavirus* genus within the *Paramyxoviridae* family (135). The type species, HeV (81), appeared first in eastern Australia in 1994 and was transmitted to humans from infected horses [reviewed in (39) and (38)]. The disease manifested in horses predominantly as a respiratory illness and in humans as an influenza-like illness. In the initial outbreak near Brisbane, 14 horses died from HeV infection, with a further 7 horses euthanized, and 1 of the 2 human cases associated with this outbreak manifested as a severe and fatal pneumonia. The isolated virus was recognized as a novel paramyxovirus and initially named equine morbillivirus, but then renamed *Hendra virus* after the suburb where the outbreak took place. At a separate location 13 months later, a person died of encephalitis and it was retrospectively recognized to be as a result of HeV infection. Over a year earlier, just prior to the Brisbane outbreak, this individual had assisted in the necropsy of 2 horses that had died of a severe respiratory illness, later recognized as HeV infection. It became apparent that he was infected at that time and experienced mild meningitis but had apparently recovered until the fatal encephalitic relapse. Subsequent outbreaks in 1999 and 2004 have been limited to individual horses. Although a number of animals were surveyed, the discovery of anti-HeV antibodies in *Pteropus* bats and the

later isolation of HeV from individual bats of two different species suggested that bats of the *Pteropus* genus were the primary animal reservoir (38, 39).

NiV was identified later during an outbreak of severe encephalitis in Malaysia and Singapore that began in 1998 and continued into 1999 [reviewed in (24) and (38)]. The disease outbreak was initially thought to be caused by Japanese Encephalitis; however epidemiological characteristics including (i) a high proportion of cases that were males who worked with pigs, (ii) few cases among children, and (iii) the apparent ineffectiveness of JE vaccination and mosquito control programs suggested a different etiology. In March of 1999, a virus was isolated from the cerebrospinal fluid of a fatally encephalitic patient, and subsequent serologic, electron microscopic, and genetic analysis led to its identification as a novel paramyxovirus, closely related to HeV, that was determined to have been responsible for the disease outbreak. The new paramyxovirus was named *Nipah virus* after the village from which the patient had come, Sungai Nipah. NiV was primarily transmitted to humans from infected pigs, although several additional animal species were also noted to have been infected. The association led to the culling of more than 1 million pigs and a prohibition of their import into Singapore from Malaysia, which, together with the development of an effective ELISA assay for the detection of infected pigs, helped to end the epidemic. In total, this outbreak resulted in 265 human cases of acute encephalitis with 105 deaths (24). Also of interest, was that 7.5% of recovered patients experienced relapse encephalitis and 3.4% of non-encephalitic or asymptomatic cases experienced late-onset encephalitis (125). Remarkably, these delayed encephalitis events have occurred as many as 4 years after initial infection, with a mean of approximately 8 months, and with 18% case fatality (23, 125). The underlying

mechanism(s) of how both NiV and HeV can persist in the infected human host and escape immune clearance is unknown. In order to determine the host reservoir, a multitude of domestic and wild animals were surveyed for evidence of NiV infection with a special focus on *Pteropus* bats. The finding of anti-NiV neutralizing antibodies in *Pteropus* bats (105), and subsequent isolation of NiV from bat urine and partially eaten fruit (26), has established *Pteropus* species of fruit bats (also known as flying foxes) as the natural reservoir hosts. There have been subsequent, and more recent outbreaks of NiV in Bangladesh (49, 57, 63-65) and India (19) from 2001 to 2005. Of particular note, the most recent episodes in 2004 and 2005 were associated with a higher incidence of acute respiratory distress syndrome in conjunction with encephalitis, person-to-person transmission, higher fatality rates (~75%), and apparently direct transmission from natural reservoir to humans. Their broad species tropism coupled with their highly pathogenic characteristics has clearly distinguished the henipaviruses from all other known paramyxoviruses [reviewed in (37)].

General Features of Paramyxoviruses

Paramyxoviruses are enveloped viruses with a single-stranded negative-sense RNA genome that replicate in the cytoplasm, and these features are shared with the *Filoviridae*, *Rhabdoviridae* and *Bornaviridae*, with which the paramyxoviruses have been grouped in the taxonomical order *Mononegavirales* (**Table 1**) (29). The family *Paramyxoviridae* is divided into two sub-families, *Paramyxovirinae* and *Pneumovirinae*. The *Paramyxovirinae* sub-family is further divided into five genera: *Respirovirus*, *Rubulavirus*, *Avulavirus*, *Morbillivirus* and *Henipavirus* (73, 81). Members of the

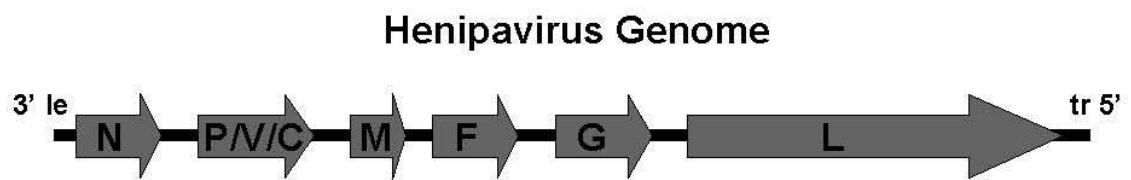
Table 1. Overview of *Mononegavirales* and Paramyxovirus Taxonomy

Family	Subfamily	Genus	Representative Virus Species
<i>Paramyxoviridae</i>			
	<i>Paramyxovirinae</i>		
		<i>Henipavirus</i>	<i>Nipah virus, Hendra virus</i>
		<i>Morbillivirus</i>	<i>Measles virus</i>
		<i>Rubulavirus</i>	<i>Simian virus 5</i>
		<i>Respirovirus</i>	<i>Sendai virus</i>
		<i>Avulavirus</i>	<i>Newcastle disease virus</i>
	<i>Pneumovirinae</i>		
		<i>Pneumovirus</i>	<i>Human respiratory syncytial virus</i>
		<i>Metapneumovirus</i>	<i>Human metapneumovirus</i>
<i>Bornaviridae</i>			<i>Borna disease virus</i>
<i>Filoviridae</i>			<i>Ebola virus, Marburg virus</i>
<i>Rhabdoviridae</i>			<i>Rabies virus, Vesicular stomatitis virus</i>

Paramyxoviridae include several well-known viruses such as *Measles virus* (MeV), *Sendai virus* (SeV), human parainfluenza viruses (hPIV) types 1-4, *Simian virus 5* (SV5), *Newcastle disease virus* (NDV), *Mumps virus*, and *Human respiratory syncytial virus* (RSV). The genome codes for six principal viral proteins: nucleocapsid protein (N), phosphoprotein (P), matrix (M), the fusion (F) and attachment (H, HN, or G) envelope glycoproteins, along with the viral RNA-dependent RNA polymerase (L). Additional viral proteins include V, C, and others that vary according to species (73). Although paramyxovirus genome lengths have traditionally clustered between 15.1 and 15.9 kb, newly discovered viruses such as HeV (18,234 nt) and NiV (18,246 nt), as well as the even longer genomes of J-virus and Beilong virus, have extended the upper limits of paramyxovirus genome length to almost 19 kb (37). Like other paramyxoviruses, the genomes of HeV and NiV are flanked by 3' leader and 5' trailer sequences that contain promoter elements for initiation of mRNA transcription and whole-genome replication (**Fig. 1**) (73, 133).

Paramyxovirus infection of a host cell is initiated by binding of the viral attachment protein to a cellular receptor followed by fusion of the viral and host cell membranes, which is mediated by the viral fusion protein. Upon release into the cytoplasm, the genome and associated proteins initiate mRNA production and subsequent rounds of genomic replication via a positive-sense RNA antigenome intermediate. The transcriptase complex is composed of the L protein along with the N and P proteins. Untranscribed intergenic sequences contain signals for termination and initiation of transcription. The viral mRNA transcripts are polyadenylated and terminated when the viral polymerase reiteratively copies a short stretch of uridylylates. After releasing the

Figure 1. Representation of Henipavirus genome organization. The Henipavirus genome consists of single stranded negative-sense RNA that contains 6 principle gene open reading frames (ORFs), which are drawn to scale. The genome is flanked by a 3' leader (le) and 5' trailer (tr) sequence. See the text for gene abbreviations. Leader and trailer sequences are not drawn to scale.



transcript, the polymerase can re-initiate transcription of the downstream gene. However, at a certain frequency the polymerase fails to re-initiate transcription, resulting in a progressively decreasing gradient of gene transcript production with genes proximal to the 3' end of the genome transcribed more than those that are distal. During full-length replicative transcription the intergenic signals are ignored by the polymerase. Exactly how the polymerase is regulated in switching between full-length replication and mRNA transcription is not known, however one leading hypothesis is that the concentration of N protein plays a role. The envelope glycoproteins are synthesized by membrane-bound ribosomes and then transported through the endoplasmic reticulum (ER) and Golgi to the cell surface where they are incorporated into viral particles during the assembly and budding process (73).

The N protein coats the genome as well as antigenome intermediates. Each N monomer associates with six nucleotides, which corresponds with the fact that paramyxovirus genome lengths are divisible by six, a feature known as the rule of six. Coating of the genome with N occurs concomitantly with full-length transcription and therefore the polymerase interacts with coated RNA rather than a naked template (73).

Depending on the viral species, the P gene can encode for as many as five different proteins. This is accomplished through the use of overlapping and altered reading frames. While transcribing the P gene the polymerase may add one or more non-templated G nucleotides at a conserved editing site, thus changing the reading frame of the gene from the editing site onward (73). In henipaviruses and morbilliviruses the V (+1 G) and W (+2 G) proteins are produced by this editing mechanism, and therefore share most of their sequence with the P protein while possessing unique C-terminal

domains. The C protein is transcribed entirely from a different open reading frame (ORF) located in the 5' portion of the P gene, as are some other species-specific proteins (37). The P protein plays a critical role in viral polymerase activity. Although the L protein is thought to contain most of the catalytic activity, P mediates the interaction of L with the N:RNA complex. The roles of some of the accessory proteins derived from the P ORF in viral replication are not well understood, and can vary between viral species (73). The V proteins of several viral species have been shown to play a role in inhibiting the host type I IFN response (37).

The M protein appears to play a central role in particle assembly in certain well-studied paramyxoviruses. Structurally, the M protein underlies the viral lipid envelope as an electron-dense layer and is the most abundant viral protein incorporated into virions. M is a basic and somewhat hydrophobic protein that, although the atomic structure has not been solved, is thought to possess amphipathic α -helices that insert into the inner leaflet of the lipid bilayer. However it is not an integral membrane protein and its interaction with the lipid membrane appears to be a result of hydrophobic, rather than electrostatic, interactions (73). In contrast to the M protein of some retroviruses (44), there is no evidence that the paramyxovirus M is modified with fatty acids (114). Although SeV M can be phosphorylated, the role of phosphorylation in replication and assembly is unknown since virions contain predominantly unphosphorylated M protein, and a mutant virus containing an M protein incapable of being phosphorylated was indistinguishable from wild-type in replication kinetics and plaque morphology (109).

The M protein is also capable of self-association and it forms paracrystalline arrays in its association with lipid membrane, and under low-salt conditions, *in vitro*, it

forms paracrystalline sheets and tubes (4, 55). In addition to self-association, certain M proteins have also been shown to interact with the viral envelope glycoproteins as well as the viral nucleocapsids (viral RNA genomes associated with N protein). Although its interaction with cellular proteins has remained relatively unexplored and may differ according to viral species, there is evidence that SeV and NDV M interacts with actin (43, 123), and the discovery of a late budding domain in SV5 M (115) strongly suggests an interaction with cellular multivesicular body proteins. It is likely that additional undiscovered interactions between M and cellular proteins exist.

All paramyxoviruses possess attachment and fusion glycoproteins, which decorate the surface of virions [reviewed in (73) and (10)], and with the exception of RSV and human metapneumovirus, both glycoproteins are required for productive cell entry and infection. Many members of the *Paramyxovirinae* sub-family have attachment proteins (HN) that possess both hemagglutinin and neuraminidase activity; however morbillivirus attachment proteins (H) lack neuraminidase activity. Henipaviruses and members of the *Pneumovirus* sub-family have structurally unrelated attachment proteins (G) that lack both hemagglutinin and neuraminidase activity. These attachment proteins are type II transmembrane proteins consisting of an amino (N)-terminal cytoplasmic and transmembrane domain, a stalk, and a globular head where receptor binding and enzymatic activity (if any) is located. They are also invariably N-glycosylated and oligomeric, consisting of disulfide-linked dimers that combine to form tetramers. Receptor engagement by the attachment protein is thought to facilitate or trigger the conformational changes in the F glycoprotein that ultimately lead to membrane fusion, however the details of this process remain poorly understood (10, 73).

The F protein is a trimeric type I transmembrane glycoprotein that mediates fusion of the viral and host cell membrane. It is synthesized as a precursor molecule (F_0) that is cleaved by host proteases into F_1 and F_2 subunits that remain linked by a disulfide bond. Whereas the C-terminus of F_1 remains anchored in the cell membrane, the new N-terminus created by cleavage is called the fusion peptide and, upon receptor engagement, is inserted into the target membrane. The F_1 subunit also contains two α -helical heptad repeats, one proximal to the N-terminus and fusion peptide (HRA), and the other proximal to the transmembrane domain (HRB). During fusion there is a conformational change in F such that HRA and HRB interact to form a six-helix bundle (6-HB), resulting in the protein adopting a hairpin conformation. This conformational change brings the two lipid membranes together allowing for pore formation and subsequent membrane fusion. This process takes place at the plasma membrane at neutral pH (10, 73).

Paramyxovirus Assembly

The assembly and morphogenesis of progeny virions requires that viral proteins, including the envelope glycoproteins and ribonucleoprotein (RNP) complex, associate at the plasma membrane for inclusion into budding virions. The M protein is thought to mediate this association, however the details of this process remain poorly understood and appear to vary among viral species [reviewed in (114)]. The interaction of M with other viral and cellular proteins has been explored using a variety of techniques including the generation of recombinant viruses using reverse-genetics, as well as recombinant expression of viral proteins to generate virus-like particles (VLPs). Recombinant MeV (17), SeV (66) and rabies virus (RV) (a rhabdovirus) (83) that lack M are impaired in

budding ability but remain infectious as demonstrated by increased cell-cell fusion. Recombinant expression of the M protein of SeV (121, 123), hPIV-1 (31), or NDV (99), in the absence of other viral proteins, leads to budding of virus-like particles (VLPs). Similar results have been observed for vesicular stomatitis virus (VSV) (54, 70, 74) and Ebola virus (EBOV) (5, 53, 69, 92, 127) (a rhabdovirus and filovirus, respectively). In addition, certain envelope glycoproteins also appear to have intrinsic budding activity, as has been shown for SeV F (121, 123), the G protein of RV and VSV (82, 107), and the envelope glycoprotein (GP) of Ebola virus (5, 92, 130). In contrast, SV5 requires expression of M along with N and at least one of its envelope glycoproteins in order for efficient budding to occur (116).

In addition to the budding ability exhibited by some paramyxovirus M proteins, M also plays an organizing role through its interactions with the envelope glycoproteins and nucleocapsid. Multiple studies have focused on the role of the envelope glycoproteins in assembly, with particular attention paid to the cytoplasmic domains of these proteins. Co-localization of M and at least one envelope glycoprotein has been observed for SeV (111, 112), SV5 (113, 116, 136), and RSV (42). For SV5 and RSV, the co-localization was disrupted by truncation or mutation of the cytoplasmic domain of the attachment protein. Ali and Nayak found that either F or HN increased the proportion of M bound to detergent-resistant membranes, a property that, for F, mapped to both the cytoplasmic and transmembrane domains (3). Recombinant MeV in which the envelope glycoproteins were replaced with VSV G failed to incorporate M, however M was incorporated when the cytoplasmic tail of VSV G was replaced with that of MeV F, thus suggesting an interaction between M and the F cytoplasmic tail. Support for a specific

interaction between M and N in SeV and hPIV-1 comes from the necessity of hPIV-1 N to be co-expressed with M in order to be incorporated into VLPs (31), and from a study that found that although mixed SeV/hPIV-1 nucleocapsids could be formed by co-expressing the N protein of both viruses, heterotypic nucleocapsids were excluded from progeny SeV (32). Under these conditions, additional co-expression of the heterotypic (hPIV-1) M protein resulted in SeV containing hPIV-1 N, suggesting a direct interaction between N and M. In a separate study, the SeV M-N interaction could be disrupted by a single amino acid mutation in M (110).

Late Budding Domains

An emerging area of interest in enveloped virus assembly and morphogenesis is the contribution of late budding domains (L-domains), which are protein motifs first identified in retroviral Gag precursor molecules that are important for late steps in assembly and budding [reviewed in (6, 33, 84)]. L-domains interact with components of cellular machinery involved in multivesicular body (MVB) formation and are thought to commandeer those proteins for use in viral budding. The involvement of L-domains in virus assembly and budding has been extended to other enveloped virus families including arenaviruses (102), filoviruses (53, 76), rhabdoviruses (52, 54, 76), and paramyxoviruses (115).

MVBs are late endosomes that are involved in the degradation of membrane proteins, and contain multiple intraluminal vesicles (ILVs) that are formed by invagination and budding into the MVB lumen, a process that is in effect topologically equivalent to the viral budding process. The protein components involved in MVB formation were

first identified and characterized in yeast, and those results have since been extended to mammalian cellular systems. The proteins are known collectively as class E Vps (for vacuolar protein sorting) proteins, many of which are found within three complexes known as Endosomal Sorting Complex Required for Transport (ESCRT-I, -II, or -III). Monoubiquitinated membrane proteins in the early endosome associate with hepatocyte growth factor-regulated tyrosine kinase substrate (Hrs), which recruits the ESCRT-I complex. The ESCRT-II and III complexes are also recruited, along with AIP1/Alix, and together these proteins play a critical, though poorly understood, role in ILV formation. The VPS4A and VPS4B ATPases then promote the disassembly of the ESCRT complexes. L-domains appear to act by interacting with one or more proteins in these complexes, or proteins associated with the complexes, and recruiting them to the plasma membrane to assist in viral budding (**Fig. 2**). L-domain amino acid motifs that have been identified (along with the MVB protein it interacts with) include: P(T/S)AP (Tsg101), PPxY (Nedd4-like E3 ubiquitin ligases), YP(x)_nL (AIP1/Alix), and ØPxV (none identified), where x is any amino acid and Ø is any aromatic amino acid (6, 33, 84). In certain cases, different L-domains can be functionally interchanged or mediate their activity in a position-independent manner within the protein molecule, however these properties are not universal and it is now apparent that the surrounding regions or context within which the L-domain motif lies can be important for its function (33, 67). There are several well-characterized examples where the mutation or removal of a viral L-domain motif within, for example, the M protein, will abrogate the protein's ability to bud from expressing cells (1, 68, 76, 104, 115). However, although deletion of the Ebola VP40 overlapping L-domains has a dramatic effect on VP40 VLP release, mutant viruses

Figure 2. Representation of Late (L)-domain interaction with multivesicular body (MVB) proteins. Normal protein trafficking and MVB protein interactions are depicted (left), as well as virus or virus-like particle (VLP) L-domain interactions with MVB machinery (right). See text for details. Monoubiquitination (mono-Ub) of a transmembrane protein is represented as a green circle. Endosomal Sorting Complex Required for Transport (ESCRT) protein complexes I, II, and III, are represented with blue, violet, and orange ovals, respectively. AIP1/Alix (green oval) and the VPS4A and B proteins (red circles) are also represented. The viral matrix protein is represented with yellow circles. The figure is modified from Demirov and Freed (33).

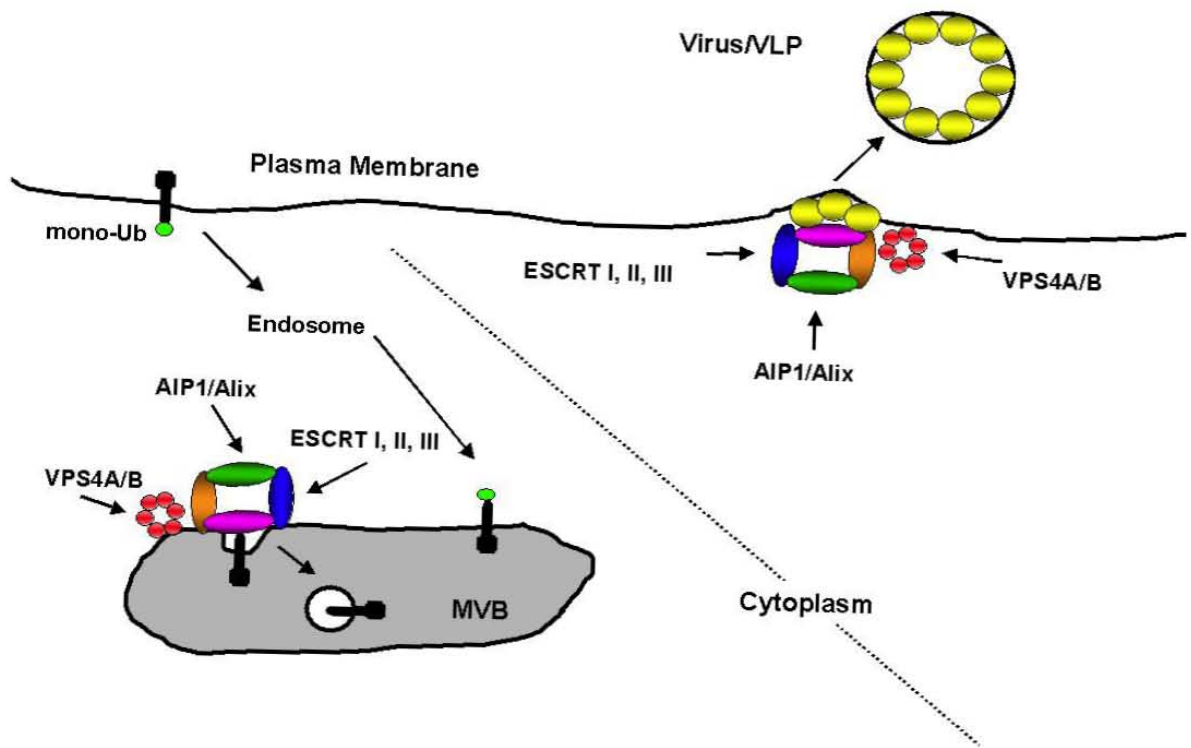


exhibit a modest attenuation in titer, indicating that in some cases the L-domain is not essential for virus replication (90). The first L-domain identified in a paramyxovirus was the novel FPIV sequence in SV5 M (115). Although several closely related paramyxoviruses share this motif, its importance in these viruses has yet to be demonstrated. In addition, yeast-two hybrid and co-precipitation experiments have suggested that the SeV C protein binds AIP1/Alix and appears to possess L-domain activity, however deletion and mutagenesis studies have failed to identify a sequence motif and the enhancement of VLP or virus production is limited to 2- to 3- fold (108).

Henipavirus Biology

The more recent discovery of HeV and NiV and their classification as BSL-4 agents has hampered studies of their cell biological properties. Nevertheless, the use of recombinant gene expression systems and *in vitro* assays have enabled the discovery of important biological features of the henipaviruses that in some cases have proven unique among the paramyxoviruses. At the time of their discovery HeV and NiV had the largest genomes of any paramyxovirus (18,234 nt and 18,246 nt, respectively) by about 15%, although the recently described J-virus and Beilong virus have larger genomes (18,954 nt and 19,212 nt, respectively). However, much of the additional length of the henipavirus genome is contained in un-translated regions located 3' (in sense orientation) to each gene except L, a feature that remains unique (37). The henipaviruses also are distinct in that their 3' leader and 5' trailer sequences are genus-specific, and in that their L protein contains the sequence GDNE rather than the highly conserved GDNQ motif found in all

but three (subsequently discovered) non-segmented negative sense RNA viruses (37, 50, 135). The significance of this change is unknown.

The envelope glycoproteins have been the focus of much of the research conducted on henipaviruses, primarily because they are the mediators of viral attachment and infection, and are the principal viral surface antigens to which neutralizing antibodies are directed (12, 13, 47, 73, 86, 124, 137). The F proteins are similar to other paramyxovirus fusion proteins in their overall processing, structure, and mechanism. They are synthesized as precursor molecules (F_0) that are cleaved into disulfide-linked subunits F_1 and F_2 , and mediate fusion via 6-HB formation (12, 13, 124). Most paramyxovirus F proteins contain a conserved RXXR motif that is cleaved by the ubiquitous cellular protein furin in the *trans*-Golgi network. The ubiquitous expression of furin enables these viruses to spread systemically. In contrast, a few paramyxovirus F proteins, like that of SeV, are cleaved by an extracellular trypsin-like protease. Such viruses are limited in their distribution and produce a more localized infection (10, 73). HeV and NiV are unique among paramyxoviruses in that their F proteins contain a cleavage site that is relatively insensitive to mutagenesis and contains only one basic residue, which is dispensable, and are cleaved by the endosomal protease cathepsin L. In contrast to other paramyxovirus F proteins, which are cleaved in the secretory pathway, henipavirus F proteins are cleaved in endosomal compartments and processed F molecules are subsequently returned to the cell surface (37, 95-97).

In contrast to the attachment protein of many *Paramyxovirinae* sub-family members, henipavirus G proteins lack both hemagglutinin and neuraminidase activity. They are otherwise similar to other paramyxovirus attachment proteins in that they (i) are

type II transmembrane proteins, (ii) can oligomerize into disulfide-linked dimers that can further form tetramers (iii) and appear to have a similar overall structure. Another unique feature of the henipavirus envelope glycoproteins is their ability to function in bi-directional heterotypic combinations (13, 124), a property that has only been observed for MeV and canine distemper virus (CDV); SeV F paired with hPIV-1 HN is also functional, however the reciprocal combination is not (10). The cellular receptor for HeV and NiV has been determined to be ephrin-B2 ligand (with ephrin-B3 serving as an alternate receptor), a glycoprotein that is expressed in a variety of organs and tissues including neurons and arterial endothelial cells, and is involved in development, cell-to-cell communication, and attachment (8, 88, 89). HeV and NiV are unique among paramyxoviruses in their ability to replicate in a broad range of animal species, a property that is attributed to the conserved expression of ephrin-B2 across many animal species (37).

The HeV and NiV M proteins are 89 percent identical at the amino acid level and have greater sequence homology to other paramyxovirus M proteins than do the other HeV and NiV proteins to their homologous paramyxovirus proteins. Compared to morbilliviruses, henipavirus M proteins have an additional 12 N-terminal amino acids (133), a feature also found in the more closely related Tupaia paramyxovirus (TPMV) (see Chapter 4). For NiV, the M protein has retained a methionine that aligns with the morbillivirus N-terminal methionine, while in HeV a point mutation has changed the methionine to isoleucine (see Chapter 4). Interestingly, there is zero percent identity between the HeV and NiV M proteins in this region, which accounts for approximately one-third of the amino acid differences between the two proteins (133).

The henipavirus P/V/C gene codes for the P, V, W and C proteins, which are produced from edited and alternate reading frames, as described above. HeV contains an additional ORF not found in NiV that codes for a putative protein called small basic (SB) protein (133). The henipavirus P protein is more than 100 amino acids longer than those of other paramyxoviruses. The roles of the P/V/C gene products in the viral lifecycle and pathogenesis have yet to be fully characterized. Recombinant protein expression in cell culture has demonstrated that the P, V, and W proteins can interfere with IFN induction and signaling, however their contribution to pathogenesis has yet to be established (37).

Ultrastructural studies of HeV (62) and NiV (45, 62) have revealed properties similar to other paramyxoviruses including the herringbone appearance of nucleocapsids, the formation of syncytia and nucleocapsid aggregates, assembly and budding at the plasma membrane, and production of pleomorphic particles that for HeV and NiV can range from 40 to 1900 nm in diameter. HeV and NiV infection can be distinguished from one another by the location of the giant cell nuclei and nucleocapsid aggregates, with those of HeV remaining in the center of the syncytia while those of NiV tend to be peripheral. Another distinguishing feature is the ‘double-fringed’ appearance of surface projections observed on HeV virions, versus the uniform appearance of NiV surface projections. The formation of a network of membrane-like tubules and reticular structures in the cytoplasm of infected cells is a distinctive feature found for both HeV and NiV. Although they remain poorly characterized, *in situ* hybridization studies suggest that these reticular structures play a role in transcription (45, 62).

NiV infection in humans is characterized by endothelial cell infection and extensive vasculitis of small blood vessels in multiple organs including the central

nervous system, heart, lungs, and kidneys. Multinucleated endothelial cells have been found in approximately a quarter of autopsied cases and constitute a pathognomonic feature. Common symptoms exhibited in patients with acute encephalitis included fever, drowsiness, headache, dizziness, vomiting, and reduced consciousness. Although most acute symptoms involved the CNS, many patients also had respiratory symptoms (139). In pigs NiV caused both neurological and respiratory manifestations, with respiratory manifestations dominating in pigs younger than 6 months old. However the overall mortality in pigs was comparatively low (5-15%), with many having no illness (24).

Flying foxes are some of the largest bats in the world. They navigate by sight and smell and can travel long distances (up to 600 km) (39). There are 65 species of flying foxes that range from Madagascar to Southeast Asia and Australia, to the Cook Islands. Only 3 geographically overlapping species are needed to link Pakistan to eastern Australia, and camps of flying foxes can contain multiple species (37, 39). Evidence of henipavirus infection of bats has been obtained in Australia, Malaysia, Cambodia, and Thailand (93, 105, 132, 142) and virus has been isolated from bat urine and partially eaten fruit (26, 105). In the Malaysian and Australian outbreaks, human cases were a result of interaction with pigs and horses, respectively. In contrast, evidence for animal intermediaries are lacking in Bangladesh outbreaks, suggesting a more direct route of transmission such as from contaminated fruit. Henipavirus infection of flying foxes appears to be largely sub-clinical, and experimental infection of flying foxes with HeV results in occasional and sporadic vasculitis (138). Viral antigen has been detected in the tunica media of blood vessels (138) rather than endothelial cells, and this may help to explain the relative lack of vasculitis and systemic disease in flying foxes (37). An

additional hypothesis is that a factor not found in other mammals limits HeV replication in flying foxes (36).

At present, there are no approved vaccines or therapeutics for treatment of henipavirus infection (38). During the initial Malaysian outbreak of NiV, 140 patients were treated with ribavirin, which apparently lowered mortality from 54% (of 54 patient controls) to 32%, which represents a 36% reduction in mortality (22). However, ribavirin had little effect in a hamster model of acute NiV infection (41). Peptides designed to bind the F protein and block formation of the 6-HB inhibit HeV and NiV envelope glycoprotein-mediated membrane fusion *in vitro* (11-13). This mechanism of fusion inhibition is identical in concept to that used in the treatment of HIV-1 infection with the antiviral drug enfuvirtide (T-20) (18), and such peptides may eventually play a role in therapeutic treatment of henipavirus infections. In hamster (47) and pig (137) models, animals immunized with recombinant poxviruses expressing either NiV F or G were protected against NiV challenge. Cats immunized with a recombinant subunit vaccine comprised of soluble HeV or NiV G were also protected against NiV challenge (86). Humoral immunity can clearly offer significant antiviral benefits, since hamsters were protected by passive transfer of antibodies against either NiV F or G (47, 48). These studies suggest that immunization directed against the henipavirus envelope glycoproteins may be an effective vaccine strategy in humans or livestock.

Hypotheses

Work with infectious NiV is restricted to BSL-4 containment, which imparts significant limitations on experimentation aimed at exploring the biology of the virus. As

a result, the determinants of NiV assembly and morphogenesis have remained relatively unexplored. The subject of this dissertation is the development and utilization of a recombinant gene expression system for the major structural proteins of NiV. We intend to use this experimental approach to investigate the assembly and budding process of the virus by generating VLPs, and also to examine the role of the M protein in VLP formation. The overall hypothesis of my dissertation is that the M protein plays a central role in henipavirus budding. Specific hypotheses include:

Hypothesis #1: Expression of NiV matrix protein results in virus-like particle (VLP) formation.

Hypothesis #2: Envelope glycoproteins and other structural proteins can be incorporated into VLPs, are dependent on co-expression of matrix protein for release, and enhance VLP formation.

Hypothesis #3: NiV matrix protein contains a late budding domain required for efficient budding.

Chapter 2

Methods

Cell lines. Vero cells, provided by Alison O'Brien (Uniformed Services University), and primary chicken embryo fibroblast cells (Charles River Laboratories, Inc, Wilmington, MA) were maintained in Eagle's minimal essential medium (Quality Biologicals, Gaithersburg, MD) supplemented with 10% cosmic calf serum (Hyclone, Logan, UT), 2mM L-glutamine, and 100 units/ml penicillin and streptomycin (Quality Biologicals, Gaithersburg, MD) (EMEM-10). 293T cells were maintained in Dulbecco's modified Eagle's medium (Quality Biologicals, Gaithersburg, MD) supplemented as described above (DMEM-10). BSR T7/5 cells (15) were kindly provided by Karl-Klaus Conzelmann (Max-von-Pettenkofer Institute and Gene Center, Germany) and were maintained in DMEM-10, which was supplemented with 1 mg/ml Geneticin (G-418) (Invitrogen, Carlsbad, CA) every second passage. All cultures were maintained at 37°C in 7.5% CO₂.

Antibodies. The following antibodies were used in immunoprecipitations: polyclonal rabbit antiserum against NiV F was obtained by immunization of rabbits with a synthetic peptide of the following sequence: CNTYSRLEDRRVRPTSSGDL, which corresponds to the cytoplasmic tail of NiV F. The peptide was conjugated to keyhole limpet hemocyanin (KLH) for immunization. Monoclonal antibodies (MAbs) F45G5 (anti-M) and F45G6 (anti-N) were kindly provided by Jody Berry and Hana Weingartl (National Centre for Foreign Animal Disease, Canadian Food Inspection Agency). MAb M-h (anti-

SV5 M) and rabbit anti-SV5 serum were kindly provided by Robert Lamb (Northwestern University). Mouse antiserum specific for HeV G was provided by Andrew Hickey (Uniformed Services University). Polyclonal sera from a rabbit immunized with gamma-irradiated NiV and from a rabbit immunized with soluble HeV G, as well as ascites fluid containing monoclonal antibody against the *c-myc* epitope were also used. Rabbit polyclonal antisera against the green fluorescent protein (GFP) (Invitrogen, Carlsbad, CA) and against DsRed (BD Biosciences, San Jose, CA) were purchased.

Plasmid and Recombinant MVAs. A system for recombinant gene expression using modified vaccinia virus Ankara (MVA) has been described (16). pMC03ΔE/L, which was made by removing the vaccinia virus promoter from pMC03 by ligation of the vector after *Pst*I digestion, was provided by Katharine Bossart (CSIRO Livestock Industries, Australian Animal Health Laboratory). To introduce the bacteriophage T7 promoter into the vector, complementary oligonucleotides 5' - GGAAATTAATACGACTCACTATAGGGAGACCACAACGGTTTAAACGGCGCGC CGGA (T7S) and 5' - GATCTCCGGCGCGCCGTTTAAACCGTTGTGGTCTCCCTATAGTGAGTCGTATT AATTCCTGCA (T7AS) were mixed in equal molar amounts, heated to 65°C, then allowed to cool and ligated into the *Pst*I and *Bgl*II sites of pMC03ΔE/L to form pMC03T7.

The NiV N ORF was PCR amplified from pCP629 (NiV N gene in pFastBac HTc) using primers 5' - GTTTAAACCACCATGAGTGATATCTTTG (NIVNS) and 5' - GTTTAAACTCACACATCAGCTCTG (NIVNAS). The NiV M ORF was PCR

amplified from pCP630 (NiV M gene in pFastBac HTa) using primers 5'-GTTTAAACCACCATGGAGCCGGACATC (NIVMS) and 5'-GTTTAAACTTAGCCCTTTAGAATTCTC (NIVMAS). The NiV F ORF was PCR amplified from pMC02 NiV F (13) using the primers 5'-GTTTAAACCACCATGGTAGTTATACTTGAC (NF2) and 5'-GGCGCGCCCTATGTCCCAATGTAGTAG (NFAS2). The NiV G ORF was PCR amplified from pMC02 NiV G (13) using the primers 5'-GTTTAAACCACCATGCCGGCAGAAAAC (NIVGS) and 5'-GTTTAAACTTATGTACATTGCTCTGG (NIVGAS). The HeV M ORF was PCR amplified from pCP436 (HeV M gene in pTD1) using the primers 5'-GTTTAAACCACCATGGATTTTAGTGTG (HEVMS) and 5'-GTTTAAACTCACCCCTTTAGGATCTTC (HEVMAS). PCR was done using Accupol DNA polymerase (PGS Scientifics Corp., Gaithersburg, MD) with the following settings: 94°C for 5 min, then 25 cycles of 94°C for 1 min, 55°C for 2 min, then 72°C for 3 min. The resulting PCR products were sub-cloned into pCRII-Blunt-TOPO (Invitrogen, Carlsbad, CA). TOPO constructs were digested with *PmeI* or *PmeI* and *AscI*, as appropriate, and inserted into *PmeI* or *PmeI-AscI* sites in pMC03T7.

The pCAGGS/MCS eukaryotic expression vector has been described previously (72, 91). In order to introduce an *AscI* site into pCAGGS, 128 pmol of the oligonucleotide 5' – TCGACGGCGCGCCG (CAG1) was heated to 65°C, allowed to cool, and then ligated into the *XhoI* site of pCAGGS/MCS to form pCAGGS-*AscI*. The ORFs for NiV N, M, G, and HeV M were digested from pMC03T7 as *PmeI* fragments and ligated into the pCAGGS *SmaI* site. The ORF for NiV F was digested from

pMC03T7 as a *PmeI*-*AscI* fragment and ligated into the pCAGGS-*AscI* *SmaI*-*AscI* site. pCAGGS-SV5 M, pCAGGS-SV5-NP, pCAGGS-SV5-F, and pCAGGS-SV5-HN were kindly provided by Robert Lamb.

Amino acid changes were introduced into NiV M by PCR site-directed mutagenesis using the QuickChange II Site-Directed Mutagenesis Kit (Stratagene, La Jolla, CA). NiV M P35A was PCR amplified using the primers 5'-CTTGATAAGGTTGAAGCAGAAATTGATGAAAATG (P35S) and 5'-CATTTTCATCAATTTCTGCTTCAACCTTATCAAG (P35AS). NiV M P93A was PCR amplified using the primers 5'-GACAATTGCTGCCTACGCTCTGGGTGTTGGTAAG (P93S) and 5'-CTTACCAACACCCAGAGCGTAGGCAGCAATTGTC (P93AS). NiV M P329A was PCR amplified using primers 5'-GCAGCTGTGTTGCAGGCTTCTATTCCAAGAGAG (NMSA329) and 5'-CTCTCTTGAATAGAAGCCTGCAACACAGCTGC (NMAA329). NiV M P332A was PCR amplified using primers 5'-GTTGCAGCCTTCTATTGCAAGAGAGTTCATGATC (NMSA332) and 5'-GATCATGAACTCTCTTGCAATAGAAGGCTGCAAC (NMAA332). NiV M Δ 92-97 was PCR amplified using primers 5'-CAGGACAATTGCTGCCAAGAGTGCCTCTCATC (93DS) and 5'-GATGAGAGGCACTCTTGGCAGCAATTGTCCTG (93DAS). NiV M Y92A was PCR amplified using primers 5'-CAGGACAATTGCTGCCGCCCTCTGGGTGTTGGTAAG (Y92S) and 5'-CTTACCAACACCCAGAGGGGCGGCAGCAATTGTCCTG (Y92AS). NiV M L94A was PCR amplified using primers 5'-

CAGGACAATTGCTGCCTACCCTGCGGGTGTGGTAAGAGTGCCTCTC (L94S2) and 5'– GAGAGGCACTCTTACCAACACCCGCAGGGTAGGCAGCAATTGTCCTG (L94AS2). NiV M encoded in pMC03T7 was used as the template in PCR for mutants P35A, P93A, P329A, and P332A, and mutagenesis PCR was performed using the following settings: 95°C for 5 min, then 10 cycles of 95°C for 1 min, 54°C for 2 min, then 68°C for 30 min. NiV M in pCRII-Blunt-TOPO was used as the template in PCR for mutants Δ 92-97, Y92A, and L94A, and mutagenesis PCR was performed using the following settings: 95°C for 5 min, then 15 cycles of 95°C for 1 min, 50°C for 2 min, then 68°C for 30 min. All mutants were sub-cloned as *PmeI* fragments into the *SmaI* site of pCAGGS-*AscI*.

S-tagged NiV M protein was created by PCR amplification of NiV M in pCAGGS-*AscI* using primers 5'-
 GTTTAAACCACCATGAAGGAAACAGCAGCTGCCAAGTTCGAACGACAACATA
 TGGATAGCATGGAGCCGGACATCAAGAGTATTTC (SNMS) and NIVMAS, and
 was carried out according to the settings described above. S-tagged SV5 M was created
 by PCR amplification of pCAGGS-SV5 M using primer
 5'-
 GTTTAAACCACCATGAAGGAAACAGCAGCTGCCAAGTTCGAACGACAACATA
 TGGATAGCATGCCATCCATCAGCATTCCCGC (SSV5S) and primer 5'-
 GGCGCGCCTCATTCCAGCTCCGTCAGGTTAGGCAGTG (SV5AS), and was carried
 out according to the settings described above except with an annealing temperature of
 56°C. Both products were cloned into pCRII-Blunt-TOPO, and further sub-cloned into
 pCAGGS-*AscI* as either *PmeI* or *PmeI-AscI* fragments. To create S-tagged chimeras, the

following gene fragments were PCR amplified: (i) the 5' half of S-tagged NiV M was amplified with primers 5'- GTTTAAACCACCATGAAGGAAACAGC (STAG5) and 5'- TGTGATACTGAGAAAAAATATTCTCAGAGCTTGATG (NMM3), (ii) the 3' half of S-tagged NiV M was amplified with primers 5'- AAGCTCAATGATTCTGGAATCTAC (NMM5) and NIVMAS, (iii) the 5' half of S-tagged SV5 M was amplified with primers STAG5 and 5'- AGTCACTGACAGAAATGTCGGAATGAAGAG (SMM3), (iv) the 3' half of S-tagged SV5 M was amplified with primers 5'- TACTGTCCAGCTGCAATCAAATTCAG (SMM5) and SV5AS. PCR was carried out as described above with an annealing temperature of 54°C. Gene fragments were gel purified and extracted using the QIAquick gel extraction kit (Qiagen, Valencia, CA), mixed in heterotypic combinations, and ligated. Chimeric products were PCR amplified with primers STAG5 and NIVMAS, or STAG5 and SV5AS, as appropriate. Resulting products were cloned into pCRII-Blunt-TOPO, and further sub-cloned into pCAGGS-AscI as either *PmeI* or *PmeI-AscI* fragments. We failed to detect expression of the S-tagged M constructs so un-tagged chimeras were generated by PCR amplification of the tagged chimeras with primers NIVMS and SV5AS (NiV-179/SV5 M), or SV5S and NIVMAS (SV5-176/NiV M), as appropriate, using the settings described above with an annealing temperature of 53°C. The resulting products were cloned into pCRII-Blunt-TOPO, and further sub-cloned into pCAGGS-AscI as either *PmeI* or *PmeI-AscI* fragments.

HeV and NiV M protein N-terminal chimeras were created by *PciI* digestion of pCRII-Blunt-TOPO containing HeV or NiV M, followed by reciprocal ligation of digestion fragments. This resulted in chimeric M genes containing the first 64 amino

acids of either HeV (H/N) or NiV (N/H). Both chimeric genes were sub-cloned as *PmeI* fragments into the *SmaI* site of pCAGGS-AscI. However, because we failed to detect expression of N/H M, a new mutant was made by PCR amplification of HeV M using primers 5'-

GTTTAAACCACCATGGAGCCGGACATCAAGAGTATTTCAAGTGAGTCAATGG
AAGGTGTTTCAGATTTTAGTCCC (N/HS) and HEVMAS, as described above. The resulting product (N/H2 M) was identical to HeV M except for the first 13 amino acids, which corresponded to those of NiV M. The PCR product was cloned into pCRII-Blunt-TOPO and further sub-cloned as a *PmeI* fragment into the *SmaI* site of pCAGGS-AscI. H/N and N/H2 M are called HeV/NiV M and NiV/HeV M, respectively, in Chapter 4.

NiV/HeV 2-5 M was created by PCR amplification of NiV M with primers 5'-
GATTTTAGTGTGAAGAGTATTTCAAGTGAGTCAATGG (NH1I) and NIVMAS. The resulting product was cloned into pCRII-Blunt-TOPO and used as the template for PCR amplification using primers 5'-

AGCTTTGTTTAAACCACCATGGATTTTAGTGTGAAGAGTATTTCAAGTGAG
(NH1S3) and 5'- TTGGCGCGCCTTAGCCCTTTAGAATTCTC (NMASC). NiV/HeV

6-9 M was created by PCR amplification of NiV M with primers 5'-

AGTGATAACCTTAGTGAGTCAATGGAAGGAGTATCT (NH2I) and NIVMAS.

The resulting product was cloned into pCRII-Blunt-TOPO and used as the template for PCR amplification using primers 5'-

AGCTTTGTTTAAACCACCATGGAGCCGGACATCAGTGATAACCTTAGTGAGT
CAATGGAAGG (NH2S3) and NMASC. NiV/HeV 10-13 M was created by PCR

amplification of NiV M with primers 5'-

GATGGTCCAATGGAAGGAGTATCTGATTCAGCCC (NH3I) and NIVMAS. The resulting product was cloned into pCRII-Blunt-TOPO and used as the template for PCR amplification using primers 5'-

AGCTTTGTTTAAACCACCATGGAGCCGGACATCAAGAGTATTCAGATGGTC
CAATAGAAGGAGTATCTGATTCAGC (NH3S3) and NMASC. All PCR was done using the settings described above except for an annealing temperature of 54°C. Final PCR products were digested with *PmeI* and *AscI* and ligated into the *SmaI-AscI* site of pCAGGS-*AscI*.

NiV M Δ 1-12 was created by site-directed mutagenesis PCR of NiV M in pCRII-Blunt-TOPO using primers 5'-

GCCCTTGTTTAAACCACCATGGAAGGAGTATCTGATTCAGC (NMDS) and 5'-
GCTGAAATCAGATACTCCTTCCATGGTGGTTTAAACAAGGGC (NMDAS) as described above. The gene was sub-cloned as a *PmeI* fragment into the *SmaI* site of pCAGGS-*AscI*.

HeV M Δ 2-13 was created by PCR amplification of HeV M using primers 5'-
AGCTTTGTTTAAACCACCATGGAAGGTGTTTCAGATTTTAGTCCCACCTCATG
GGAG (*HdeI*2) and 5'- TTGGCGCGCCTCACCCCTTAGGATCTTCCC (*HMASC*),
digesting the PCR product with *PmeI* and *AscI*, and ligating it into the *SmaI-AscI* site of pCAGGS-*AscI*. PCR was done using the settings described above except for an annealing temperature of 54°C.

Wesley Sundquist (University of Utah) kindly provided pEGFP-VPS4A-WT, pEGFP-VPS4A-E228Q, pDsRed-VPS4B-WT, pDsRed-VPS4B-E235Q, pcDNA3.1*mycHisA*(-), and pcDNA3.1-AIP1*mycHis*.

To create recombinant MVAs, chicken embryo fibroblasts (CEFs) were infected with wild-type MVA at a multiplicity of infection (MOI) of 0.1. At 2 h post-infection, the CEFs were transfected with 8 μ g of the appropriate pMC03T7 construct using Profection Mammalian Transfection System – Calcium Phosphate (Promega, Madison, WI). At 4 h post-transfection, cells were washed, given fresh EMEM-10, and then incubated for 3 days at 37°C. Cells were harvested by scraping, pelleted, and then resuspended in 0.5 ml EMEM-2.5 as crude recombinant virus. After 3 cycles of freezing and thawing, virus was diluted and CEF monolayers were infected overnight at 37°C. Monolayers were then overlaid with EMEM-10 containing 1% low-melting point agarose (Invitrogen, Carlsbad, CA) and incubated for 2 days. A final overlay of EMEM-10 containing 1% low-melting point agarose and 0.2 mg/ml 5-bromo-4-chloro-3-indolyl- β -D-glucuronic acid (X-Gluc) (Clontech, Palo Alto, CA) was added to the monolayers and over the following 72 h cells that showed blue staining were picked, resuspended in 0.5 ml EMEM-2.5, and used for repeated positive selection. After 5 or more rounds of purifying positive selection, recombinant MVAs were amplified in CEFs to make crude stocks.

Recombinant MVA expressing the bacteriophage T7 RNA polymerase (MVAGKT7) was provided by Gerald R. Kovacs (National Institutes of Health, Bethesda, MD).

Transfection, MVA Infection, and Metabolic Labeling. 293T cells in 6-cm wells were transfected in duplicate with expression plasmids using FuGene 6 transfection reagent (Roche, Indianapolis, IN) according to the manufacturer's instructions. Unless otherwise

specified, 1 μg of each plasmid was used per well. Empty vector was used to make the total DNA amount equivalent between groups. For experiments described in Chapter 3, a total DNA amount of 4 $\mu\text{g}/\text{well}$ was used. Vero cells were infected with recombinant MVAs at an MOI of 3-5 in a minimal volume of EMEM containing 2.5% serum. At 24 h post transfection or 6 h post infection, cells were overlaid with methionine- cysteine-free minimal essential medium (MEM) (Invitrogen, Carlsbad, CA) containing 2.5% dialyzed fetal calf serum (Invitrogen, Carlsbad, CA) and 100 $\mu\text{Ci}/\text{ml}$ ^{35}S -cys/met Redivue Promix (Amersham Pharmacia Biotech, Piscataway, NJ), and incubated at 37°C for transfected cells, or 31°C for infected cells. For pulse-chase labeling, cells were washed then starved in methionine-cysteine-free MEM for 45 min followed by metabolic labeling as, as described above, for 15 min. Cells were washed once then chased with DMEM-10.

Immunoprecipitation. Cells were harvested by scraping, pelleted by centrifugation at 5000 X g for 5 min, and then washed once with PBS and pelleted again. The pellet was resuspended in 200 μl lysis buffer (100 mM Tris-HCl, pH 8.0; 100 mM NaCl; 1.0% Triton-X 100) containing Complete, Mini protease inhibitors at a 1X concentration (Roche, Indianapolis, IN), and incubated on ice for 10 min. After removing nuclei by centrifugation, lysates were pre-cleared by incubation with Protein G-Sepharose (Amersham Pharmacia Biotech, Piscataway, NJ) for 30 min. Lysates derived from a VLP detection assay were frozen at -80°C until immunoprecipitation. Typically 1-2 μl of appropriate antiserum was used for each sample and antiserum and lysates were incubated at 4°C overnight, followed by addition of Protein G-Sepharose for 45 min. Protein G beads were washed twice with lysis buffer followed by one wash with lysis

buffer containing 0.1% sodium deoxycholate and 0.1% SDS. Proteins were separated either by SDS-polyacrylamide gel electrophoresis (SDS-PAGE) on a 10% polyacrylamide gel, or by a NuPAGE Novex 4-12% Bis-Tris gel (Invitrogen, Carlsbad, CA) and visualized by autoradiography.

VLP Assay. 293T cells were transfected, and Vero cells were infected with recombinant MVAs, as described above. At 20-24 h p.t. or 48 h p.i., the cell culture medium was removed, clarified, and then centrifuged through a cushion of 10% sucrose (w/vol) in NTE (100 mM NaCl; 10 mM Tris-HCl, pH 7.5; 1 mM EDTA) at 200,000 X g for 2 h at 4°C. The resulting pellet was re-suspended in 4 ml NTE and 1.3 ml 80% sucrose. A discontinuous sucrose gradient was formed by overlaying with 1.8 ml 50% followed by 0.6 ml 10% sucrose in NTE. The gradient was centrifuged at 200,000 X g for 16 h at 4°C in a SW50.1 rotor. Typically, two 0.7 ml fractions were removed from the top of the gradient, diluted with 2X lysis buffer, and analyzed by immunoprecipitation. The two fractions were combined during the first wash after Protein G-Sepharose addition. Proteins from 1/20 of cell lysates from MVA infections, and half of cell lysates from transfected cells, were used for immunoprecipitation. For samples derived from transfection, 1/3 of each sample was loaded and analyzed by SDS-PAGE followed by autoradiography (equivalent to 1/6 total lysate). The release efficiency of protein was quantified by performing densitometry analysis on the scanned film images using AlphaEaseFC software (Alpha Innotech Corporation, San Leandro, CA). Percent release was calculated as the fraction of protein derived from the supernatant divided by total protein detected (total lysate + supernatant). Experiments described in Chapter 4 did not

include a flotation step. Rather, following the pelleting phase through the sucrose cushion, the released protein was resuspended in 200 μ l of lysis buffer and then immunoprecipitated.

Proteasome Inhibition. Proteasome inhibition was performed essentially as described by Schmitt and co-workers (115). Transfected cells were treated with increasing concentrations of the proteasome inhibitor MG-132 (Calbiochem, EMD Biosciences, San Diego, CA) for 30 min prior to addition of ^{35}S -containing medium. Cells were then washed and metabolically labeled as described above, except with continued treatment with MG-132. Extra DMSO was added as needed to make the total DMSO concentration equal between groups. NiV M release was analyzed by harvesting cell lysates and supernatants as described above.

Equilibrium Centrifugation. Clarified culture supernatants of MVA-infected Vero cells were centrifuged at 200,000 X g for 2 h at 4°C. The resulting pellet was resuspended in 200 μ l NTE and added to the top of a continuous gradient of 5-45% sucrose. Clarified supernatants from transfected cells were added directly to the gradient. The gradient was centrifuged in an SW40 Ti rotor at 200,000 X g for 16 h at 4°C. Fractions were collected from the bottom and 50 μ l of each fraction was set aside for density measurement. The remainder of each fraction was combined with 4X lysis buffer (pH 7.5) and immunoprecipitated as described. Density was determined based on refractive index as measured with a refractometer. Culture supernatants of NiV-infected Vero cells were

clarified at 20,000 X g for 10 min at room temperature and 100 µl of clarified supernatant containing approximately 10^6 TCID₅₀ was added to the top of a continuous gradient of 5-45% sucrose. The gradient was then centrifuged in an SW41 Ti rotor at 200,000 X g for 16 h at 4°C. Fractions were collected from the bottom and 50 µl of each fraction was set aside for density measurement. A portion (140 µl) of each fraction was extracted using the QIAamp Viral RNA Mini kit (Qiagen GmbH, Hilden) and extracted RNA was analyzed by quantitative real-time PCR as previously described (86). Threshold cycle (Ct) values were used as a proxy for virus concentration and density was determined based on refractive index as measured with a refractometer.

Electron Microscopy. VLPs released from transfected 293T cells into the culture supernatant were prepared as described above except the top 1.4 ml of the flotation gradient was mixed with 3 ml of PBS and centrifuged for an additional 2 h after which the pellet was resuspended in 60 µl PBS. VLPs were adsorbed onto carbon-coated parlodion copper grids and immunolabeled using either polyclonal HeV G-specific mouse antiserum (1:2500) or anti-NiV M monoclonal antibody F45G5 (1:1), followed by secondary antibody (1:50) conjugated to 12 nm gold beads. For detection of M, immunolabeling was done in the presence of 0.05% saponin. Samples were negatively stained with 1% uranyl acetate and examined with a Hitachi 7600 transmission electron microscope operated at 80 kV.

Protein Sequence Alignment. ClustalW protein alignment was performed using the ClustalW program of the European Bioinformatics Institute

(<http://www.ebi.ac.uk/clustalw>). The Jalview (28) multiple alignment editor was used to view the ClustalW alignment, as well as to make pairwise amino acid alignments. Matrix gene sequences were derived from the following GenBank accession numbers: Nipah virus (NP_112025.1); Tupaia paramyxovirus (NP_054694.1); Measles virus (NP_056921.1); Sendai virus (NP_056876.1); Newcastle disease virus (NP_071468.1); Simian virus 5 (YP_138514.1). The sequence for Hendra virus was derived from sequencing pCP436. Measles subacute sclerosing panencephalitis (SSPE) mutant sequences were from accession numbers: BAA09963.1; BAA09956.1; P16628; BAA00381.1; AAN09804.1; AAN09800.1; AAN09803.1.

Ebola VP40 budding assay. The expression plasmids for Ebola VP40 and glycoprotein GP have been generated as described previously (75, 76). A plasmid encoding the VP40/NiV protein chimera was produced by introducing the putative L-domain of NiV in place of the VP40 L-domain by PCR and inserted into vector pCAGGS using EcoRI and XhoI restriction endonucleases. All introduced mutations were confirmed by automated DNA sequencing. Human 293T cells in six-well plates were transfected with 2 μ g plasmid DNA of Ebola GP plus 2 μ g plasmid DNA of VP40WT or VP40/NiV chimera by using the Lipofectamine reagent (Invitrogen, Carlsbad, CA) and the protocol of the supplier. At 20-24 h post-transfection, proteins were metabolically labeled with 150 μ Ci of 35 S Met-Cys (Perkin-Elmer, Wellesley, MA) for 5 h. Culture media was centrifuged at 2,500 rpm for 10 min to remove cellular debris, layered onto a 20% sucrose cushion in STE buffer (0.01 M Tris-HCl [pH 7.5], 0.01 M NaCl, 0.001 M EDTA [pH 8.0]), and centrifuged at 36,000 rpm for 2 h at 4°C. The resulting pellet containing VLPs was

suspended in 100 μ l of STE buffer followed by 300 μ l of RIPA buffer (50 mM Tris [pH 8.0], 150 mM NaCl, 1.0% NP-40, 0.5% deoxycholate, 0.1% SDS) overnight at 4°C. The VLPs were immunoprecipitated with the anti-VP40 monoclonal antibody at 4°C overnight. The immune complexes were then precipitated with 50 μ l of a 20% protein A agarose bead suspension and analyzed by SDS-PAGE. Protein bands were visualized by autoradiography and quantified by phosphorimager analysis.

VP40 indirect immunofluorescence. COS-1 cells were transfected with plasmids encoding VP40WT, VP40 Δ PT/PY or VP40/NiV proteins using Lipofectamine and the protocol of supplier (Invitrogen, Carlsbad, CA). The cells were fixed with 4.0% paraformaldehyde in 1 \times PBS (fresh-made) at room temperature for 10 min at 20-24 h post-transfection, washed three times with 1 \times PBS, permeabilized with 0.2% Triton X-100 in 1 \times PBS on ice for 10 min, and washed three times with 1 \times PBS. The cells were incubated with mouse anti-VP40 monoclonal antibody (1:100) in 3% BSA/PBS at 37°C in dark for 30 min and washed three times, and then incubated with Alexa Fluor 488 donkey anti-mouse antibody (1:500) (Molecular Probes, Invitrogen, Carlsbad, CA) in 3% BSA/PBS at 37°C in dark for 30 min. The cells were washed three times with 1 \times PBS and one time with water, and then mounted with Prolong antifade solution (Molecular Probes, Invitrogen, Carlsbad, CA) and analyzed by confocal microscopy.

Chapter 3

Quantitative analysis of *Nipah virus* proteins released as virus-like particles reveals central role for the matrix protein

Introduction

The recent emergence of NiV and its requirement for BSL-4 containment has hampered investigation of its assembly and budding. Studies of the replication of live NiV in mammalian cell culture have yielded some general characteristics of viral morphogenesis (45, 62), however underlying mechanisms and the properties and contributions of individual viral proteins have remained unexplored. Recombinant expression and VLP production have been employed as a means of studying the assembly and budding of other paramyxoviruses including hPIV-1, SeV, NDV, and SV5 (31, 99, 116, 121, 123). As described above, solo expression of the M protein of several of these viruses, as well members of the filovirus (5, 53, 69, 92, 127) and rhabdovirus (54, 70, 74) families, results in the release of M in VLPs. In order to address the contribution of NiV structural proteins to the assembly and budding process, we sought to develop a VLP system using recombinant gene-expression techniques. We hypothesized that the NiV M protein could form VLPs when expressed alone, and that when co-expressed, other structural proteins, particularly the envelope glycoproteins, could be incorporated into and enhance VLP formation.

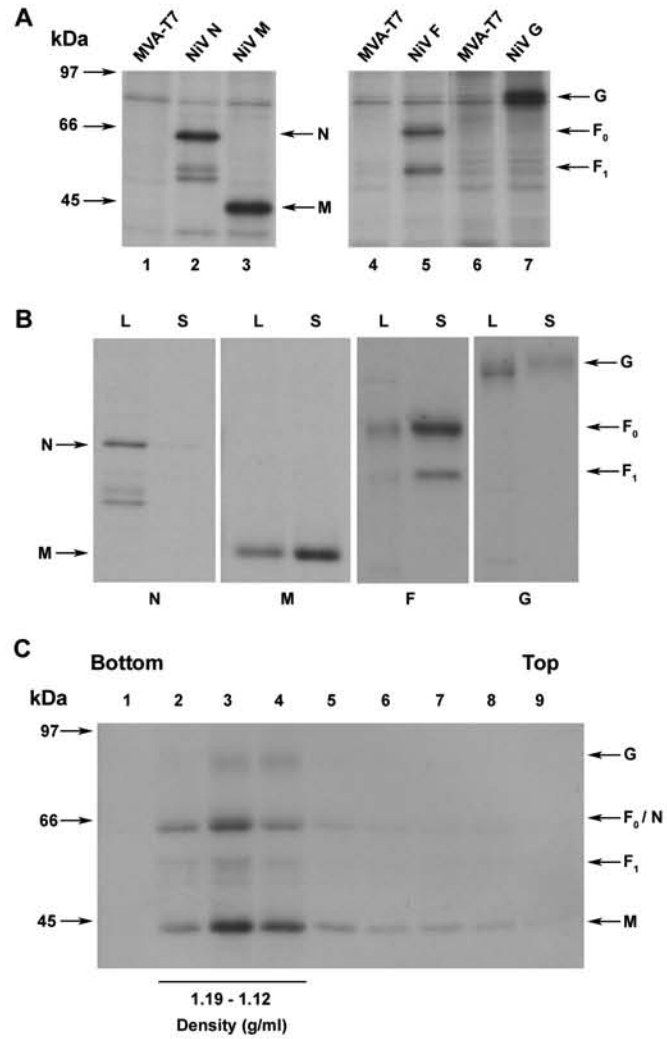
Results

MVA expression of NiV Proteins. We first sought to develop a NiV VLP expression system using recombinant MVA poxvirus-based technology as a means of gene delivery and expression. The NiV N, M, F and G ORFs were sub-cloned into the pMC03-based vector (16) in which the vaccinia virus early-late promoter was replaced with the bacteriophage T7 promoter. These constructs were then used to create the various rMVAs containing the individual NiV genes under the control of the T7 promoter. To test for NiV protein expression, Vero cells were infected with individual rMVAs expressing N, M, F, or G, along with MVAGKT7 encoding the T7 RNA polymerase. Infected cells were metabolically labeled overnight. Cell lysates were prepared and the NiV proteins were immunoprecipitated with NiV-specific polyclonal rabbit serum or rabbit anti-F polyclonal serum (**Fig. 3**). Analysis of immunoprecipitated proteins revealed bands corresponding to NiV N and M (**Fig. 3A**, lanes 2 and 3) which migrated at the expected apparent molecular weights of ~58 kDa (N) and ~42 kDa (M) respectively (117, 134). The NiV F₀ (~61 kDa), F₁ (~49 kDa), and G (~74 kDa) shown in **Fig 3A** (lanes 5 and 7), were found to be consistent with patterns reported previously (13).

In subsequent experiments to evaluate whether expression of NiV proteins can lead to VLP formation, cells were infected with rMVAs and metabolically labeled for 44 h followed by collection of both the cells and culture supernatant. Vesicles in the culture supernatant were pelleted by centrifugation through a 10% sucrose cushion and then floated by centrifugation in a discontinuous sucrose gradient as described in the Methods chapter.

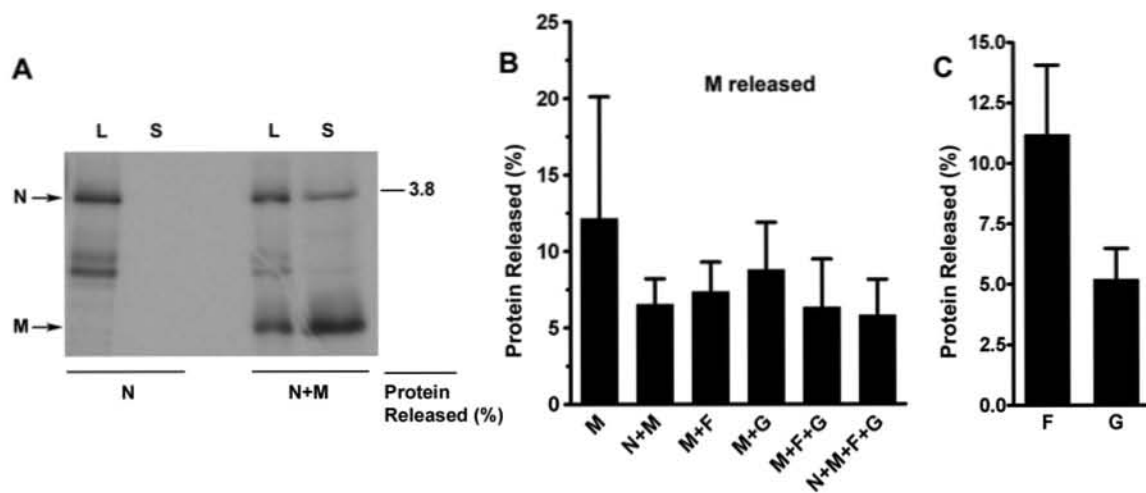
Figure 3. MVA expression of NiV structural proteins results in protein release.

Panel A: Vero cells were infected with rMVAs expressing NiV N, M, F, or G, along with MVAGKT7 and then metabolically labeled. Lysates were immunoprecipitated with either rabbit anti-NiV polyclonal serum (N, M, G) or rabbit anti-F polyclonal serum. **Panel B:** Vero cells were infected with rMVAs and MVAGKT7 and metabolically labeled. Released protein was purified by centrifugation through a 10% sucrose cushion followed by flotation in a sucrose gradient. Proteins derived from cell lysates (L) or culture supernatants (S) were immunoprecipitated and analyzed as described above and in the Methods chapter. Lysate bands represent 1/20 of total lysate. **Panel C:** Supernatant from metabolically labeled cells expressing N, M, F, and G was clarified and released protein was layered onto a 5-45% sucrose gradient followed by centrifugation for 16 h as described in the Methods chapter. Fractions were obtained and proteins were analyzed by immunoprecipitation. A portion of each fraction was also used to determine density.



Membrane-associated proteins were collected from the top of the gradient and detected by immunoprecipitation and analyzed by SDS-PAGE followed by autoradiography. Whereas minimal membrane-associated N was detected in culture supernatants, individual expression of M, F, and G resulted in detectable membrane-associated protein release (**Fig. 3B**). To characterize the protein release as genuine VLPs, the culture supernatant of metabolically labeled cells expressing N, M, F, and G together was layered onto a 5-45% sucrose gradient, which was then centrifuged to allow membrane-associated proteins to migrate to their given buoyant density. Fractions of the gradient were then collected with a portion of each fraction set aside for sucrose density determination. The proteins in the remaining portion of the fractions were then recovered by immunoprecipitation and analyzed by SDS-PAGE followed by autoradiography. NiV proteins were found predominantly in fractions 2 through 4, which corresponded to a density range of 1.12-1.19 g/ml (**Fig. 3C**). This density range was consistent with the density reported for SeV and NDV VLPs (99, 121, 123), as well as authentic NiV (see below). To examine the contribution of each viral protein to overall protein release, NiV proteins were expressed in different combinations and their release was quantified. Release of N was not detected when expressed alone, however co-expression of M with N resulted in release of both proteins into the supernatant (**Fig. 4A**). Quantification of expression of M protein with other viral proteins indicated a reduction in the mean M released (~12%) compared to its expression alone; however this reduction did not reach statistical significance among repeated experiments (**Fig. 4B**). We also confirmed that expression of multiple proteins simultaneously did not reduce the overall N, M, F, or G

Figure 4. Quantified release of MVA-expressed NiV structural proteins. Cells were infected with rMVAs in order to express NiV proteins alone or in combination. Cells and supernatants were treated as in **Fig. 3B**. Membrane-associated protein release of N (**Panel A**), M (**Panel B**), and F and G (**Panel C**) was quantified by densitometry. A representative experiment is shown in Panel A. The mean and standard deviation of three or more independent experiments are shown in Panels B and C.



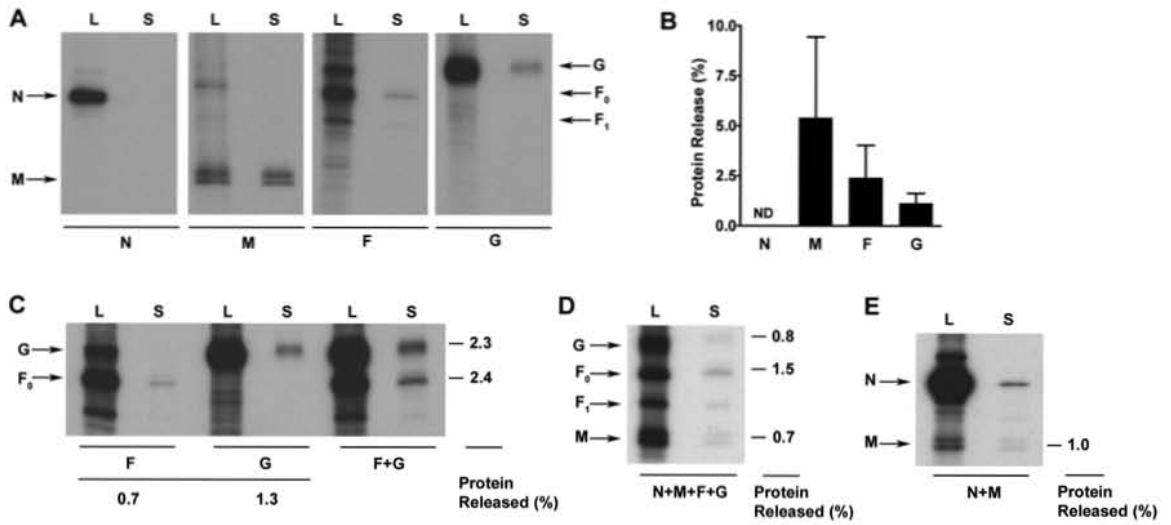
expression levels (data not shown). The quantification of envelope glycoprotein release revealed that approximately 11% of F and 5% of G was released when each was expressed alone (**Fig. 4C**).

NiV protein release and VLP production is not dependent on MVA co-infection.

Although less cytopathic than its wild-type parental strain, MVA does retain the ability to block host protein synthesis and otherwise interfere with normal cellular metabolism (85). To determine whether the protein release we observed was an accurate reflection of NiV biology or an artifact resulting from poxvirus infection, we employed a transfection plasmid-based expression system using the pCAGGS eukaryotic expression vector, which has also been used in other paramyxovirus VLP assays (31, 99, 116, 121, 123). The NiV N, M, F, and G genes were sub-cloned into the pCAGGS vector and expression was verified in separate experiments by immunoprecipitation (data not shown).

To determine whether the various NiV proteins produced by this method were also released from cells, cultures were transfected with individual plasmid constructs for 24 h, followed by metabolic labeling for another 20 h. Cells and culture supernatants were harvested and processed as described above and in the Methods chapter. We again observed membrane-associated release of M, F and G but no detectable release of N as predicted (**Fig. 5A**). Immunoprecipitation analysis of M expressed by plasmid-transfected cells consistently revealed a doublet of bands that were both released into the culture supernatant (**Fig. 5A**). When M was expressed by MVA, the doublet was usually only revealed by Western Blot (data not shown). We have been unable to determine the nature of the doublet, but it could reflect a post-translational modification of M.

Figure 5. NiV structural proteins are released in the absence of MVA. 293T cells were transfected with pCAGGS constructs containing the various NiV genes. **Panel A:** Proteins released into the supernatant were purified by gradient centrifugation as described in the Methods chapter. The proteins were immunoprecipitated with MAbs F45G6 (anti-N), F45G5 (anti-M) or rabbit polyclonal anti-serum against NiV F or HeV G, and analyzed by SDS-PAGE and autoradiography. **Panel B:** The proteins released in Panel A were quantified by densitometry. The means and standard deviations of three or more independent experiments are shown. ND = not detectable. Release of proteins from cells expressing combinations of F and G (**Panel C**) N, M, F, and G (**Panel D**) or N and M (**Panel E**) are shown along with the percent protein released. N was not immunoprecipitated in Panel D to allow for visualization of F₀. The quantification in Panel C was performed at a lighter exposure. Proteins derived from cell lysates (L) or culture supernatants (S) are indicated. Lysate bands represent 1/6 of the total lysate. Representative experiments are shown.



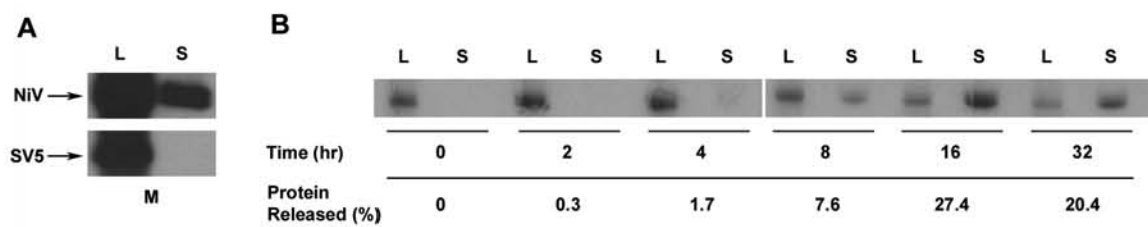
Although NiV M does contain a second potential AUG start codon 36 nt downstream of the first start codon (51), this does not account for the doublet appearance because a truncation mutant that begins at the second start codon, as well as HeV M, which lacks the second AUG codon, also appear as doublets (see Chapter 4). Quantification of protein release following plasmid system transfections revealed an overall reduction in protein release compared to that seen in the MVA system (**Fig. 5B**, compare with **Fig. 4**). Several studies have provided evidence for a physical interaction between paramyxovirus attachment and fusion proteins (77, 119, 141). For NiV F and G this interaction is apparent from their ability to be co-precipitated without cross-linking (Bossart and Broder, unpublished data). We, therefore, sought to determine the effect of F and G co-expression on their release. Under these conditions, the expression of F and G together resulted in greater release of both proteins together in comparison to expression of each protein individually (**Fig. 5C**). This observed increase of F and G release did not appear to be a result of increased protein expression or cell-surface expression (data not shown). We also noted that when N, M, F and G were all co-expressed using equivalent amounts of transfected plasmids, an overall reduction in protein release from cells occurred (data not shown). Indeed, in certain other recombinant VLP expression systems, the amounts of transfected plasmids have been adjusted to more accurately reflect or achieve cellular expression levels of the individual viral proteins produced using infectious virus (99, 116, 121). In an attempt to increase the amount of protein release in our system, we performed similar experimental variations in the amounts of transfected plasmids and estimated envelope glycoprotein expression in authentic NiV infection as one third of M expression and adjusted plasmid ratios accordingly (56, 117, 140). In additions, we

further reduced the transfected amount of plasmid containing N to 50 ng per well. However, even when the adjusted plasmid ratio was used, overall protein release remained low (**Fig. 5D**). We verified that the low level of protein release was not due to a reduction of protein expression due to multiple gene expression (data not shown); thus we interpret the reduction in protein release as indicative of a more organized assembly and budding process. In addition, the co-expression of N and M resulted in the release of N but with modest release of both proteins (**Fig. 5E**). The release of N was in agreement with our previous results obtained using the MVA expression system, which demonstrated that M facilitated the release of N. However, in contrast to the MVA expression system, we observed that N reduced overall M release. (**Fig. 5E**, compare with **Fig. 4A** and **B**).

Specific M release and kinetic analysis. To ensure that NiV M release was accomplished by a mechanism specific to itself, release of NiV M was again examined in parallel with SV5 M, which requires co-expression of N and one of the envelope glycoproteins in order to form VLPs that are released into the culture supernatant (116). **Fig. 6A** shows that analysis of culture supernatants revealed release of NiV M but no detectable release of SV5 M (**Fig. 6A**), which suggests that the observed release of NiV M was specific to its biological properties and not due to a non-specific mechanism such as cell lysis. In this respect, NiV M was similar to the M proteins of SeV, NDV, and hPIV1, all of which have been reported to form VLPs in the absence of other viral proteins (31, 99, 121, 123).

Figure 6. Comparison of NiV M release with SV5 M and kinetics of NiV M

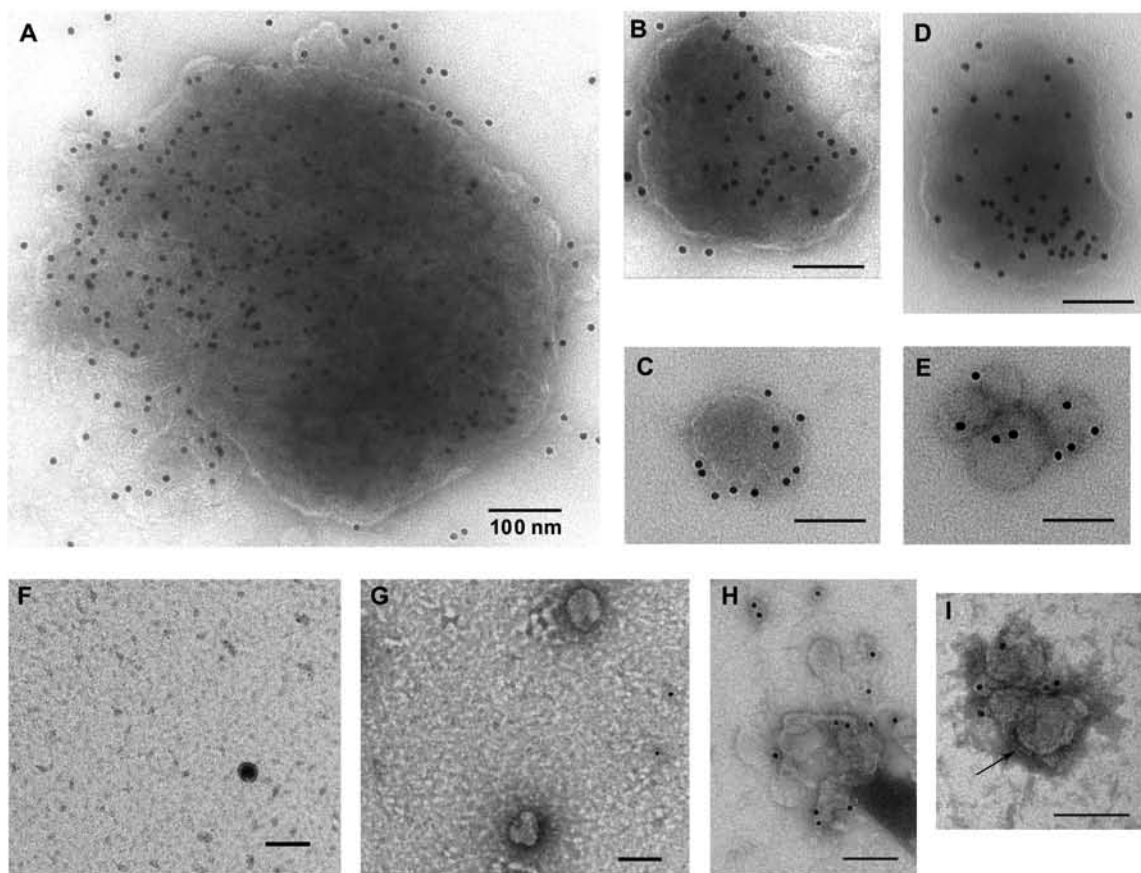
release. Panel A: Culture supernatants were analyzed for release of either NiV or SV5 M. Released protein was analyzed as described in the Methods chapter and immunoprecipitated using either rabbit anti-NiV polyclonal serum or MAb M-h (anti-SV5 M) followed by SDS-PAGE and autoradiography. The image is deliberately over-exposed to show the contrast between the two M proteins. **Panel B:** Cells expressing NiV M were starved for 45 min in met/cys-free medium, ³⁵S-met/cys-metabolically pulse-labeled for 15 min, then chased with complete medium for the indicated time intervals. Proteins from the lysates or supernatants were then immunoprecipitated with MAb F45G5 and analyzed by SDS-PAGE followed by autoradiography. The percentages of protein released were determined by densitometry. Proteins derived from cell lysates (L) or culture supernatants (S) are indicated. Lysate bands represent 1/6 of total lysate.



We also wanted to explore the kinetics of M expression and its eventual release from cells in order to determine the temporal progression of M release. For this analysis, plasmid-transfected cells were starved for 45 min, ^{35}S -met/cys metabolically pulse-labeled for 15 min, and then chased for varying lengths of time up to 32 h. At each time point cells and supernatants were harvested. Vesicles released into the supernatant were purified by centrifugation through a 10% sucrose cushion followed by sucrose gradient flotation. M derived from supernatants or cell lysates was immunoprecipitated with a monoclonal antibody and visualized by SDS-PAGE and autoradiography. The percentage M protein release was quantified by densitometry. The presence of membrane-associated protein in the supernatant was barely detectable at 2 h with 0.3% release, but then readily detected at 4 h with 1.7% release (**Fig. 6B**). Maximum M release of 27.4% was observed by 16 h.

Electron microscopy analysis of VLPs. The biochemical analysis of the NiV proteins released from expressing cells in a membrane-associated manner suggested that VLPs were being generated. To analyze the released material visually, VLPs were prepared and isolated by sucrose gradient flotation. VLPs from the resulting fractions were adsorbed to copper grids and immunolabeled using antibodies against NiV M or HeV G followed by a secondary antibody conjugated to gold beads. After negative staining, the samples were examined by electron microscopy. Expression of NiV M alone resulted in the release of roughly spherical enveloped structures that varied in size from approximately 100 to 700 nm in diameter (**Fig. 7A-C**). Immunogold labeling, which was dense in some cases, revealed the presence of M. In addition, negative staining revealed

Figure 7. Immunoelectron microscopy shows particles consistent in size and morphology with authentic NiV virions. VLPs released from transfected 293T cells were purified by gradient centrifugation, labeled using immunogold techniques, negatively stained, and viewed by electron microscopy as described in Methods. VLPs were derived from cells that expressed M (**Panels A to C**) or N, M, F, and G (**Panels D to E, and I**). Immunolabeling against M was done using MAb F45G5 (**Panels A to D**) and G was detected with mouse anti-HeV G polyclonal serum (**Panels E and I**). VLPs shown in Panel I were derived from BSR T7/5 cells that were transfected with NiV genes in pMC03T7. The arrow indicates the presence of spikes. Vesicles derived from cells expressing GFP were not immunolabeled by Mab F45G5 (**Panel F**) or mouse anti-HeV polyclonal serum (**Panel G**). Representative background immunolabeling of samples from cells expressing M is shown (**Figure H**). Bars represent 100 nm.

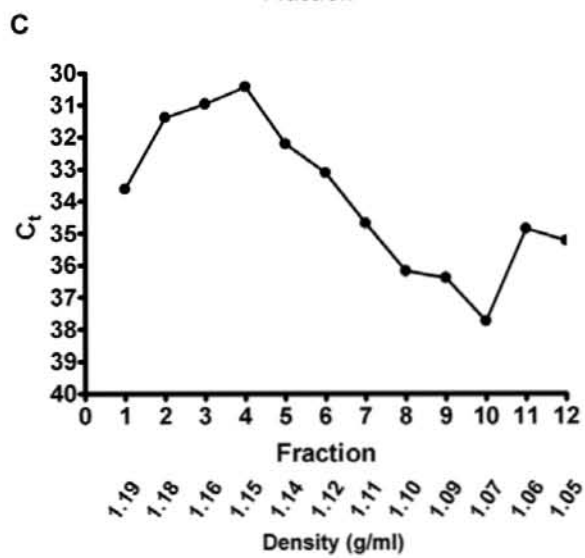
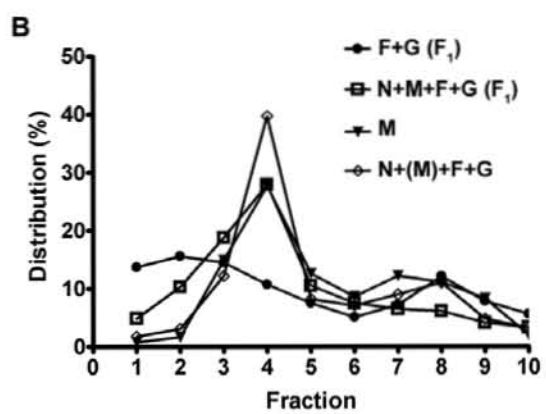
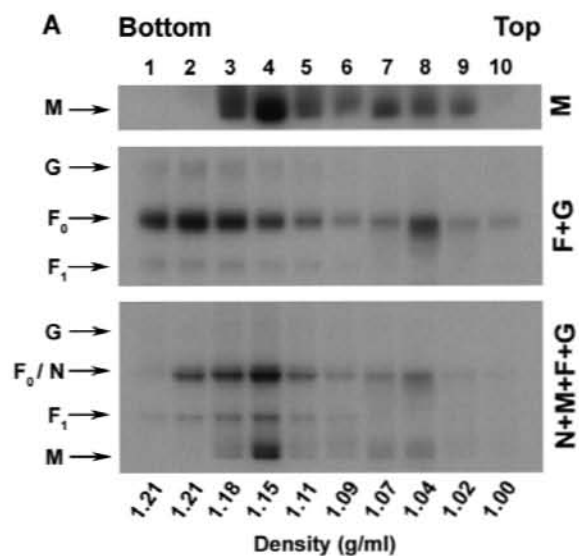


that some VLPs contained dense material of unknown composition. Expression of NiV N, M, F, and G resulted in similar results: release of VLPs with detectable M (**Fig. 7D**) or G (**Fig. 7E and I**) with a diameter of approximately 100 to 300 nm. Although immunogold labeling indicated the presence of G, spikes were occasionally visualized (**Fig. 7I**). This observation is in agreement with Goldsmith and co-workers, who reported that spikes on NiV virions were only occasionally prominent (45). The sizes of the VLPs observed are consistent with observations made of authentic NiV virions, which have been reported to range from 40 to 1900 nm (45, 62). The observed dense immunogold and negative staining was also similar to henipavirus virions [compare, especially, **Fig. 7A** with Fig. 1B and C in (62) and Fig. 1B in (45).] Although sporadic vesicles were observed from cells expressing green fluorescent protein (GFP) as a negative control, immunolabeling of the vesicles was not observed (**Fig. 7F and G**), which suggested specificity of the primary and secondary antibodies. Samples derived from cells expressing NiV M exhibited a low level of background immunolabeling; however, background immunolabeling was generally not associated with vesicles, and the occasional immunolabeling of questionable membranous structures contrasted with dense labeling of structures judged to be VLPs (**Fig. 7H**, compare with **A-D**).

Interaction between proteins during VLP formation. To further investigate the interaction of F and G with M during VLP release, we performed sucrose density gradient analyses to determine whether the buoyant density of released particles varied depending on the viral proteins present. M produced alone, F produced with G, or the combination of N, M, F and G were expressed in cells, metabolically labeled, and the

culture supernatants were harvested and layered onto 5-45% continuous sucrose gradients. After centrifugation, the gradients were fractionated and analyzed by immunoprecipitation and SDS-PAGE. The M protein was again recovered predominantly in fractions 3 to 5, corresponding to a density range of 1.11-1.18 g/ml (**Fig. 8A and B**). We noted that the M protein could also be found in less dense fractions, especially when it was expressed in the absence of any other viral proteins. When F was co-expressed with G, both proteins were recovered predominantly in fractions 1 to 3, which correspond to a density of 1.18-1.21 g/ml (**Fig. 8A and B**). However, the co-expression of N, M, F, and G led to a greater concentration of M in fraction 4 and, importantly, co-expression also resulted in a shift of the fractionation profile of F and G distribution to fractions 3 to 5 (**Fig. 8A and B**). This density range was also consistent with the previous results obtained using rMVAs (**Fig. 3C**). Further, sucrose density gradient analysis of authentic infectious NiV revealed peak virus concentration at a density of 1.15 g/ml, which corresponded well with our VLP results (**Fig. 8C**). Taken together, these findings suggest that although F and G can direct budding when produced alone, the co-expression of M facilitates F and G incorporation into VLPs with a density that is more consistent with that of an authentic virion.

Figure 8. Sucrose gradient density analysis of NiV VLPs. Panel A: Clarified culture supernatants from cells expressing different combinations of NiV proteins were layered onto 5-45% sucrose gradients and centrifuged. Fractions were immunoprecipitated with MAbs F45G6 (anti-N), F45G5 (anti-M) or rabbit polyclonal anti-serum against NiV F or HeV G, and analyzed by SDS-PAGE followed by autoradiography. A portion of each fraction was also used to determine density. Densitometry analysis of the autoradiographs shown in Panel A was used to determine the quantitative distribution of proteins shown in **Panel B**. Where more than one protein was expressed, the protein analyzed by densitometry is indicated by parentheses. **Panel C:** Supernatant from cells infected with NiV was layered onto a 5-45% sucrose gradient and centrifuged. RNA was extracted from fractions and used for real-time PCR. The threshold cycle (Ct) value was used as a proxy for virus concentration. The distribution and density of infectious NiV was determined in collaboration with Gary Crameri under appropriate biosafety containment (CSIRO Livestock Industries, Australian Animal Health Laboratory).



Discussion

The advent of reverse-genetics coupled with the *in vitro* techniques of VLP production has made it possible to examine the cell biology of viruses in increasing detail. However, certain highly pathogenic viruses such as the henipaviruses are restricted to BSL-4 containment, making such studies impractical, and in the absence of a henipavirus reverse-genetics system, there are considerable obstacles that inhibit the dissection of an individual protein's role(s) in virus particle formation. To circumvent some of these obstacles, we have established a VLP system to permit the investigation of NiV assembly and release. Our first attempt to produce VLPs utilized a recombinant poxvirus platform using MVA because of its high efficiency in gene delivery and expression and for its reduced level of cytopathic effect as compared to vaccinia virus. Further, poxviruses have been successfully employed in reverse-genetics systems and virus budding assays with success (30, 53, 54, 70, 130). Using rMVAs to deliver NiV genes, we observed membrane-associated release of M, F, and G. The ability of an M protein to be released from cells when expressed alone has also been observed for some other paramyxoviruses including SeV (121, 123), hPIV-1 (31), and NDV (99), as well as viruses in other related virus families including Ebola (5, 53, 92, 127) and VSV (54, 70, 74). In addition, Ciancanelli and Basler have recently independently reported that expression of NiV M leads to VLP formation (27). Release of F when expressed alone has been observed for SeV (121, 123), and release of HN has been noted for NDV (99). Ebola virus (5, 92, 130), VSV (82, 107), and rabies virus (82, 107) each contain a single envelope glycoprotein that can also direct budding of vesicles; thus our observation that NiV F and G can be independently released is not unprecedented. In contrast to these

other viruses, individual viral proteins expressed alone from SV5 are not released from cells, and particle formation requires the expression of M, N, and at least one envelope glycoprotein in order for any significant VLP release to occur (116).

Typically, viruses rescued using reverse-genetics techniques that employ vaccinia virus are subsequently purified from contaminating poxvirus and amplified by growth in cell culture. In such cases, the alteration of cellular metabolism by vaccinia virus is therefore of little concern because it is ultimately unimportant to the outcome. However, we were concerned that the effects of MVA infection might confound the interpretation of our VLP studies. Therefore, we employed a eukaryotic plasmid-based system as a means of gene expression in order to determine whether the results obtained using rMVAs faithfully reflected NiV biology.

When individual NiV proteins were produced in cells by transfection, M, F and G were each independently released into culture supernatants in a membrane-associated manner. In contrast, N was not detected in culture supernatants, as predicted, and these results were in agreement with those observations made using rMVAs. However, the percent of protein released was higher in the MVA system, which may reflect an effect of MVA on cellular metabolism or overall expression levels of the individual genes. When M was expressed in combination with various NiV proteins using rMVAs, we observed little change in M release, irrespective of which other NiV proteins were present. Expression of M with N enabled greater release of membrane-associated N, which is consistent with the model that M and N interact, and that this interaction facilitates the incorporation of the genome into budding virions (31, 32, 114). The dynamics of protein release were somewhat different when a plasmid-based transfection and

expression system was used. Under these conditions, we found that co-expression of M with N, or M with N, F and G lead to a reduction in M release. We obtained a similar result when F and M were co-expressed (data not shown). We also found that F and G co-expression led to greater release of both proteins than when either was expressed independently. Notably, in both the MVA and plasmid-based expression systems, we predominantly detected F₀ in both cell lysates and supernatants (**Fig. 3B** and **Fig. 5A, C-D**). In contrast, NiV virions appear to contain completely processed F (133). The reason for the difference in F processing is not known, but we and others have consistently observed greater levels of F₀ when recombinant expression systems are employed, which could bias its incorporation into particles (2, 13, 34). Alternatively, perhaps additional viral factors present during natural viral replication result in greater F processing or a biased incorporation of processed F.

The context-dependent variations in protein release and buoyant density suggest that the viral proteins interact either directly or indirectly to orchestrate the particle budding process. The differences observed in protein release, when a comparison is made between the transfected plasmid-based and rMVA systems, are likely a result of the alterations of cellular metabolism brought about by MVA infection. Although VLPs can be produced using either system, our results suggest that the two methods have different applications. We believe that the cell biology of NiV is more accurately reflected in the plasmid-based transfection system in the absence of poxvirus infection. This conclusion was reached because the MVA system has more efficient gene delivery and expression, and the percentage of viral protein released is greater. Thus, the MVA system is more useful when the number of VLPs is of primary importance. VLPs have been reported to

elicit a protective immune response against Ebola and Marburg viruses in animal models (122) and may serve as a more efficient method of NiV VLP production for immunization studies or perhaps as a potential livestock vaccine.

To ensure that NiV M was not released into culture supernatants by a non-specific means such as cell lysis, we assayed SV5 M in parallel as a control. As expected, we detected the release of M for NiV but not for SV5. However, SV5 M budding could readily be detected when it was co-expressed with its HN, F, and N genes (see Chapter 4). Pulse-chase analysis of NiV M expression revealed detectable release from expressing cells by 2 to 4 h with a maximal release of at least 27% by 16 h. This percentage of release is greater than that observed during standard budding assays, which were not performed as a pulse-chase. The percentages of protein release reported in our budding assays, as well as for SeV (121, 123) and SV5 (116) have been reported as non-pulse-chased systems. As a result, any nascent protein produced in the cell is included in the overall calculation. This method is useful as a relative measure between groups, but probably underestimates the true budding efficiency. Here, pulse-chase not only reveals the timing of release but also likely gives a more accurate picture of the kinetics of M production and its ultimate destination, release from producing cells.

Ultrastructural studies of NiV have revealed pleomorphic virions that range from 40-1900 nm (45, 62). In our studies, expression of M alone or along with N, F and G, resulted in VLPs containing the various proteins as shown by immunogold labeling and electron microscopy (**Fig. 7**). The VLPs ranged in size from approximately 100 to 700 nm, consistent with the range reported for live virus. Using both the MVA and transfection systems we observed NiV proteins migrating as membrane vesicles at a

density range of 1.11-1.19 g/ml. Authentic NiV migrated to a similar density range with peak detection at 1.15 g/ml. This range is consistent with the density of SeV and NDV VLPs as well as SeV virions (99, 121, 123). Paramyxovirus N proteins are known to assemble on cellular RNAs in the absence of genome, and these pseudo-RNPs can be incorporated into VLPs [see (116) and citations therein]. Based on the identical density distribution of NiV VLPs and live virus, we speculate that a similar process is likely occurring with the formation of NiV VLPs in the context of N expression in the present studies; however, we did not directly address whether the VLPs contained RNA. Using a plasmid transfection system we further evaluated the release of M alone, and with co-expression of N, F, and G. Although a greater percentage of M was detected in additional fractions when expressed alone, it was predominately concentrated in fractions 3 to 5 when co-expressed along with N, F, and G. Particles containing F and G migrated to denser fractions when additional NiV proteins were absent, but the position of both proteins in the gradient shifted to fractions 3 to 5 when M was present, suggesting that M interacts with F and G either directly or indirectly during assembly to facilitate the incorporation the envelope glycoproteins into the particles. The reason for the greater density of particles containing only F and G is unknown, but it is likely a reflection of altered lipid or protein incorporation relative to particle size. Taken together, the density and ultrastructural characteristics of the membrane-associated NiV proteins reported here are suggestive of authentic VLP formation.

Ciancanelli and Basler recently observed NiV VLPs when M was expressed alone or with envelope glycoproteins (27), which is supportive of our data. Although they did not perform quantitative analysis in their study, M release was apparently unaffected by

the presence of one or both of the envelope glycoproteins. As mentioned above, in our hands plasmid-based co-expression of M and F resulted in a distinct reduction in M release. This apparent discrepancy may be attributable to differences in the VLP purification techniques, especially our inclusion of an additional particle flotation step. Another difference between the two studies is our inclusion of the N protein, which was found to also reduce M release and this was not examined in the Ciancanelli and Basler report. VLP formation has been evaluated for other paramyxoviruses including SeV, hPIV-1, SV5, and NDV (31, 99, 116, 121, 123). Of these, only SV5, SeV, and NDV have been analyzed quantitatively. Two independent studies of SeV VLP formation reported that M and F can be released independently but that co-expression of M and F results in a greater release of each protein (121, 123). However, the percentage of protein released differed dramatically between the studies. Takimoto and co-workers (123) reported that approximately 50% of M was released. In contrast, Sugahara and co-workers (121) reported that 14.5% of M was released. Using avian cells and a pulse-chase system, Pantua and colleagues reported that NDV M is both necessary and sufficient for VLP release, with solo expression of NDV M resulting in 90% release efficiency (99). Whereas SV5 VLP release was most efficient (32% of M released) when N, M, F, and HN were expressed together (116), a decrease in M release was observed when the equivalent SeV or NDV proteins were co-expressed (99, 121). These results are comparable to our results observed with NiV N, M, F and G.

Sugahara and co-workers (121) have also shown that expression of the C protein with N, M, F, and HN leads to an increase in VLP release by 2- to 3-fold. This increase was subsequently shown to be due to the interaction of C with AIP1/Alix, a cellular

protein involved in multivesicular body formation; however an interaction between AIP1/Alix and measles C was not detected, suggesting that this mechanism of budding is not applicable to all paramyxoviruses (108). Nevertheless, this finding raises the possibility that additional NiV proteins not evaluated here may increase VLP release; however, additional experiments will be necessary to examine this premise. It is also important to recognize that because the various studies on several paramyxovirus VLPs each employed slightly differing methodologies in their analysis, the calculated percentage of released proteins among the various reports are not directly comparable. However, the qualitative differences observed between these viruses suggest that beneath the generalized model of paramyxovirus assembly and budding lay differences in the specific mechanisms employed, and these differences remain to be determined.

Chapter 4

Mutational analysis of *Nipah virus* matrix protein reveals a domain required for budding

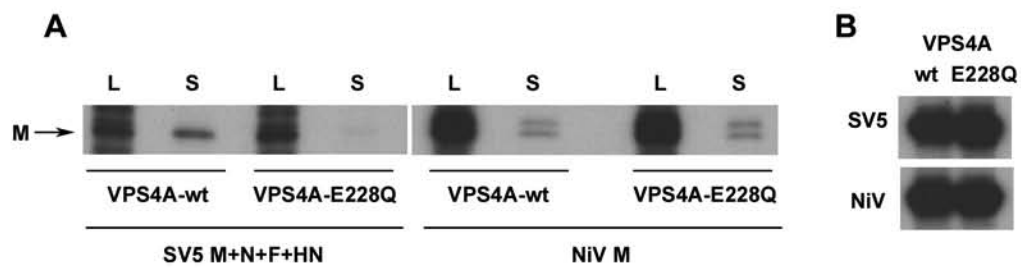
Introduction

As obligate cellular parasites, viruses have evolved many ways of exploiting cellular machinery to accomplish their own replication. In the past decade, it has become clear that some enveloped viruses use proteins involved in MVB formation as a means of accomplishing budding [reviewed in (6, 33, 84)]. The interaction between the viral M (or equivalent) protein and MVB proteins occurs via defined amino acid motifs located in the viral protein. These L-domains were first characterized among retroviruses (6, 33, 84); however the exploitation of MVB proteins was subsequently recognized to occur in the assembly and budding of members of other enveloped virus families including arenaviruses (102), filoviruses (53, 76), and rhabdoviruses (52, 54, 76). Based on the lack of any known L-domain motif in NiV (or HeV) M, and the taxonomical grouping of paramyxoviruses with filoviruses and rhabdoviruses into a common order, we hypothesized that NiV M contains a novel L-domain that is required for efficient budding. The subsequent identification of a novel L-domain in SV5 M (FPIV) (115), which is not present in NiV M, lent support to our hypothesis. We used the NiV M VLP budding assay as a tool for testing this hypothesis, and employed a combination of mutagenesis and perturbation of MVB machinery as strategies to identify the hypothesized L-domain.

Results

NiV M release is not dependent on VPS4A/B. As discussed earlier, the involvement of certain components of the cellular MVB machinery has been demonstrated in several other viral systems [reviewed in (6, 33, 84)]. A powerful technique that has helped facilitate the demonstration of these relationships has been the use of dominant-negative mutant versions of one or more of the protein components of the MVB complexes (33). Dominant-negative (DN) mutants of the paralogous multivesicular body (MVB) proteins VPS4A and VPS4B have been shown to impair release of most viruses that use a late budding domain (L-domain) to accomplish budding (84). To determine whether VPS4A has a functional role in NiV M VLP formation, we evaluated NiV M release in the presence of VPS4A-E228Q, a DN VPS4A mutant. SV5 VLP release, which is significantly reduced in the presence of DN VPS4A (115), was evaluated in parallel as a control. Cells were transfected with expression plasmids for SV5 proteins (M, N, F, and HN) or NiV M, along with 100 ng (per well) of plasmid containing Green Fluorescent Protein (GFP) fused to either wild-type or DN VPS4A. The quantities of the SV5 plasmids used were as described by Schmitt and co-workers (116) (N: 50ng; M: 0.4 µg; F: 0.75 µg; HN: 0.75 µg), and 0.4 µg (per well) of NiV M was used along with empty vector for equivalent total DNA. Culture supernatants were clarified and VLPs were centrifuged through a 10% sucrose cushion. Immunoprecipitation and SDS-PAGE analysis of the pellet revealed that SV5 VLPs (as indicated by M detection) were released in the presence of wild-type VPS4A, but not in the presence of DN VPS4A, as expected (**Fig. 9A**). In contrast, DN VPS4A had no effect on NiV M release (**Fig. 9A**). The

Figure 9. NiV M release is insensitive to VPS4A inhibition. Panel A: Cells were transfected with expression plasmids for SV5 N, M, F and HN, or NiV M, along with either wild-type or the dominant-negative VPS4A, followed by ³⁵S-metabolic labeling. Released protein was pelleted through 10% sucrose, as described in the Methods, and proteins derived from cell lysates (L) and culture supernatants (S) were immunoprecipitated with either rabbit anti-SV5 polyclonal serum or MAb F45G5 (anti-NiV M) and analyzed by SDS-PAGE followed by autoradiography. **Panel B:** Expression of VPS4A was detected in cell lysates from the material analyzed in Panel A by immunoprecipitation with rabbit polyclonal antiserum against GFP, followed by SDS-PAGE and autoradiography.



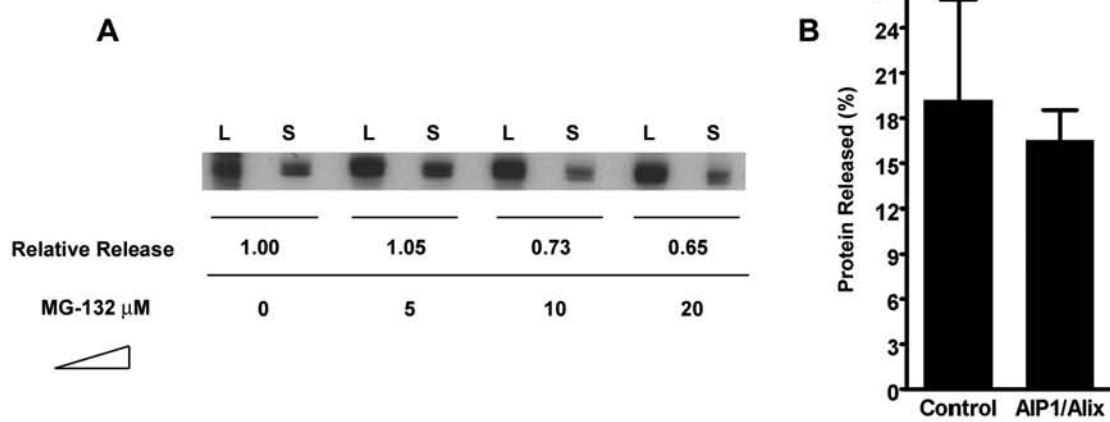
difference observed between SV5 and NiV M release was not due to unequal VPS4A expression, which was equivalent in each group (**Fig. 9B**). To determine whether NiV M release is dependent on VPS4B, cells were transfected with expression plasmids for NiV M along with either wild-type or DN VPS4A or VPS4B. In addition, to ensure that DN VPS4 proteins were not complemented by the cellular wild-type paralog, cells were transfected with either wild-type or DN VPS4A and VPS4B together. The total amount of transfected VPS4 plasmid (per well) was increased to 1 μg , as was the amount of NiV M plasmid, and culture supernatants were treated as before. Again, no effect of DN VPS4A on NiV M release was observed, with the same result for DN VPS4B (**Fig. 10A**). Importantly, no difference was observed when both DN VPS4A and DN VPS4B were expressed together (**Fig. 10A**). Since over-expression of wild-type VPS4 proteins can result in some reduction of virus or VLP release (40, 115), they are included as a control. Although wild-type VPS4B was not expressed to the same level as DN VPS4B (**Fig. 10B**), this does not affect the interpretation of the results because no further reduction of M protein release from cells expressing DN VPS4B was observed.

NiV M release is insensitive to proteasome inhibition and AIP1/Alix over-expression. Ubiquitin appears to play an important, though poorly defined role, in the budding of several viruses that possess an L-domain, including SV5 (33, 115). To determine whether NiV M protein release was dependent on ubiquitination, cells expressing NiV M were treated with increasing concentrations of the proteasome inhibitor MG-132, which depletes the available cellular ubiquitin (129), and VLPs were centrifuged through a 10% sucrose cushion and analyzed by immunoprecipitation and

Figure 10. NiV M release is insensitive to VPS4B inhibition. Panel A: Cells were transfected with the NiV M expression plasmid along with plasmids encoding wild-type or dominant-negative VPS4A and/or VPS4B. The released M protein was pelleted and processed as described in **Fig. 9A** and the Methods chapter. The proteins derived from cell lysates (L) and culture supernatants (S) were immunoprecipitated with MAb F45G5 (anti-NiV M) and analyzed by SDS-PAGE followed by autoradiography. **Panel B:** Expression of VPS4A and VPS4B was detected in parallel samples of cell lysates as in Panel A by immunoprecipitation with rabbit polyclonal antiserum against GFP or DsRed, followed by SDS-PAGE and autoradiography.



Figure 11. NiV M release is insensitive to proteasome inhibition and AIP1/Alix over-expression. Panel A: Cells expressing NiV M were treated with increasing concentrations of MG-132, as described in the Methods. The released protein was pelleted through 10% sucrose. Proteins derived from cell lysates (L) or culture supernatants (S) were immunoprecipitated with MAb F45G5 and analyzed by SDS-PAGE followed by autoradiography. The M protein release was quantified by densitometry and expressed as a ratio relative to the samples obtained from untreated cells in parallel. Lysate bands represent 1/6 of total lysate. **Panel B:** Cells were transfected with expression plasmids for NiV M, along with either AIP1/Alix or empty vector as control. The released protein was pelleted through 10% sucrose. Proteins were immunoprecipitated with MAb F45G5 (anti-M) and analyzed by SDS-PAGE followed by autoradiography and quantified by densitometry, as described in the Methods. AIP1/Alix expression was confirmed by immunoprecipitation with an anti-*myc* antibody (not shown). The mean and standard deviation of 3 independent experiments are shown.



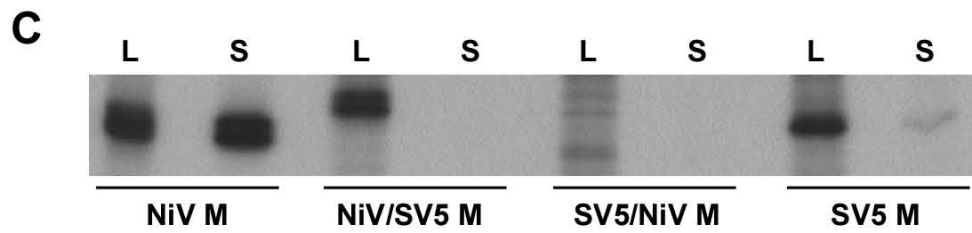
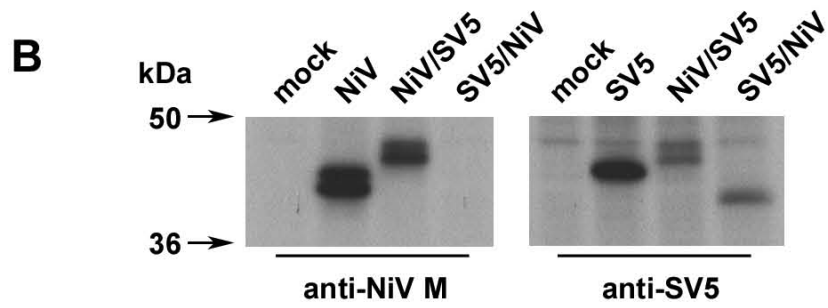
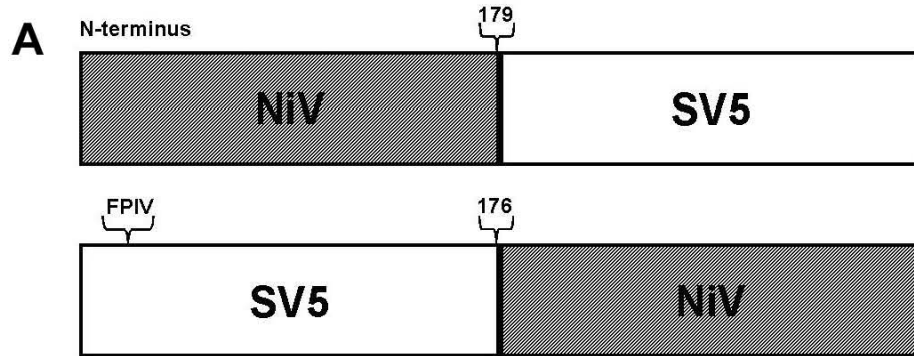
SDS-PAGE, followed by autoradiography. The quantification of the relative amounts of M protein release revealed that increasing concentrations of MG-132 had a modest decreasing effect on its release, with only a 35% reduction with a 20 μ M MG-132 concentration (**Fig. 11A**). In contrast, Schmitt and co-workers (115) reported that SV5 VLP release was reduced by 91% at 10 μ M. The insensitivity of NiV M release to proteasome inhibition suggests that ubiquitin plays a minor role, if any, in NiV M release.

As discussed earlier, the cellular protein AIP1/Alix is a component of the MVB machinery that facilitates budding of the retroviruses equine infectious anemia virus (EIAV) and human immunodeficiency virus (HIV-1) (21, 38, 79, 87, 120, 131), as well as the paramyxovirus SeV (108). Over-expression of AIP1/Alix has been shown to enhance SeV budding (108) and HIV-1 VLP (120) release, but decrease EIAV release (21). As a consequence of these observations, we sought to determine whether AIP1/Alix might play a role in NiV M protein release. Cells were transfected with the pCAGGS NiV M expression plasmid along with either a plasmid encoding a *myc*-tagged AIP1/Alix protein or an empty plasmid vector as a control, and the resulting released M protein was purified and recovered by centrifugation through a 10% sucrose cushion, and analyzed by immunoprecipitation, SDS-PAGE and autoradiography as described earlier. We found that over-expression of AIP1/Alix had no effect on NiV M protein release, suggesting that M is released by a mechanism clearly independent of AIP1/Alix (**Fig. 11B**).

NiV-SV5 M chimeras are not released. In spite of the fact that SV5 M possesses an L-domain (115), as discussed earlier, it is not released from cells when expressed alone, and

SV5 M protein requires the additional co-expression of viral N and at least one of the two viral envelope glycoproteins to produce VLPs (116). However, in contrast, we have shown that NiV M protein is released when expressed alone [see Chapter 3, (100)], and this finding was recently confirmed by others (27). The independent ability of M protein release (budding) is a property shared by some other paramyxoviruses including SeV (121, 123), hPIV-1 (31), and NDV (99). Although exceptions exist, the transferability of L-domain activity is considered to be one of the inherent characteristics of L-domains (33). We therefore hypothesized that the determinant of the budding ability of NiV M is localized to a protein domain that could be transferred to an M protein of a virus that did not possess intrinsic budding activity (SV5), and that such a domain might represent a novel L-domain. To test this hypothesis, we first constructed reciprocal chimeras of NiV and SV5 M with the chimeric junction located in approximately the middle of the molecule following a well-conserved amino acid sequence (**Fig. 12A**). Expression and detection of the chimeric proteins was verified by radioimmunoprecipitation, SDS-PAGE and autoradiography. The SV5/NiV chimera was not expressed to the same level as either of the wild-type M proteins or the NiV/SV5 chimera. Both chimeras migrated at a slightly higher (NiV/SV5) or lower (SV5/NiV) apparent molecular weight than the wild-type proteins (**Fig. 12B**). In each case, the M protein released into the supernatant was purified through a 10% sucrose cushion and analyzed by immunoprecipitation, SDS-PAGE and autoradiography. Although NiV M protein release was readily detected, along with a low level of SV5 M release, no release of either chimera was detected (**Fig. 12C**), which suggested that the budding property of NiV M might not be localized to a single

Figure 12. NiV and SV5 M protein chimeras are not released. Panel A: a cartoon representation of chimeric NiV and SV5 M proteins. At the chimera junction, the amino acid position relative to the N-terminal portion of the protein is indicated. The approximate location of the known SV5 L-domain (FPIV) is indicated. **Panel B:** Cells expressing NiV M, SV5 M, or the chimeric proteins illustrated in Panel A were metabolically labeled, and cell lysates were immunoprecipitated with antibodies against NiV M (F45G5) or SV5 (whole-virus antiserum). Precipitated proteins were analyzed by SDS-PAGE and autoradiography. **Panel C:** Cells expressing NiV M, SV5 M, or the chimeric proteins were metabolically labeled and the culture supernatants were centrifuged on 10% sucrose as described in Methods. Proteins derived from cell lysates (L) or culture supernatants (S) were immunoprecipitated with antibodies against NiV M or SV5 and analyzed by SDS-PAGE followed by



transferable domain. However, recent studies by others suggested that L-domain motifs may be sensitive to the surrounding context (33, 67). Alternatively, the proteins may be conformationally altered in such a way as to negate proper association with the cellular factors involved in biologically relevant budding.

The NiV M N-terminus is dispensable for budding. NiV and HeV M are 89 percent identical at the amino acid level (133), which suggested to us that HeV M, like NiV M, could be released from cells in a membrane-associated manner. Indeed, when HeV M was expressed alone, we did observe membrane-associated release as determined by sucrose gradient flotation, immunoprecipitation and SDS-PAGE. However HeV M release was consistently much less efficient than NiV M protein with comparative values ranging from 50-75% of the value of NiV M protein release (data not shown). We noted, that with the exception of the initiating methionine residue of the two M proteins, the N-terminal 13 amino acids of the NiV and HeV M proteins have no sequence identity and constitute approximately one-third of the amino acid differences between the two proteins (**Fig. 13**). We hypothesized that a sequence unique to the NiV M N-terminus might be responsible for the greater efficiency of NiV M protein release, and that this sequence might constitute an L-domain. To determine whether the N-terminus was responsible for the difference in observed release efficiency, chimeric M genes were constructed that contained the N-terminal sequence of NiV or HeV M (including residues 1 through 59), combined with the remainder of the sequence derived from their heterotypic counterpart (NiV/HeV M and HeV/NiV M, respectively). Although

Figure 13. Alignment of the NiV and HeV M proteins. Amino acid alignment of NiV and HeV M is shown with non-identical residues shaded. Alignment was done using the Jalview multiple alignment editor, as described in the Methods.

NiV 1 MEPDIKSISSESEMEGVSDFSPTSWEHGGYLDKVEPEIDENGSMIPKYKIYTPGANERKY
 HeV 1 MDFSVDNLDGPIEGVSDFSPTSWEHGGYLDKVEPEIDKHGSMIPKYKIYTPGANERKF

NiV 60 NNYMYLICYGFVEDVERTPETGKRKKIRTAAYPLGVGKSASHPQDLLEELCSLKVTVR
 HeV 60 NNYMYMICYGFVEDVERSPESGKRKKIRTAAYPLGVGKSTSHPQDLLEELCSLKVTVR

NiV 119 RTAGSTEKIVFGSSGPLNHLVPWKKVLTSGSIFNAVKVCRNVDQIQLDKHQALRIFFLS
 HeV 119 RTAGATEKIVFGSSGPLHLLPWKKILTGGSIFNAVKVCRNVDQIQLEKQQLRIFFLS

NiV 178 ITKLNDSGIYMIPTMLEFRRNNAIAFNLLVYLKIDADLSKMGIQGSLDKDGFKVASFM
 HeV 178 ITKLNDSGIYMIPTMLEFRRNNAIAFNLLVYLKIDADLAKAGIQGSFDKDGTKVASFM

NiV 237 LHLGNFVRRAGKYYSVDYCRRKIDRMKLQFSLGSIGGLSLHIKINGVISKRLFAQMGFQ
 HeV 237 LHLGNFVRRAGKYYSVEYCKRKIDRMKLQFSLGSIGGLSLHIKINGVISKRLFAQMGFQ

NiV 296 KNLCFSLMDINPWLNRLTWNNSCEISRVAAVLQPSIPREFMIYDDVFIDNTGRILKG
 HeV 296 KNLCFSLMDINPWLNRLTWNNSCEISRVAAVLQPSVREFMIYDDVFIDNTGKILKG

HeV/NiV M was readily expressed and detected, we were unable to detect expression of the original NiV/HeV M chimeric protein (data not shown). Therefore, a second NiV/HeV M gene was constructed that encoded the first 13 amino acids of NiV M, with the remainder derived from HeV M. We confirmed expression of this alternate NiV/HeV M protein (data not shown) and used it in subsequent experiments. As a result, HeV/NiV M contained an additional 5 HeV-derived amino acids beyond the N-terminal 13 amino acids, and therefore the chimeras were not exactly reciprocal (**Fig. 14A**, compare with **Fig. 13**). Expression of the chimeric proteins and analysis of culture supernatants by centrifugation through 10% sucrose followed by immunoprecipitation and SDS-PAGE showed that the N-terminus determined whether chimera release efficiency was like that of NiV or HeV M (**Fig. 14B**).

To further characterize the NiV M N-terminal sequence, stretches of 4 amino acids were mutated to the cognate HeV sequence, and an additional mutant was constructed by removing the first 12 amino acids of NiV M so that translation would begin at the second methionine (**Fig. 14C**). The release of the various mutant M proteins was analyzed as before. M mutants NiV/HeV 2-5 and NiV/HeV 6-9 were released with similar efficiency as wild-type NiV, while in contrast NiV/HeV 10-13 was expressed and released poorly (**Fig. 14D**). Notably, however, the NiV M Δ 1-12 protein was released with an efficiency that was comparable to, or even slightly better than, wild-type NiV M (**Fig. 14D**). This latter result clearly demonstrated that the N-terminal 12 amino acids are dispensable for NiV M protein release, and further indicated that any hypothesized L-domain is likely not located within this N-terminal amino acid stretch. However, the N-terminal amino acids were influencing the observed difference in HeV and NiV M

Figure 14. NiV M protein N-terminus is dispensable for budding. Panel A:

Shown is a cartoon representation of the chimeric NiV and HeV M proteins. At the chimera junction, the amino acid position relative to the N-terminal portion of the protein is indicated. **Panel B:** N-terminal chimeras of NiV and HeV M were constructed as depicted in Panel A and expressed in cells. The released proteins were pelleted through 10% sucrose and proteins derived from the cell lysate (L) and culture supernatant (S) were immunoprecipitated with rabbit polyclonal antiserum raised against NiV and analyzed by SDS-PAGE followed by autoradiography. **Panel C:** Mutant NiV M genes were constructed such that groups of 4 amino acids (underlined) were changed to the HeV sequence. In addition, the first 12 amino acids were deleted (dashes) from NiV M. **Panel D:** The mutant proteins illustrated in Panel C were expressed in cells, as well as wild-type NiV and HeV M proteins. The released proteins were processed and analyzed as in Panel B. Proteins were immunoprecipitated using either MAb F45G5 (anti-NiV M) or rabbit polyclonal antiserum against NiV and analyzed by SDS-PAGE followed by autoradiography.

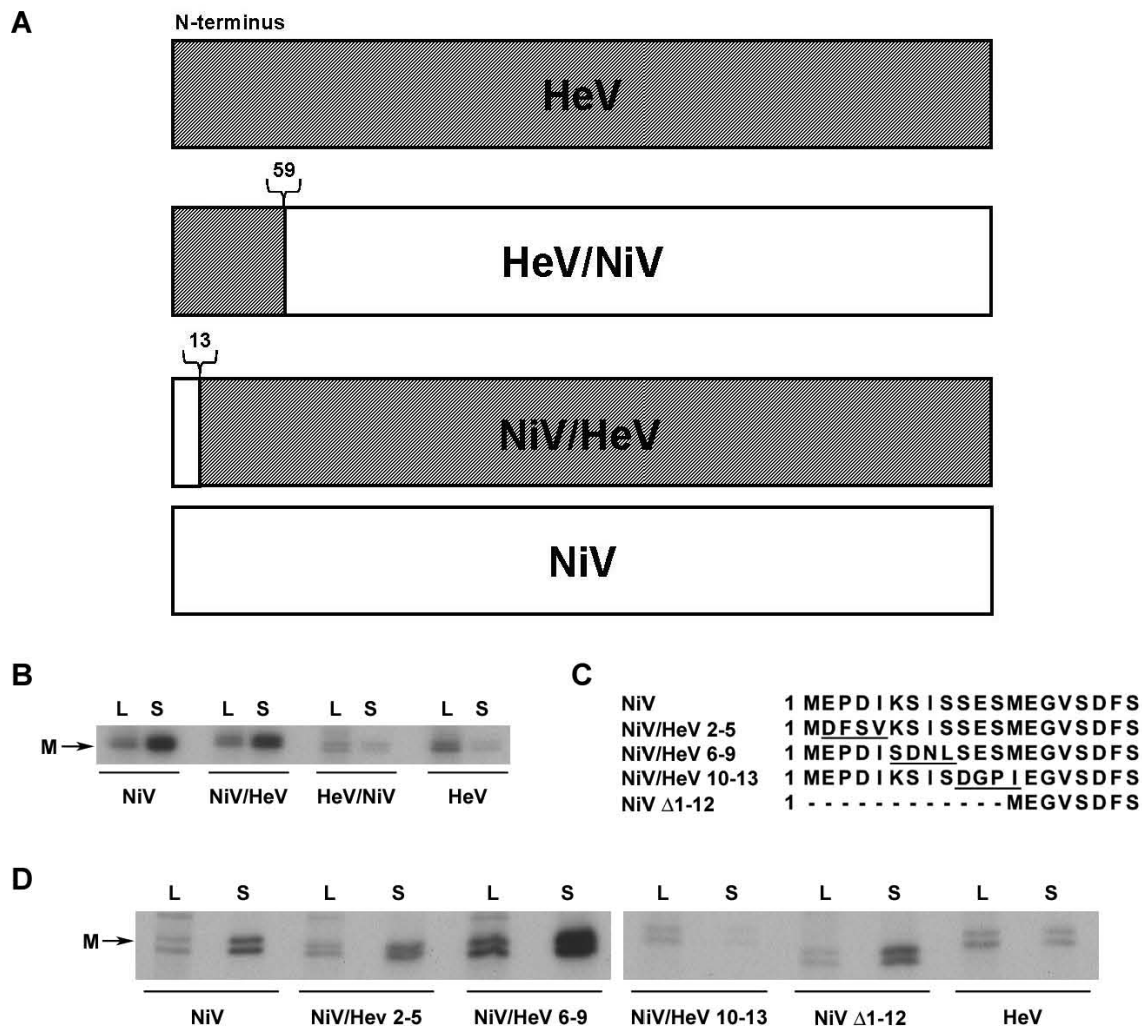
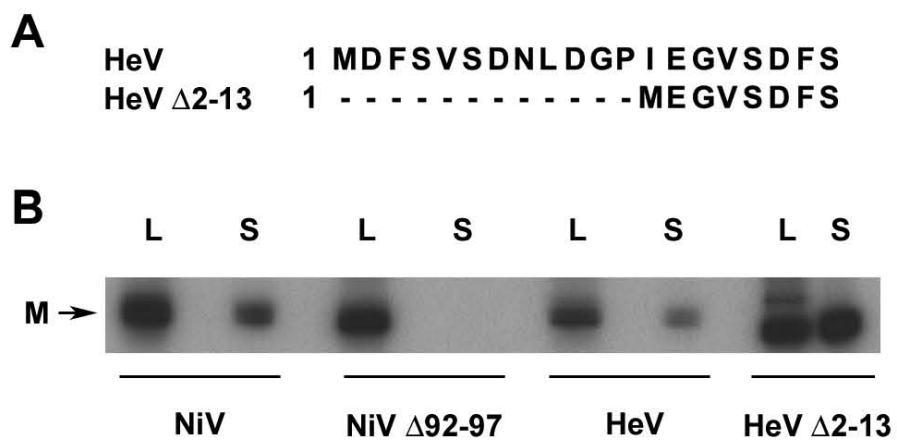


Figure 15. The N-terminus of HeV M confers a decrease in release. Panel A:

HeV M amino acids were deleted (dashes) such that the mutant N-terminus is identical to NiV M Δ 1-12, shown in **Fig. 14C**. **Panel B:** Wild-type HeV M and the mutant illustrated in Panel A were expressed in cells and released protein was pelleted through 10% sucrose. Budding controls NiV M (positive) and NiV M Δ 92-97 (negative) were included in parallel. Proteins were immunoprecipitated using either MAb F45G5 (for NiV) or rabbit polyclonal antiserum raised against NiV (for HeV) and analyzed by SDS-PAGE followed by autoradiography.



release efficiency, although the NiV sequence did not increase NiV M protein release. These observations suggested that the N-terminal amino acids of HeV M protein might be contributing to the observed decrease in the release efficiency of HeV M. To test this hypothesis, amino acids 2-13 of HeV M were removed (**Fig. 15A**), and this mutant, HeV M Δ 2-13, was tested for release and compared with wild-type HeV M. Wild-type NiV M and NiV M Δ 92-97 (see below) were included as positive and negative controls. In agreement with our hypothesis, HeV M Δ 2-13 was in fact released into the supernatant with 2-fold greater efficiency than wild-type HeV M (**Fig. 15B**). The mechanism underlying this restriction of the budding process of the natural N-terminal sequence of HeV M is unknown.

Mutation of YPLGVG sequence abrogates NiV M budding. All L-domains described to date contain one or more proline residues. Because the NiV M protein does not contain any of these exact L-domain motifs, we examined the entire M protein sequence for proline residues with surrounding amino acids that we considered to be similar to known L-domains. Following this analysis, we identified 3 sequences of interest and subsequently carried out a mutagenesis strategy whereby the proline residues within these putative motifs were changed to alanine (**Fig. 16A and B**). The residue P35 was targeted because it aligned closely to the SV5 FPIV (\emptyset PxV) motif, although there were no further sequence similarities. The P93 is located in a sequence similar to the YP(x)_nL motif, and the P329 and P332 residues were targeted because of sequence similarity to the P(T/S)AP motif. It was also noted that P93, P329 and P332 are all well conserved among

Figure 16. Site-directed proline mutagenesis. Panel A: ClustalW alignment of the M proteins from Nipah virus (NiV), Hendra virus (HeV), Tupaia paramyxovirus (TPMV), measles virus (MeV), Newcastle disease virus (NDV), and simian virus 5 (SV5). Sequences of interest are boxed. Alignment was performed as described in the Methods. **Panel B:** Known L-domains are shown along with corresponding hypothetical L-domain sequences of NiV M (boxed in A). Underlined prolines were mutated to alanine. **Panel C:** Mutant NiV M proteins, along with wild-type, were expressed in cells and released protein was pelleted through 10% sucrose. Proteins derived from the cell lysate (L) or culture supernatant (S) were immunoprecipitated using MAb F45G5 and analyzed by SDS-PAGE followed by autoradiography as described earlier and in the Methods chapter.

A

```

NiV      1 MEPDIKSISSSEMEGVS-DFSPSSWEHGGYLDKVEPEIDENGSMIPKYKIYTPGANERKYNMYMLICYGFVEDVERTPETG
HeV      1 MDFSVDNLDGPIEGVS-DFSPTSWENGGYLDKVEPEIDKHGSMIPKYKIYTPGANERKFNNYMYMICYGFVEDVERSPESG
TPMV     1 MYPSAPRIDEAPVVDCEYEFIPPTWLEKGYLSAMKVESDHNGKIIPSVRVVNPWGGERKTSGYMYLIMHGIYEDVPKDGDE
MeV      1 -----MTEIY-DFDKSAWDIKGSIAPIQPTTYS DGRLVPQVRVIDPGLGDRKDECFMYMFLGLGVVDES DPLGPP-
SeV      1 -----MADIY-RFPKFSYEDNGTVEPLRLRTGPDKKAIPHIRIVKVGDPKPKHGVRVLDLLLLGFFETPKQTASLG
NDV      1 -----MSSRTIGLYFDSAHSNLLAFPIVLQDTGGGKKQIAPQYR IQRLLDWTDSKEDSVFITTYGFI FQVGN EATV
SV5      1 -----MPSISIPADPTNPRQSIKAFPIVINSDDGGEKGRVLVQLRTTYLNDLDTHEPLVTFINTYGF IYEQDRGNTIV

NiV      82 -----KRKKIRTIAAYPLGVGKKSASHPQDLLEE LCSLKVTVRRTAGSTEKIVFGSSGPNLHLLVPPWKKVLTSGSIFNAVK
HeV      82 -----KRKKIRTIAAYPLGVGKKSASHPQDLLEE LCSLKVTVRRTAGSTEKIVFGSSGPNLHLLVPPWKKVLTSGSIFNAVK
TPMV     83 -----QRYSGKTYAAYPLGVGKKSATPDDL TSMNKLOITVRRTAGAGERIVFGNNAPL GALFPWRRVLD FGA VFTAYK
MeV      69 -----IGRAFGLPLGVGRSTAKPEELLKEATELDIVRRTAGLNEKLVFYNNPTLTLTPWRKVLTTGVSFNANQ
SeV      70 SVS DLT EHTGYSICGSGSLPIGVAKYHGSDQELLKACTDLRITVRRTRV RAGEMIYVMVDSIGAPLLPWSGR L RQGMIFNANK
NDV      76 G--IIDDKPKRELLSAAMLCLGSLVPNTGDLELARACLMMVTCKKSATNTERMVFSVVQAPQVLQSCRVVANKYSSVNAVK
SV5      73 G--EDQLGKKREAVTAAAMVTLGCGPNLPSLGNVLGQLRE FQVTVRKTSSKAEMEVMFIVKYPRI FRGHTLIQKGLVCSVAEK

NiV      156 VCRNV DQIQLDKHKQALRIFFLSITKLNDSGIYIMPRTMLEFRRNNAIAFNLLVY LKIDADLSKMGIQGSLDKDGFK--VASF
HeV      156 VCRNV DQIQLEKQQLRIFFLSITKLNDSGIYIMPRTMLEFRRNNAIAFNLLVY LKIDADLAKAGIQGSDKDGTK--VASF
TPMV     157 VCLSVESISLFTPQRFRLFLTVTLTLDNGLYKAPSLFADFRASKAVSFNLLARLTVNNKSGKDYLATAPASDTKQ--VVSF
MeV      140 VCN AVNLIPLDTPQRF RVVYMSITRLSDNGYITVPRRMLEFRSVNAVAFNLLVTLRIDKAI GPGKI IDN--AEQLP--EATF
SeV      152 VALAPQCLPVDKDIRFRVVFVNGTSLGAIITIAKIPKTLADLALPNSIVSNLLVTLKTGISTEQKGVLPVLDQDQGEK--KLN F
NDV      156 HVK APEKIPGSGTLEYKVN FVSLTVVPK KD VYKIPAAV LKISGSSLYNLALNVTINVEVDPRSPLVKLSKSDSGY--YANL
SV5      153 FVKS PGKIQSGMDYLFIP TFLSVTYCPAAIKFQVPGPMLKMSRYTQSLQLLELMIRILCKP DSPLMKVHTPDKEGRGCLVSV

NiV      236 MLHLGNFV--RRAGKYYSVDYCRRKIDRMK LQFSLGSI GGLSLHIKINGVISKRLFAQMGFQKNLCFSLMDINPWLNR L TWN
HeV      236 MLHLGNFV--RRAGKYYSVEYCRRKIDRMK LQFSLGSI GGLSLHIKINGVISKRLFAQMGFQKNLCFSLMDINPWLNR L TWN
TPMV     237 MVHIGNFV--RKGGDVYSNSYCKKKIDRM D LQFALGAVGGLSFHIKINGKMSKTLMTQLGFHRNLCYSIMDINPDLNKKIWN
MeV      218 MVHIGNFR--RKKSEVYSADYCKMKIEKMG L VFALGGIGGTSLHIRSTGKMSKTLHAQLGFKKTLCYPLMDINEDLNRLLWR
SeV      232 MVHLG LIR--RKVKIYSVEYCKSKIERMRLIFSLGLIGGISFHVQVTGTL SKTFMGQLAWKRAVCFPLMDVNP H MNLV IWA
NDV      236 FLHIGLMTTVDRKGGKVTFDKLEKKIRSLDLSVGLSDV LGPSVLVKARGARTKLLAPFFSSSGTACYP IANASQVAKI LWS
SV5      235 WLHVCNIFKSGNKNGSEWQEYWMRKC ANMQLEVISADMWGPTIIHARGHIPKSAKLF FGGKGGWSCHP LHEVVVSVTKTLWS

NiV      316 NSCEISRVAAVLQPSIPREFMIYDDVFI DNTGRILKG-----
HeV      316 NSCEISRVAAVLQPSVPREFM IYDDVFI DNTGKILKG-----
TPMV     317 SSCRITSVAAI LQPSVSKDFKIYH D VFI DNTGKIMG-----
MeV      298 SRCKIVRIQAVLQPSV P QEFRIYDDVI I NDDQGLFKVL-----
SeV      312 ASVEITD VDAVFPAPIPRDFRYYPNVVAKNIGRI RKL-----
NDV      318 QTA CLR SVKIIIQAGTQRAVAVTADHEVTSTKLEKHTLAKYNPFKK-----
SV5      317 VGCEITKAKAI IQESSISLLVETTDIISP KVKISSKHRRFVKS NWGLFKKTKSLPNLTELE

```

B

L-domains	NiV M Sequences
ØPxV	29 YLDKVEPEID
YP(x) _n L	92 YPLGVG
P(T/S)AP	329 PSIP

C

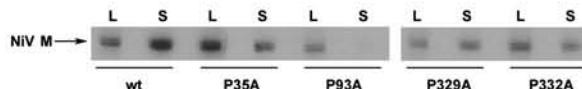
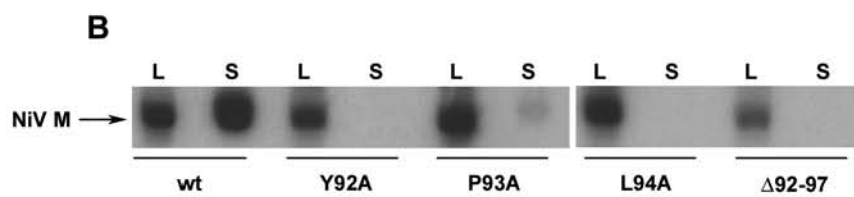


Figure 17. NiV M sequence required for budding and possible late domain

element. Panel A: NiV M mutants were constructed with single alanine substitution mutations in the YPLGVG sequence (underlined), or with the whole sequence deleted (dashes). **Panel B:** Wild-type NiV M and the mutants depicted in Panel A were all expressed in cells and released protein was pelleted through a 20% sucrose cushion. Proteins derived from the cell lysate (L) or culture supernatant (S) were immunoprecipitated with MAb F45G5 and analyzed by SDS-PAGE followed by autoradiography.

A

NiV M	TIAAY <u>PLGVG</u> KSAS
Y92A	APLGVG
P93A	YALGVG
L94A	YPAGVG
Δ 92-97	-----

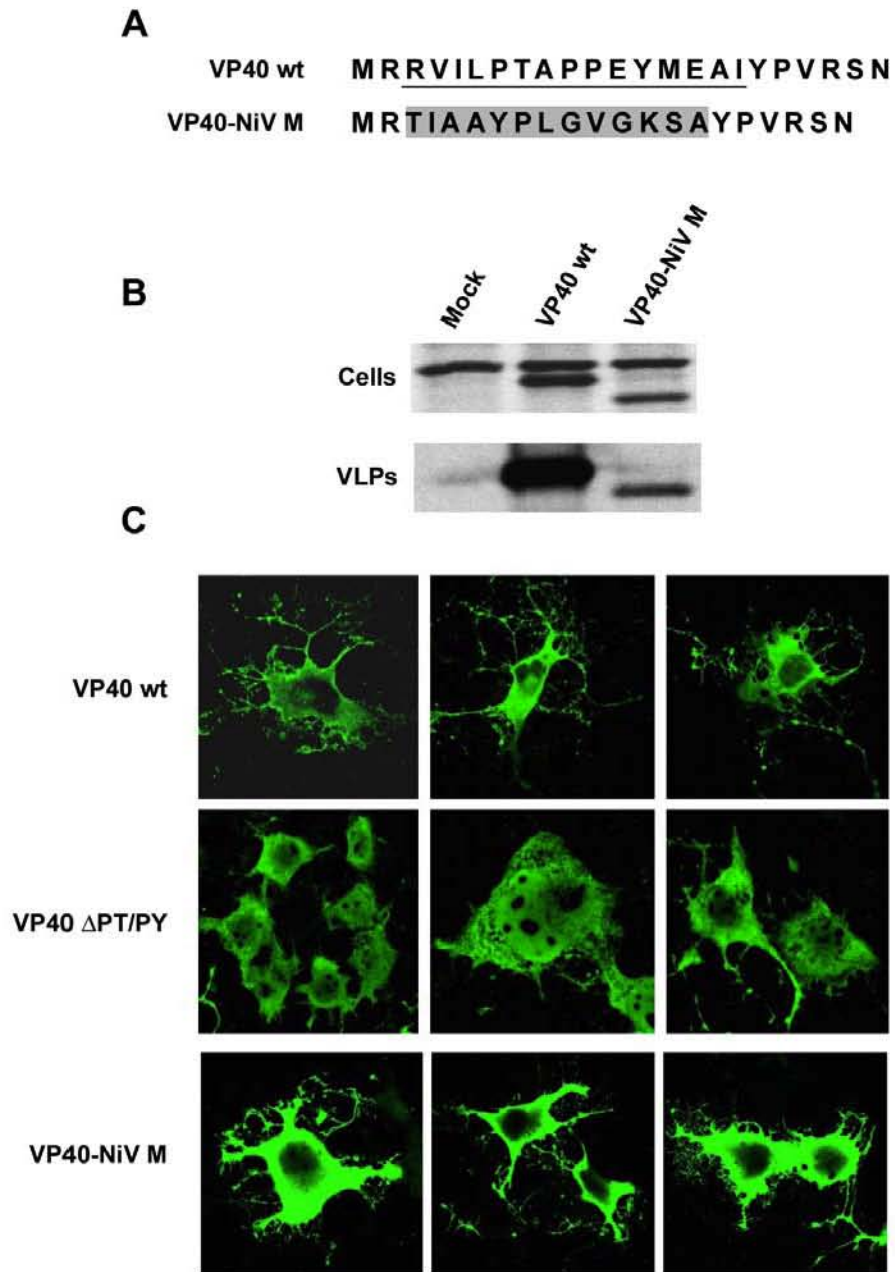


paramyxovirus M proteins but are absent in SV5 M (**Fig. 16A**), which further suggested that these proline residues might be part of an L-domain.

The mutant M gene cassettes were expressed in cells and pelleted through a 10% sucrose cushion and analyzed by immunoprecipitation and SDS-PAGE followed by autoradiography. The result of this comparison revealed that each of the mutant M proteins retained budding ability except for the P93A mutant, which exhibited a marked reduction in M protein release (**Fig. 16C**). The P93 residue is part of an amino acid sequence (YPLGVG) that resembles the YP(x)_nL motif and also contains residues that are well conserved among paramyxovirus M proteins (**Fig. 16A**). To confirm this important observation and further characterize the role of this sequence in M protein release, a series of additional M mutants was constructed: Y92A, L94A, and Δ 92-97 (**Fig. 17A**), that were then tested in the budding assay. The result of this experiment revealed that none of the additional mutant M proteins, with the exception of the P93A mutant, which retained a low level of budding activity, were released from expressing cells (**Fig. 17B**). All of the mutants expressed at levels similar to wild-type NiV M, and these findings confirm the importance of this motif.

As discussed earlier, one notable feature of most viral L-domain motifs is their inherent ability to be transferable to other M proteins defective in budding (33, 68, 115). Therefore, we sought to determine whether this newly identified NiV M sequence could impart budding activity within the context of a different viral background. Using the Ebola VP40 protein in which its native overlapping L-domain motifs, the PTAPPEY sequence, are deleted, thus rendering the protein defective in release (76), we inserted the NiV M protein YPLGVG motif (**Fig. 18A**) and then tested whether budding activity was

Figure 18. NiV late domain can rescue Ebola VP40 budding. **Panel A:** The L-domain and flanking sequence of VP40 (underlined) was replaced with a sequence derived from NiV M (shaded) containing the YPLGVG sequence. **Panel B:** 293T cells were transfected with plasmids containing Ebola GP along with either wild-type VP40 or VP40-NiV M for 20 h and then ^{35}S labeled for 5 h. Culture supernatants were clarified and VLPs were centrifuged through 20% sucrose. The proteins were immunoprecipitated with an antibody against VP40 and analyzed by SDS-PAGE and autoradiography. **Panel C:** COS-1 cells were transfected with plasmids encoding VP40 wt, VP40 $\Delta\text{PT/PY}$, or VP40-NiV M. Cells were fixed 20-24 h post-transfection, permeabilized, and incubated with mouse anti-VP40 monoclonal antibody followed by Alexa Fluor 488 donkey anti-mouse antibody and analyzed by confocal microscopy. The VP40-NiV M immunofluorescence experiment was performed separately; all images are representative. All VP40 experiments were performed in collaboration with Ziyang Han and Ronald Harty (University of Pennsylvania), and are included with permission.



restored. The results of this experiment revealed that indeed the NiV M protein YPLGVG motif successfully restored significant VP40 budding (**Fig. 18B**).

Furthermore, immunofluorescent confocal microscopy revealed that cells expressing VP40-NiV M had a similar morphology to those expressing wild-type VP40, which was characterized by extensive membrane fragmentation. In contrast, this morphology was not seen when the L-domain was deleted from VP40 (VP40 Δ PT/PY) (**Fig. 18C**). These results strongly support the hypothesis that the NiV M protein YPLGVG motif plays an important role in NiV M budding, and that it acts through a mechanism that is transferable to other viruses.

Discussion

The involvement of MVB proteins in viral assembly and release, and their recruitment by L-domain motifs residing within viral structural proteins, is an area of increasing interest in enveloped virus research. L-domains were first identified in retroviruses, and have now been discovered in a variety of enveloped virus families including arenaviruses, filoviruses, rhabdoviruses, and paramyxoviruses (6, 33, 84). Since NiV M did not contain any of the known L-domain motifs, we used a VLP budding assay and employed multiple strategies including perturbation of MVB machinery, chimeric protein construction, and targeted mutagenesis to determine whether NiV M contains a novel L-domain that is used to accomplish budding.

VPS4A and VPS4B are paralogous ATPases that are responsible for disassembly of the ESCRT complexes involved in MVB formation, and mutations that destroy their ability to bind or hydrolyze ATP result in the ability to dominantly inhibit cellular

VPS4A or VPS4B. These DN mutants inhibited the release of most viruses that use L-domains and are thought to provide a method of global inhibition of class E Vps proteins (6, 33, 84). Notably, we found that NiV M protein release was unchanged in the presence of VPS4A, while in parallel, SV5 VLP release was greatly reduced, in agreement with a previous report (115). Furthermore, NiV M protein release was also unchanged in the presence of DN VPS4B, or in the presence of both DN VPS4A and DN VPS4B, thus eliminating the possibility that NiV M protein release was accomplished either by VPS4B or that the wild-type cellular paralogs were rescuing release. In addition, NiV M protein was also relatively resistant to the proteasome inhibitor MG-132, as well as to over-expression of AIP1/Alix. In contrast, a number of viruses that contain L-domains, including SV5, are sensitive to proteasome inhibition, and over-expression of AIP1/Alix increases SeV virion (108) and HIV-1 VLP release (120), and decreases EIAV release (21). These findings indicate that the mechanisms whereby NiV M facilitates its budding and release from cells may be unique and fundamentally distinct from the known pathways of viral budding.

SV5 M contains the L-domain sequence FPIV; however SV5 M is not released efficiently from cells when expressed alone (115, 116). We attempted to transfer the budding phenotype of NiV M to SV5 M by construction of reciprocal chimeras, reasoning that the amino acid sequence responsible for NiV M budding might constitute an L-domain or budding domain acting through a different mechanism. Although both chimeras were expressed, release of neither protein was detected which suggests that either the budding phenotype of NiV M is not governed by a single short amino acid sequence or the SV5 M phenotype is dominant to the NiV sequence.

In an additional approach to the identification of a NiV M budding domain, we sought to determine the basis for the greater efficiency of NiV M release compared to HeV M. Because approximately one-third of the amino acid differences between the two proteins are located in the N-terminal 12 amino acids, which have no sequence homology, we constructed M mutants with reciprocal heterotypic N-termini and observed that the difference in budding phenotype was indeed governed by the N-terminus. To further narrow the sequence hypothesized to increase NiV M release, a series of mutants was made in which blocks of 4 amino acids were changed to the HeV M sequence. In addition, the first 12 amino acids of NiV M were removed so that translation would begin at the methionine normally at position 13. The replacement mutants were released at equivalent or lesser proportions compared to wild-type. However, and more importantly, we found that the deletion mutant was released with efficiency approximately equivalent to the wild-type. This result demonstrates that the N-terminal 12 amino acids do not increase NiV M release and are dispensable for release. The equivalent HeV M deletion mutant was also released, but with a greater efficiency than wild-type HeV M, suggesting that, at least in the context of solo expression, the N-terminus of NiV M does not increase budding whereas in HeV M it serves to reduce budding. That the M protein of NiV, HeV, and TPMV each have extended N-termini relative to the morbilliviruses, as well as other representatives of the paramyxovirinae, is suggestive of function, particularly since NiV M has a methionine that aligns with the N-terminus of morbillivirus M proteins and could thus easily lose the extra 12 amino acids by mutation of its current start codon. Our results suggest that in HeV this sequence may serve to negatively regulate virus release, however the mechanism underlying this observation is unknown and it remains

to be further explored. In contrast, our results suggest that the NiV M N-terminus does not play a role in budding, however whether this holds true in the context of other viral proteins, or live virus, also requires further testing.

We next sought to take advantage of the fact that all identified L-domains contain at least one proline residue and initiated a mutagenesis strategy whereby individual proline residues in NiV M were mutated to alanine. We identified 3 sequences (4 proline residues, total) of interest because of their similarity to known L-domain motifs, or close alignment to the SV5 FPIV motif. Using this alanine mutagenesis approach coupled with our VLP budding assay, we identified one particular M mutant, P93A, that was defective in budding and release. To confirm this observation and further characterize the surrounding amino acids, we targeted the YPLGVG motif within the M protein and additional alanine mutants were made (Y92A and L94A), as well as a deletion mutant (Δ 92-97), which were then tested for budding ability. Whereas a low level of P93A release could sometimes be detected, the additional YPLGVG mutants were totally defective in budding. HeV M contains an identical sequence at the same position, and although we have not examined its importance for HeV M release, we predict that mutation of the sequence in HeV M will yield similar results.

Finally, to determine whether this sequence has transferable L-domain activity, the L-domain sequence of Ebola VP40 was replaced with YPLGVG along with a few flanking amino acids. Although less efficient than wild-type, we found that VP40 budding was rescued by the NiV M sequence. In addition, immunofluorescence microscopy revealed that cells expressing mutant VP40 containing the YPLGVG sequence displayed a morphology consistent with those expressing wild-type VP40,

which was characterized by membrane fragmentation. These data suggest that the YPLGVG sequence is important for NiV M budding and can act as a substitute for the native VP40 L-domain sequence. Experiments to determine whether mutation of the Y, P, or L residues abrogate rescue of VP40 budding are in progress.

We initially noticed the YPLGVG sequence because of its similarity to the L-domain motif YP(x)_nL. This motif was first discovered in EIAV (YPDL) (104) and then identified in the p6 domain of HIV-1 Gag (YPLTSL) (120). Initial characterization of this motif in EIAV determined that the Y, P, and L residues are critical for viral budding, however the motif was designated YxxL because of the similarity to the YxxL endocytosis motif, and it was hypothesized that the EIAV motif interacted with endocytosis machinery (104). In fact, evidence suggests that EIAV Gag does interact with the AP-2 complex (21), however it appears that AIP1/Alix is the primary protein that interacts with this L-domain, and the EIAV motif is now usually designated as YP(x)_nL or YPxL because the proline residue is critical for AIP1/Alix binding and viral budding (6, 33, 84). Both HIV-1 and EIAV contain a sequence just downstream of the YP(x)_nL motif that is also important for AIP1/Alix binding, and it has recently been suggested that the two motifs are actually a single motif that can be summarized as (L)[F/Y]Px₁₋₃LXX[I/L] (87).

This background notwithstanding, Hui and co-workers identified a sequence, YRK_L, in influenza A M1 that served as an L-domain through its interaction with VPS28 and Cdc42, but importantly, the tyrosine and leucine residues were not important for function, thus suggesting a fundamental difference from the YP(x)_nL motif (58, 59). However, the papers describing these findings have since been retracted and it remains

unclear whether the sequence is, in fact, an L-domain (60). Using the YxxL designation as a guide, Ciancanelli and Basler have identified 62-YMYL-65 as a sequence important for NiV M budding (27). Their study found that alanine mutation of Y62, Y62 and L65, or deletion of the whole sequence resulted in defective M budding. They also established the functional rescue of L-domain-mutant VP40 budding by appending the YMYL (and flanking) sequence to the C-terminus of VP40. However, when we attempted to confirm their findings by directly replacing the native VP40 L-domain with the identical NiV sequence used by Ciancanelli and Basler, rather than appending it to the C-terminus, we failed to detect rescue of VP40 budding (data not shown). The reason for the difference is not known; however L-domains can be context-dependent, which may account for our differing result (33, 67). Interestingly, the equivalent sequence in HeV M is YMYM, and as our experiments show, HeV M is also released into the supernatant with the difference of efficiency compared to NiV M mapping to the N-terminus. In addition, mutation of the NiV YMYL sequence to the HeV sequence (YMYM) does not appear to adversely affect NiV M release (data not shown). In light of our results, the role of this sequence in henipavirus budding remains to be clarified.

Our findings suggest that the NiV M (YPLGVG) sequence may represent a novel L-domain motif, and this suggestion is based on the necessity of the sequence for NiV M release and the ability of the sequence to rescue mutant VP40 release while also correlating with the production of a cellular morphology consistent with wild-type VP40 expression. The P(T/S)AP and PPxY L-domain motifs, both of which are present and functional in VP40, interact with cellular proteins Tsg101 and Nedd4-like E3 ubiquitin ligases, respectively (33, 76, 84, 126). In the case of the P(T/S)AP motif, specific

contacts are made between each residue and the binding pocket of Tsg101 (84, 103). This specificity of interaction and the proteasome insensitivity of NiV M suggest that the YPLGVG sequence does not rescue VP40 budding by restoring interactions with Tsg101 or Nedd4-like E3 ubiquitin ligases. That YPLGVG enables budding in both NiV and VP40 by an alternative mechanism that is independent of MVB machinery is a formal possibility.

L-domains, with their interactions with MVB machinery, most likely represent a subset of protein domains involved in virus budding. An early observation made regarding Gag truncation mutants of HIV-1, which did not express the L-domain-containing p6 protein, was the apparent tethering of budding virions to the cell surface (33, 46). This phenotype appears to represent a defect in the final step of virus budding and suggests that mechanisms other than those underlying L-domain function also play an important role in HIV-1 budding. In addition, deletion of the Ebola virus overlapping L-domains in VP40 results in a modest defect in live virus production and suggests that mechanisms independent of MVB machinery play a dominant role in Ebola virus budding (90). The NiV YPLGVG sequence may facilitate budding of NiV M via interactions with non-MVB-associated cellular proteins or another conformation-dependent mechanism, and may complement VP40 budding by this alternative mechanism.

Further, the observation that NiV M release is insensitive to DN VPS4 proteins and proteasome inhibition lends some support to this alternative interpretation. However, both influenza A and vesicular stomatitis virus (VSV) are reported to be insensitive to DN mutants of either VPS4A (VSV) (68) or VPS4B (influenza) (58), and both EIAV and

influenza A budding are insensitive to proteasome inhibitors (61, 71, 94, 101). Thus, insensitivity to DN VPS4 proteins and proteasome inhibitors are apparently not sufficient grounds to rule out L-domain activity. Further characterization of the YPLGVG sequence and determination of any interaction with MVB machinery will be needed to definitively establish whether the NiV YPLGVG budding domain possesses classical L-domain activity. Current evidence suggests that, whatever the role of the YPLGVG sequence in NiV budding, it is distinct from the similar YP(x)_nL motif represented by EIAV.

Chapter 5

Discussion

Nipah virus is an emerging viral pathogen that has a demonstrated ability to infect a broad variety of animals and, in human infections, to cause significant morbidity and mortality. Although outbreaks of the virus since its discovery in 1999 have been limited, the ability of pigs to serve as an amplifying host serves as a reminder of the potential for large outbreaks. The classification of Nipah virus as a BSL-4 pathogen has hampered the study of its lifecycle, while in general, the mechanisms of paramyxovirus assembly remain poorly understood.

We have established a virus-like particle (VLP) system as a means of exploring NiV assembly and morphogenesis under regular laboratory conditions. In accordance with our hypothesis, by using a combination of biochemical and electron microscopy techniques we found that expression of NiV M alone, or in combination with N, F and G, leads to the release of membrane-associated M, and that the resulting particles are consistent in size and density with authentic NiV. Although the envelope glycoproteins contain some intrinsic budding ability, the central role of the M protein was demonstrated by its ability to incorporate the envelope glycoproteins into particles of a slightly different density than those containing only envelope glycoproteins, and its facilitation of N release. Co-expression of M, N, F and G lead to a reduction in overall protein release, which we interpret as the result of a more organized assembly process via direct or indirect viral protein interactions.

In recent years, many enveloped viruses have been shown to possess one or more important protein motifs, typically residing in their matrix protein, which are termed L-domains and are important in associating with host factors and facilitating the budding and release of viral particles (6, 33, 84). We found that NiV M release was not affected by (i) blocking the action of VPS4A and VPS4B, (ii) proteasome inhibition, or (iii) over-expression of AIP1/Alix. These findings indicate that the nature of the NiV M protein budding activity appears unique and quite distinct from other known viral systems. Importantly, we identified a sequence motif in NiV M (YPLGVG) that was essential for its release and that could functionally complement the Ebola VP40 overlapping L-domain sequence. These findings strongly suggest that the YPLGVG sequence serves as an L-domain in NiV M.

Cytoskeletal Proteins

An important component of future research on NiV assembly will be to characterize the protein interactions involved. Little is known about the structure of M, and the domains responsible for interacting with the envelope glycoproteins and the nucleocapsid are undefined. In addition, interactions with cellular proteins also remain largely unexplored. Aside from potential interactions with components of ESCRT complexes, it is likely that cytoskeletal proteins play a role in NiV assembly and budding as well. Indeed, several lines of evidence suggest a role for cellular actin in paramyxovirus budding. Using biochemical techniques, Giuffre and co-workers determined that the M protein of NDV and SeV interacts with cellular actin (43). Treatment of cells with cytochalasin B, which inhibits actin polymerization, has been

shown to reduce MeV release by at least 88%, and an association between budding virions and actin has been observed by electron microscopy (7, 118). In addition, vesicles derived from solo expression of either SeV M or F contain actin, and mutation in each protein of amino acid residues similar to an actin-binding domain results in a lack of particle formation (123). In contrast, hPIV-3 release was unaffected by treatment of cells with cytochalasin D but was inhibited by nocodazole, thus indicating a role for microtubules rather than actin filaments in hPIV-3 release (9). However, NiV M and F do not contain the amino acid motifs described for SeV, but the close relationship of NiV to MeV is suggestive of a role for actin. It is interesting to note that the L-domain identified in influenza A (YRKL) was reported to interact with the ESCRT-I protein VPS28, as well as Cdc42, a member of the Rho G protein family that plays a role in cytoskeletal remodeling, and depletion of either protein by small interfering RNA resulted in reduced virus production (58). The paper describing these results has been retracted, thus casting doubt on the results (60). Nevertheless the paper raises the possibility that some L-domains may be multifunctional and may promote involvement of the cytoskeleton, in addition to MVB machinery, in assembly and budding.

Our VLP system can be used to investigate cytoskeletal involvement in NiV budding by determining the effect of inhibition of actin or microtubule polymerization on VLP release. As a more general approach to investigating the involvement of cellular proteins, we also intend to employ a yeast two-hybrid analysis to screen for cellular proteins that interact with NiV M. We anticipate that this technique will play an important role in the identification of cellular proteins and pathways involved in NiV

budding, and the VLP system will be an important tool in the confirmation of these interactions.

Lipid Rafts

Lipid rafts are microdomains of lipid membranes that are enriched in cholesterol and sphingolipids, and are insoluble in nonionic detergents, particularly TX-100, at 4°C (20). They play a role in the assembly and budding of a number of enveloped viruses including HIV, influenza, Ebola, and MeV and are thought to facilitate the selective accumulation of viral, as well as cellular, proteins [reviewed in (20)]. Among paramyxoviruses, the role of lipid rafts in assembly has received the most attention for MeV. The measles F and H glycoproteins associate with lipid rafts in the *trans*-Golgi network, however only processed F is included and it mediates the co-association of H, which does not have raft affinity on its own. The M protein has a low but significant affinity for rafts, and associates with the viral ribonucleoprotein complex. Thus, lipid rafts are thought to serve as a platform for assembly by facilitating the co-localization of the envelope glycoproteins and the M-RNP complex (78, 128). Additional support for lipid raft involvement in paramyxovirus assembly comes from SeV, NDV and RSV, which have one or more lipid raft-associated viral proteins (3, 14, 35, 80). Lipid rafts also appear to facilitate the interaction of viral and cellular proteins. For example, Tsg101 is a component of the ESCRT-I complex that interacts with the L-domain motif P(T/S)AP, and is located in raft domains. Ebola VP40 also associates with membrane rafts and recruits Tsg101 to the plasma membrane via the VP40 L-domain (76, 98).

Whether NiV assembly and budding involves lipid rafts and what role they might play are questions that remain to be explored.

Persistent Infection

A remarkable feature of NiV and HeV is their ability to cause a persistent sub-clinical infection that can result in late-onset or relapse encephalitis up to 4 years after initial infection (23, 125). This ability is reminiscent of MeV, which is the causative agent of subacute sclerosing panencephalitis (SSPE), a progressive neurological disease that is universally fatal and occurs between 9 months and 30 years (average is 8 years) following acute MeV infection. The mechanism of MeV persistence and the pathogenesis of SSPE are poorly understood. However, defects in viral assembly, due especially to mutations of M, as well as the cytoplasmic tail of F, appear to be important [reviewed in (106)]. Attempts to isolate NiV from late encephalitic events have not been reported, so the nature of the persisting virus is unknown. Nevertheless, an attractive speculation is that similar mutations as those found in MeV of SSPE patients are involved in NiV persistence. In that regard, it is interesting to note that, in some cases, the M protein of SSPE viruses contain a mutation in the sequence homologous to the NiV M YPLGVG sequence (**Fig. 19**). However, such mutations are not universal among SSPE viruses and when they are present they co-exist with other mutations, so any causal relationship between these mutations and SSPE is a matter of speculation. Based on results reported here, however, it would not be surprising if mutation of this sequence is an important contributor to defective assembly in some SSPE viruses, and this correlation may have implications for persistent henipavirus infections.

Figure 19. Alignment of mutations in Measles virus M. A portion of the wild-type MeV M amino acid sequence was aligned with that of neurotropic and SSPE isolates. Amino acids corresponding to the NiV M YPLGVG sequence are underlined, and amino acid differences in several neurotropic and SSPE isolates relative to the wild-type sequence are shaded.

Accession Number	MeV Type	
NP_056921.1	wt	70 GRAFGS <u>L</u> PLGVGRS
BAA09963.1	Neurotropic	70 GRAFGS <u>L</u> LLGVGRS
BAA09956.1	Neurotropic	70 GRAFGS <u>L</u> LLGVGRS
P16628	SSPE	70 GRAFGS <u>P</u> PLGVGRS
BAA00381.1	SSPE	70 GRAFGS <u>P</u> PLGVGRS
AAN09804.1	SSPE	70 GRAFGS <u>P</u> PLGVGRS
AAN09800.1	SSPE	70 GRA <u>P</u> GS <u>L</u> PLG <u>A</u> GRS
AAN09803.1	SSPE	70 GRAFGS <u>L</u> P <u>S</u> GVGRS

Limitations and Future Directions

The VLP system described here will serve as a useful platform for exploring further details in the cell biology of NiV, however it does have several limitations. The VLP system is, in the end, an artificial system and does not reflect all aspects of NiV replication. We speculate that the inclusion of additional viral proteins as well as an artificial mini- or reporter genome may better approximate certain NiV cell biological events or processes. Experiments showing that the loss of the Ebola VP40 L-domain results in only a modest decrease in virus titer serve as a reminder that results obtained in a VLP budding assay do not necessarily directly apply to live virus. Experiments with live recombinant NiV will be required to confirm our results derived from mutation of M.

The work presented here has focused almost exclusively on NiV. Because of its close relationship to NiV, we speculate that the results described here should also apply to HeV as well. However, this assumption remains to be tested and further experiments will be required to determine whether the dynamics of VLP release by HeV proteins are similar to that of NiV, whether HeV M is sensitive to inhibition of VPS4 proteins, and whether the YPLGVG sequence is also critical for HeV M release. Additionally, it will be interesting to determine whether NiV and HeV proteins can function in heterotypic combinations in VLP formation. Failure to find heterotypic function may aid in the identification of domains important for protein interactions, such as between M and N.

Chapter 6

Bibliography

1. **Accola, M. A., B. Strack, and H. G. Gottlinger.** 2000. Efficient particle production by minimal Gag constructs which retain the carboxy-terminal domain of human immunodeficiency virus type 1 capsid-p2 and a late assembly domain. *J Virol* **74**:5395-402.
2. **Aguilar, H. C., K. A. Matreyek, C. M. Filone, S. T. Hashimi, E. L. Levroney, O. A. Negrete, A. Bertolotti-Ciarlet, D. Y. Choi, I. McHardy, J. A. Fulcher, S. V. Su, M. C. Wolf, L. Kohatsu, L. G. Baum, and B. Lee.** 2006. N-glycans on Nipah virus fusion protein protect against neutralization but reduce membrane fusion and viral entry. *J Virol* **80**:4878-89.
3. **Ali, A., and D. P. Nayak.** 2000. Assembly of Sendai virus: M protein interacts with F and HN proteins and with the cytoplasmic tail and transmembrane domain of F protein. *Virology* **276**:289-303.
4. **Bachi, T.** 1980. Intramembrane structural differentiation in Sendai virus maturation. *Virology* **106**:41-9.
5. **Bavari, S., C. M. Bosio, E. Wiegand, G. Ruthel, A. B. Will, T. W. Geisbert, M. Hevey, C. Schmaljohn, A. Schmaljohn, and M. J. Aman.** 2002. Lipid raft microdomains: a gateway for compartmentalized trafficking of Ebola and Marburg viruses. *J Exp Med* **195**:593-602.
6. **Bieniasz, P. D.** 2006. Late budding domains and host proteins in enveloped virus release. *Virology* **344**:55-63.

7. **Bohn, W., G. Rutter, H. Hohenberg, K. Mannweiler, and P. Nobis.** 1986. Involvement of actin filaments in budding of measles virus: studies on cytoskeletons of infected cells. *Virology* **149**:91-106.
8. **Bonaparte, M. I., A. S. Dimitrov, K. N. Bossart, G. Crameri, B. A. Mungall, K. A. Bishop, V. Choudhry, D. S. Dimitrov, L. F. Wang, B. T. Eaton, and C. C. Broder.** 2005. Ephrin-B2 ligand is a functional receptor for Hendra virus and Nipah virus. *Proc Natl Acad Sci USA* **102**:10652-7.
9. **Bose, S., A. Malur, and A. K. Banerjee.** 2001. Polarity of human parainfluenza virus type 3 infection in polarized human lung epithelial A549 cells: role of microfilament and microtubule. *J Virol* **75**:1984-9.
10. **Bossart, K. N., and C. C. Broder.** 2007. Paramyxovirus Entry. *In* S. Pohlmann and G. Simmons (ed.), *Viral Entry into Host Cells*. Landes Bioscience, Austin, Tx.
11. **Bossart, K. N., B. A. Mungall, G. Crameri, L. F. Wang, B. T. Eaton, and C. C. Broder.** 2005. Inhibition of Henipavirus fusion and infection by heptad-derived peptides of the Nipah virus fusion glycoprotein. *Virol J* **2**:57.
12. **Bossart, K. N., L. F. Wang, B. T. Eaton, and C. C. Broder.** 2001. Functional expression and membrane fusion tropism of the envelope glycoproteins of Hendra virus. *Virology* **290**:121-35.
13. **Bossart, K. N., L. F. Wang, M. N. Flora, K. B. Chua, S. K. Lam, B. T. Eaton, and C. C. Broder.** 2002. Membrane fusion tropism and heterotypic functional activities of the Nipah virus and Hendra virus envelope glycoproteins. *J Virol* **76**:11186-98.

14. **Brown, G., H. W. Rixon, and R. J. Sugrue.** 2002. Respiratory syncytial virus assembly occurs in GM1-rich regions of the host-cell membrane and alters the cellular distribution of tyrosine phosphorylated caveolin-1. *J Gen Virol* **83**:1841-50.
15. **Buchholz, U. J., S. Finke, and K. K. Conzelmann.** 1999. Generation of bovine respiratory syncytial virus (BRSV) from cDNA: BRSV NS2 is not essential for virus replication in tissue culture, and the human RSV leader region acts as a functional BRSV genome promoter. *J Virol* **73**:251-9.
16. **Carroll, M. W., and B. Moss.** 1995. E. coli beta-glucuronidase (GUS) as a marker for recombinant vaccinia viruses. *Biotechniques* **19**:352-4, 356.
17. **Cathomen, T., B. Mrkic, D. Spehner, R. Drillien, R. Naef, J. Pavlovic, A. Aguzzi, M. A. Billeter, and R. Cattaneo.** 1998. A matrix-less measles virus is infectious and elicits extensive cell fusion: consequences for propagation in the brain. *Embo J* **17**:3899-908.
18. **Cervia, J. S., and M. A. Smith.** 2003. Enfuvirtide (T-20): a novel human immunodeficiency virus type 1 fusion inhibitor. *Clin Infect Dis* **37**:1102-6.
19. **Chadha, M. S., J. A. Comer, L. Lowe, P. A. Rota, P. E. Rollin, W. J. Bellini, T. G. Ksiazek, and A. Mishra.** 2006. Nipah virus-associated encephalitis outbreak, Siliguri, India. *Emerg Infect Dis* **12**:235-40.
20. **Chazal, N., and D. Gerlier.** 2003. Virus entry, assembly, budding, and membrane rafts. *Microbiol Mol Biol Rev* **67**:226-37.

21. **Chen, C., O. Vincent, J. Jin, O. A. Weisz, and R. C. Montelaro.** 2005. Functions of early (AP-2) and late (AIP1/ALIX) endocytic proteins in equine infectious anemia virus budding. *J Biol Chem* **280**:40474-80.
22. **Chong, H. T., A. Kamarulzaman, C. T. Tan, K. J. Goh, T. Thayaparan, S. R. Kunjapan, N. K. Chew, K. B. Chua, and S. K. Lam.** 2001. Treatment of acute Nipah encephalitis with ribavirin. *Ann Neurol* **49**:810-3.
23. **Chong, H. T., and C. T. Tan.** 2003. Relapsed and late-onset Nipah encephalitis, a report of three cases. *Neurol J Southeast Asia* **8**:109-12.
24. **Chua, K. B.** 2003. Nipah virus outbreak in Malaysia. *J Clin Virol* **26**:265-75.
25. **Chua, K. B., W. J. Bellini, P. A. Rota, B. H. Harcourt, A. Tamin, S. K. Lam, T. G. Ksiazek, P. E. Rollin, S. R. Zaki, W. Shieh, C. S. Goldsmith, D. J. Gubler, J. T. Roehrig, B. Eaton, A. R. Gould, J. Olson, H. Field, P. Daniels, A. E. Ling, C. J. Peters, L. J. Anderson, and B. W. Mahy.** 2000. Nipah virus: a recently emergent deadly paramyxovirus. *Science* **288**:1432-5.
26. **Chua, K. B., C. Lek Koh, P. S. Hooi, K. F. Wee, J. H. Khong, B. H. Chua, Y. P. Chan, M. E. Lim, and S. K. Lam.** 2002. Isolation of Nipah virus from Malaysian Island flying-foxes. *Microbes Infect* **4**:145-51.
27. **Ciancanelli, M. J., and C. F. Basler.** 2006. Mutation of YMYL in the Nipah virus matrix protein abrogates budding and alters subcellular localization. *J Virol* **80**:12070-8.
28. **Clamp, M., J. Cuff, S. M. Searle, and G. J. Barton.** 2004. The Jalview Java Alignment Editor. *Bioinformatics* **20**:426-7.

29. **Condit, R. C.** 2001. Principles of Virology, p. 19-51. *In* D. M. Knipe, P. M. Howley, D. E. Griffin, R. A. Lamb, M. A. Martin, B. Roizman, and S. E. Straus (ed.), *Fields Virology*, 4 ed. Lippincott Williams & Wilkins, Philadelphia, PA.
30. **Conzelmann, K. K.** 2004. Reverse genetics of mononegavirales. *Curr Top Microbiol Immunol* **283**:1-41.
31. **Coronel, E. C., K. G. Murti, T. Takimoto, and A. Portner.** 1999. Human parainfluenza virus type 1 matrix and nucleoprotein genes transiently expressed in mammalian cells induce the release of virus- like particles containing nucleocapsid-like structures. *J Virol* **73**:7035-8.
32. **Coronel, E. C., T. Takimoto, K. G. Murti, N. Varich, and A. Portner.** 2001. Nucleocapsid incorporation into parainfluenza virus is regulated by specific interaction with matrix protein. *J Virol* **75**:1117-23.
33. **Demirov, D. G., and E. O. Freed.** 2004. Retrovirus budding. *Virus Res* **106**:87-102.
34. **Diederich, S., M. Moll, H. D. Klenk, and A. Maisner.** 2005. The nipah virus fusion protein is cleaved within the endosomal compartment. *J Biol Chem* **280**:29899-903.
35. **Dolganiuc, V., L. McGinnes, E. J. Luna, and T. G. Morrison.** 2003. Role of the cytoplasmic domain of the Newcastle disease virus fusion protein in association with lipid rafts. *J Virol* **77**:12968-79.
36. **Eaton, B. T.** 2001. Introduction to Current focus on Hendra and Nipah viruses. *Microbes Infect* **3**:277-8.

37. **Eaton, B. T., C. C. Broder, D. Middleton, and L. F. Wang.** 2006. Hendra and Nipah viruses: different and dangerous. *Nat Rev Microbiol* **4**:23-35.
38. **Eaton, B. T., J. S. Mackenzie, and L. F. Wang.** 2006. Henipaviruses, p. 1587-1600. *In* D. M. Knipe, P. M. Howley, D. E. Griffin, R. A. Lamb, M. A. Martin, B. Roizman, and S. E. Straus (ed.), *Fields Virology*, 5 ed, vol. 2. Lippincott Williams & Wilkins.
39. **Field, H., P. Young, J. M. Yob, J. Mills, L. Hall, and J. Mackenzie.** 2001. The natural history of Hendra and Nipah viruses. *Microbes Infect* **3**:307-14.
40. **Garrus, J. E., U. K. von Schwedler, O. W. Pornillos, S. G. Morham, K. H. Zavitz, H. E. Wang, D. A. Wettstein, K. M. Stray, M. Cote, R. L. Rich, D. G. Myszka, and W. I. Sundquist.** 2001. Tsg101 and the vacuolar protein sorting pathway are essential for HIV-1 budding. *Cell* **107**:55-65.
41. **Georges-Courbot, M. C., H. Contamin, C. Faure, P. Loth, S. Baize, P. Leysen, J. Neyts, and V. Deubel.** 2006. Poly(I)-poly(C12U) but not ribavirin prevents death in a hamster model of Nipah virus infection. *Antimicrob Agents Chemother* **50**:1768-72.
42. **Ghildyal, R., D. Li, I. Peroulis, B. Shields, P. G. Bardin, M. N. Teng, P. L. Collins, J. Meanger, and J. Mills.** 2005. Interaction between the respiratory syncytial virus G glycoprotein cytoplasmic domain and the matrix protein. *J Gen Virol* [10.1099/vir.0.80829-0](https://doi.org/10.1099/vir.0.80829-0) **86**:1879-1884.
43. **Giuffre, R. M., D. R. Tovell, C. M. Kay, and D. L. Tyrrell.** 1982. Evidence for an interaction between the membrane protein of a paramyxovirus and actin. *J Virol* **42**:963-8.

44. **Goff, S. P.** 2001. *Retroviridae: The Retroviruses and Their Replication*, p. 1871-1939. In D. M. Knipe, P. M. Howley, D. E. Griffin, R. A. Lamb, M. A. Martin, B. Roizman, and S. E. Straus (ed.), *Fields Virology*, 4 ed. Lippincott Williams & Wilkins, Philadelphia, PA.
45. **Goldsmith, C. S., T. Whistler, P. E. Rollin, T. G. Ksiazek, P. A. Rota, W. J. Bellini, P. Daszak, K. T. Wong, W. J. Shieh, and S. R. Zaki.** 2003. Elucidation of Nipah virus morphogenesis and replication using ultrastructural and molecular approaches. *Virus Res* **92**:89-98.
46. **Gottlinger, H. G., T. Dorfman, J. G. Sodroski, and W. A. Haseltine.** 1991. Effect of mutations affecting the p6 gag protein on human immunodeficiency virus particle release. *Proc Natl Acad Sci USA* **88**:3195-9.
47. **Guillaume, V., H. Contamin, P. Loth, M. C. Georges-Courbot, A. Lefevre, P. Marianneau, K. B. Chua, S. K. Lam, R. Buckland, V. Deubel, and T. F. Wild.** 2004. Nipah virus: vaccination and passive protection studies in a hamster model. *J Virol* **78**:834-40.
48. **Guillaume, V., H. Contamin, P. Loth, I. Grosjean, M. C. Courbot, V. Deubel, R. Buckland, and T. F. Wild.** 2006. Antibody prophylaxis and therapy against Nipah virus infection in hamsters. *J Virol* **80**:1972-8.
49. **Harcourt, B. H., L. Lowe, A. Tamin, X. Liu, B. Bankamp, N. Bowden, P. E. Rollin, J. A. Comer, T. G. Ksiazek, M. J. Hossain, E. S. Gurley, R. F. Breiman, W. J. Bellini, and P. A. Rota.** 2005. Genetic characterization of Nipah virus, Bangladesh, 2004. *Emerg Infect Dis* **11**:1594-7.

50. **Harcourt, B. H., A. Tamin, K. Halpin, T. G. Ksiazek, P. E. Rollin, W. J. Bellini, and P. A. Rota.** 2001. Molecular characterization of the polymerase gene and genomic termini of nipah virus. *Virology* **287**:192-201.
51. **Harcourt, B. H., A. Tamin, T. G. Ksiazek, P. E. Rollin, L. J. Anderson, W. J. Bellini, and P. A. Rota.** 2000. Molecular characterization of Nipah virus, a newly emergent paramyxovirus. *Virology* **271**:334-49.
52. **Harty, R. N., M. E. Brown, J. P. McGettigan, G. Wang, H. R. Jayakar, J. M. Huibregtse, M. A. Whitt, and M. J. Schnell.** 2001. Rhabdoviruses and the cellular ubiquitin-proteasome system: a budding interaction. *J Virol* **75**:10623-9.
53. **Harty, R. N., M. E. Brown, G. Wang, J. Huibregtse, and F. P. Hayes.** 2000. A PPxY motif within the VP40 protein of Ebola virus interacts physically and functionally with a ubiquitin ligase: implications for filovirus budding. *Proc Natl Acad Sci USA* **97**:13871-6.
54. **Harty, R. N., J. Paragas, M. Sudol, and P. Palese.** 1999. A proline-rich motif within the matrix protein of vesicular stomatitis virus and rabies virus interacts with WW domains of cellular proteins: implications for viral budding. *J Virol* **73**:2921-9.
55. **Heggeness, M. H., P. R. Smith, and P. W. Choppin.** 1982. In vitro assembly of the nonglycosylated membrane protein (M) of Sendai virus. *Proc Natl Acad Sci USA* **79**:6232-6.
56. **Homann, H. E., P. H. Hofschneider, and W. J. Neubert.** 1990. Sendai virus gene expression in lytically and persistently infected cells. *Virology* **177**:131-40.

57. **Hsu, V. P., M. J. Hossain, U. D. Parashar, M. M. Ali, T. G. Ksiazek, I. Kuzmin, M. Niezgoda, C. Rupprecht, J. Bresee, and R. F. Breiman.** 2004. Nipah virus encephalitis reemergence, Bangladesh. *Emerg Infect Dis* **10**:2082-7.
58. **Hui, E. K., S. Barman, D. H. Tang, B. France, and D. P. Nayak.** 2006. YRKL sequence of influenza virus M1 functions as the L domain motif and interacts with VPS28 and Cdc42. *J Virol* **80**:2291-308.
59. **Hui, E. K., S. Barman, T. Y. Yang, and D. P. Nayak.** 2003. Basic residues of the helix six domain of influenza virus M1 involved in nuclear translocation of M1 can be replaced by PTAP and YPDL late assembly domain motifs. *J Virol* **77**:7078-92.
60. **Hui, E. K., S. Barman, T. Y. Yang, D. H. Tang, B. France, and D. P. Nayak.** 2006. Retraction. *J Virol* **80**:10289.
61. **Hui, E. K., and D. P. Nayak.** 2001. Role of ATP in influenza virus budding. *Virology* **290**:329-41.
62. **Hyatt, A. D., S. R. Zaki, C. S. Goldsmith, T. G. Wise, and S. G. Hengstberger.** 2001. Ultrastructure of Hendra virus and Nipah virus within cultured cells and host animals. *Microbes Infect* **3**:297-306.
63. **ICDDRБ.** 2004. Nipah encephalitis outbreak over wide area of western Bangladesh, 2004. *Health Science Bulletin* **2**:7-11.
64. **ICDDRБ.** 2003. Outbreaks of encephalitis due to Nipah/Hendra-like viruses, western Bangladesh. *Health Science Bulletin* **1**:1-6.
65. **ICDDRБ.** 2004. Person-to-person transmission of Nipah virus during outbreak in Faridpur District, 2004. *Health Science Bulletin* **2**:5-9.

66. **Inoue, M., Y. Tokusumi, H. Ban, T. Kanaya, M. Shirakura, T. Tokusumi, T. Hirata, Y. Nagai, A. Iida, and M. Hasegawa.** 2003. A new Sendai virus vector deficient in the matrix gene does not form virus particles and shows extensive cell-to-cell spreading. *J Virol* **77**:6419-29.
67. **Irie, T., and R. N. Harty.** 2005. L-domain flanking sequences are important for host interactions and efficient budding of vesicular stomatitis virus recombinants. *J Virol* **79**:12617-22.
68. **Irie, T., J. M. Licata, J. P. McGettigan, M. J. Schnell, and R. N. Harty.** 2004. Budding of PPxY-containing rhabdoviruses is not dependent on host proteins TGS101 and VPS4A. *J Virol* **78**:2657-65.
69. **Jasenosky, L. D., G. Neumann, I. Lukashevich, and Y. Kawaoka.** 2001. Ebola virus VP40-induced particle formation and association with the lipid bilayer. *J Virol* **75**:5205-14.
70. **Justice, P. A., W. Sun, Y. Li, Z. Ye, P. R. Grigera, and R. R. Wagner.** 1995. Membrane vesiculation function and exocytosis of wild-type and mutant matrix proteins of vesicular stomatitis virus. *J Virol* **69**:3156-60.
71. **Khor, R., L. J. McElroy, and G. R. Whittaker.** 2003. The ubiquitin-vacuolar protein sorting system is selectively required during entry of influenza virus into host cells. *Traffic* **4**:857-68.
72. **Kobasa, D., M. E. Rodgers, K. Wells, and Y. Kawaoka.** 1997. Neuraminidase hemadsorption activity, conserved in avian influenza A viruses, does not influence viral replication in ducks. *J Virol* **71**:6706-13.

73. **Lamb, R. A., and D. Kolakofsky.** 2001. *Paramyxoviridae*: The viruses and their replication., p. 1305-1340. In D. M. Knipe, P. M. Howley, D. E. Griffin, R. A. Lamb, M. A. Martin, B. Roizman, and S. E. Straus (ed.), *Fields Virology*, 4 ed. Lippincott Williams & Wilkins, Philadelphia, PA.
74. **Li, Y., L. Luo, M. Schubert, R. R. Wagner, and C. Y. Kang.** 1993. Viral liposomes released from insect cells infected with recombinant baculovirus expressing the matrix protein of vesicular stomatitis virus. *J Virol* **67**:4415-20.
75. **Licata, J. M., R. F. Johnson, Z. Han, and R. N. Harty.** 2004. Contribution of ebola virus glycoprotein, nucleoprotein, and VP24 to budding of VP40 virus-like particles. *J Virol* **78**:7344-51.
76. **Licata, J. M., M. Simpson-Holley, N. T. Wright, Z. Han, J. Paragas, and R. N. Harty.** 2003. Overlapping motifs (PTAP and PPEY) within the Ebola virus VP40 protein function independently as late budding domains: involvement of host proteins TSG101 and VPS-4. *J Virol* **77**:1812-9.
77. **Malvoisin, E., and T. F. Wild.** 1993. Measles virus glycoproteins: studies on the structure and interaction of the haemagglutinin and fusion proteins. *J Gen Virol* **74**:2365-72.
78. **Manie, S. N., S. Debreyne, S. Vincent, and D. Gerlier.** 2000. Measles virus structural components are enriched into lipid raft microdomains: a potential cellular location for virus assembly. *J Virol* **74**:305-11.

79. **Martin-Serrano, J., A. Yarovoy, D. Perez-Caballero, and P. D. Bieniasz.** 2003. Divergent retroviral late-budding domains recruit vacuolar protein sorting factors by using alternative adaptor proteins. *Proc Natl Acad Sci USA* **100**:12414-12419.
80. **Marty, A., J. Meanger, J. Mills, B. Shields, and R. Ghildyal.** 2004. Association of matrix protein of respiratory syncytial virus with the host cell membrane of infected cells. *Arch Virol* **149**:199-210.
81. **Mayo, M. A.** 2002. Virus taxonomy - Houston 2002. *Arch Virol* **147**:1071-6.
82. **Mebatsion, T., M. Konig, and K. K. Conzelmann.** 1996. Budding of rabies virus particles in the absence of the spike glycoprotein. *Cell* **84**:941-51.
83. **Mebatsion, T., F. Weiland, and K. K. Conzelmann.** 1999. Matrix protein of rabies virus is responsible for the assembly and budding of bullet-shaped particles and interacts with the transmembrane spike glycoprotein G. *J Virol* **73**:242-50.
84. **Morita, E., and W. I. Sundquist.** 2004. Retrovirus budding. *Annu Rev Cell Dev Biol* **20**:395-425.
85. **Moss, B.** 2001. *Poxviridae: The viruses and their replication.*, p. 2849-83. *In* D. M. Knipe, P. M. Howley, D. E. Griffin, R. A. Lamb, M. A. Martin, B. Roizman, and S. E. Straus (ed.), *Fields Virology*, 4 ed. Lippincott Williams & Wilkins, Philadelphia, PA.

86. **Mungall, B. A., D. Middleton, G. Cramer, J. Bingham, K. Halpin, G. Russell, D. Green, J. McEachern, L. I. Pritchard, B. T. Eaton, L. F. Wang, K. N. Bossart, and C. C. Broder.** 2006. A feline model of acute Nipah virus infection and protection with a soluble glycoprotein-based subunit vaccine. *J. Virol.* **80**:12293-12302.
87. **Munshi, U. M., J. Kim, K. Nagashima, J. H. Hurley, and E. O. Freed.** 2006. An Alix fragment potently inhibits HIV-1 budding: Characterization of binding to retroviral YPXL late domains. *J Biol Chem* **282**:3847-55.
88. **Negrete, O. A., E. L. Levroney, H. C. Aguilar, A. Bertolotti-Ciarlet, R. Nazarian, S. Tajyar, and B. Lee.** 2005. EphrinB2 is the entry receptor for Nipah virus, an emergent deadly paramyxovirus. *Nature* **436**:401-5.
89. **Negrete, O. A., M. C. Wolf, H. C. Aguilar, S. Enterlein, W. Wang, E. Muhlberger, S. V. Su, A. Bertolotti-Ciarlet, R. Flick, and B. Lee.** 2006. Two Key Residues in EphrinB3 Are Critical for Its Use as an Alternative Receptor for Nipah Virus. *PLoS Pathog* **2**:e7.
90. **Neumann, G., H. Ebihara, A. Takada, T. Noda, D. Kobasa, L. D. Jasenosky, S. Watanabe, J. H. Kim, H. Feldmann, and Y. Kawaoka.** 2005. Ebola virus VP40 late domains are not essential for viral replication in cell culture. *J Virol* **79**:10300-7.
91. **Niwa, H., K. Yamamura, and J. Miyazaki.** 1991. Efficient selection for high-expression transfectants with a novel eukaryotic vector. *Gene* **108**:193-9.

92. **Noda, T., H. Sagara, E. Suzuki, A. Takada, H. Kida, and Y. Kawaoka.** 2002. Ebola virus VP40 drives the formation of virus-like filamentous particles along with GP. *J Virol* **76**:4855-65.
93. **Olson, J. G., C. Rupprecht, P. E. Rollin, U. S. An, M. Niezgoda, T. Clemins, J. Walston, and T. G. Ksiazek.** 2002. Antibodies to Nipah-like virus in bats (*Pteropus lylei*), Cambodia. *Emerg Infect Dis* **8**:987-8.
94. **Ott, D. E., L. V. Coren, R. C. Sowder, 2nd, J. Adams, K. Nagashima, and U. Schubert.** 2002. Equine infectious anemia virus and the ubiquitin-proteasome system. *J Virol* **76**:3038-44.
95. **Pager, C. T., W. W. Craft, Jr., J. Patch, and R. E. Dutch.** 2006. A mature and fusogenic form of the Nipah virus fusion protein requires proteolytic processing by cathepsin L. *Virology* **346**:251-7.
96. **Pager, C. T., and R. E. Dutch.** 2005. Cathepsin L is involved in proteolytic processing of the hendra virus fusion protein. *J Virol* **79**:12714-20.
97. **Pager, C. T., M. A. Wurth, and R. E. Dutch.** 2004. Subcellular localization and calcium and pH requirements for proteolytic processing of the Hendra virus fusion protein. *J Virol* **78**:9154-63.
98. **Panchal, R. G., G. Ruthel, T. A. Kenny, G. H. Kallstrom, D. Lane, S. S. Badie, L. Li, S. Bavari, and M. J. Aman.** 2003. In vivo oligomerization and raft localization of Ebola virus protein VP40 during vesicular budding. *Proc Natl Acad Sci USA* **100**:15936-41.

99. **Pantua, H. D., L. W. McGinnes, M. E. Peeples, and T. G. Morrison.** 2006. Requirements for the Assembly and Release of Newcastle Disease Virus-like particles. *J. Virol.* **80**:11062-11073.
100. **Patch, J. R., G. Crameri, L. F. Wang, B. T. Eaton, and C. C. Broder.** 2007. Quantitative analysis of Nipah virus proteins released as virus-like particles reveals central role for the matrix protein. *Virol J* **4**:1.
101. **Patnaik, A., V. Chau, F. Li, R. C. Montelaro, and J. W. Wills.** 2002. Budding of equine infectious anemia virus is insensitive to proteasome inhibitors. *J Virol* **76**:2641-7.
102. **Perez, M., R. C. Craven, and J. C. de la Torre.** 2003. The small RING finger protein Z drives arenavirus budding: implications for antiviral strategies. *Proc Natl Acad Sci USA* **100**:12978-83.
103. **Pornillos, O., S. L. Alam, D. R. Davis, and W. I. Sundquist.** 2002. Structure of the Tsg101 UEV domain in complex with the PTAP motif of the HIV-1 p6 protein. *Nat Struct Biol* **9**:812-7.
104. **Puffer, B. A., L. J. Parent, J. W. Wills, and R. C. Montelaro.** 1997. Equine infectious anemia virus utilizes a YXXL motif within the late assembly domain of the Gag p9 protein. *J Virol* **71**:6541-6.
105. **Reynes, J. M., D. Counor, S. Ong, C. Faure, V. Seng, S. Molia, J. Walston, M. C. Georges-Courbot, V. Deubel, and J. L. Sarthou.** 2005. Nipah virus in Lyle's flying foxes, Cambodia. *Emerg Infect Dis* **11**:1042-7.
106. **Rima, B. K., and W. P. Duprex.** 2005. Molecular mechanisms of measles virus persistence. *Virus Res* **111**:132-47.

107. **Rolls, M. M., P. Webster, N. H. Balba, and J. K. Rose.** 1994. Novel infectious particles generated by expression of the vesicular stomatitis virus glycoprotein from a self-replicating RNA. *Cell* **79**:497-506.
108. **Sakaguchi, T., A. Kato, F. Sugahara, Y. Shimazu, M. Inoue, K. Kiyotani, Y. Nagai, and T. Yoshida.** 2005. AIP1/Alix is a binding partner of Sendai virus C protein and facilitates virus budding. *J Virol* **79**:8933-41.
109. **Sakaguchi, T., K. Kiyotani, A. Kato, M. Asakawa, Y. Fujii, Y. Nagai, and T. Yoshida.** 1997. Phosphorylation of the Sendai virus M protein is not essential for virus replication either in vitro or in vivo. *Virology* **235**:360-6.
110. **Sakaguchi, T., T. Uchiyama, C. Huang, N. Fukuhara, K. Kiyotani, Y. Nagai, and T. Yoshida.** 2002. Alteration of Sendai virus morphogenesis and nucleocapsid incorporation due to mutation of cysteine residues of the matrix protein. *J Virol* **76**:1682-90.
111. **Sanderson, C. M., N. L. McQueen, and D. P. Nayak.** 1993. Sendai virus assembly: M protein binds to viral glycoproteins in transit through the secretory pathway. *J Virol* **67**:651-63.
112. **Sanderson, C. M., H. H. Wu, and D. P. Nayak.** 1994. Sendai virus M protein binds independently to either the F or the HN glycoprotein in vivo. *J Virol* **68**:69-76.
113. **Schmitt, A. P., B. He, and R. A. Lamb.** 1999. Involvement of the cytoplasmic domain of the hemagglutinin-neuraminidase protein in assembly of the paramyxovirus simian virus 5. *J Virol* **73**:8703-12.

114. **Schmitt, A. P., and R. A. Lamb.** 2004. Escaping from the cell: assembly and budding of negative-strand RNA viruses. *Curr Top Microbiol Immunol* **283**:145-96.
115. **Schmitt, A. P., G. P. Leser, E. Morita, W. I. Sundquist, and R. A. Lamb.** 2005. Evidence for a new viral late-domain core sequence, FPIV, necessary for budding of a paramyxovirus. *J Virol* **79**:2988-97.
116. **Schmitt, A. P., G. P. Leser, D. L. Waning, and R. A. Lamb.** 2002. Requirements for budding of paramyxovirus simian virus 5 virus-like particles. *J Virol* **76**:3952-64.
117. **Shiell, B. J., D. R. Gardner, G. Crameri, B. T. Eaton, and W. P. Michalski.** 2003. Sites of phosphorylation of P and V proteins from Hendra and Nipah viruses: newly emerged members of Paramyxoviridae. *Virus Res* **92**:55-65.
118. **Stallcup, K. C., C. S. Raine, and B. N. Fields.** 1983. Cytochalasin B inhibits the maturation of measles virus. *Virology* **124**:59-74.
119. **Stone-Hulslander, J., and T. G. Morrison.** 1997. Detection of an interaction between the HN and F proteins in Newcastle disease virus-infected cells. *J Virol* **71**:6287-95.
120. **Strack, B., A. Calistri, S. Craig, E. Popova, and H. G. Gottlinger.** 2003. AIP1/ALIX is a binding partner for HIV-1 p6 and EIAV p9 functioning in virus budding. *Cell* **114**:689-99.

121. **Sugahara, F., T. Uchiyama, H. Watanabe, Y. Shimazu, M. Kuwayama, Y. Fujii, K. Kiyotani, A. Adachi, N. Kohno, T. Yoshida, and T. Sakaguchi.** 2004. Paramyxovirus Sendai virus-like particle formation by expression of multiple viral proteins and acceleration of its release by C protein. *Virology* **325**:1-10.
122. **Swenson, D. L., K. L. Warfield, D. L. Negley, A. Schmaljohn, M. J. Aman, and S. Bavari.** 2005. Virus-like particles exhibit potential as a pan-filovirus vaccine for both Ebola and Marburg viral infections. *Vaccine* **23**:3033-42.
123. **Takimoto, T., K. G. Murti, T. Bousse, R. A. Scroggs, and A. Portner.** 2001. Role of matrix and fusion proteins in budding of Sendai virus. *J Virol* **75**:11384-91.
124. **Tamin, A., B. H. Harcourt, T. G. Ksiazek, P. E. Rollin, W. J. Bellini, and P. A. Rota.** 2002. Functional properties of the fusion and attachment glycoproteins of Nipah virus. *Virology* **296**:190-200.
125. **Tan, C. T., K. J. Goh, K. T. Wong, S. A. Sarji, K. B. Chua, N. K. Chew, P. Murugasu, Y. L. Loh, H. T. Chong, K. S. Tan, T. Thayaparan, S. Kumar, and M. R. Jusoh.** 2002. Relapsed and late-onset Nipah encephalitis. *Ann Neurol* **51**:703-8.
126. **Timmins, J., G. Schoehn, S. Ricard-Blum, S. Scianimanico, T. Vernet, R. W. Ruigrok, and W. Weissenhorn.** 2003. Ebola virus matrix protein VP40 interaction with human cellular factors Tsg101 and Nedd4. *J Mol Biol* **326**:493-502.
127. **Timmins, J., S. Scianimanico, G. Schoehn, and W. Weissenhorn.** 2001. Vesicular release of ebola virus matrix protein VP40. *Virology* **283**:1-6.

128. **Vincent, S., D. Gerlier, and S. N. Manie.** 2000. Measles virus assembly within membrane rafts. *J Virol* **74**:9911-5.
129. **Vogt, V. M.** 2000. Ubiquitin in retrovirus assembly: Actor or bystander? *Proc Natl Acad Sci USA* **97**:12945-7.
130. **Volchkov, V. E., V. A. Volchkova, W. Slenczka, H. D. Klenk, and H. Feldmann.** 1998. Release of viral glycoproteins during Ebola virus infection. *Virology* **245**:110-9.
131. **von Schwedler, U. K., M. Stuchell, B. Muller, D. M. Ward, H. Y. Chung, E. Morita, H. E. Wang, T. Davis, G. P. He, D. M. Cimborra, A. Scott, H. G. Krausslich, J. Kaplan, S. G. Morham, and W. I. Sundquist.** 2003. The protein network of HIV budding. *Cell* **114**:701-13.
132. **Wacharapluesadee, S., B. Lumlerdacha, K. Boongird, S. Wanghonga, L. Chanhome, P. Rollin, P. Stockton, C. E. Rupprecht, T. G. Ksiazek, and T. Hemachudha.** 2005. Bat Nipah virus, Thailand. *Emerg Infect Dis* **11**:1949-51.
133. **Wang, L., B. H. Harcourt, M. Yu, A. Tamin, P. A. Rota, W. J. Bellini, and B. T. Eaton.** 2001. Molecular biology of Hendra and Nipah viruses. *Microbes Infect* **3**:279-87.
134. **Wang, L. F., W. P. Michalski, M. Yu, L. I. Pritchard, G. Cramer, B. Shiell, and B. T. Eaton.** 1998. A novel P/V/C gene in a new member of the Paramyxoviridae family, which causes lethal infection in humans, horses, and other animals. *J Virol* **72**:1482-90.

135. **Wang, L. F., M. Yu, E. Hansson, L. I. Pritchard, B. Shiell, W. P. Michalski, and B. T. Eaton.** 2000. The exceptionally large genome of Hendra virus: support for creation of a new genus within the family Paramyxoviridae. *J Virol* **74**:9972-9.
136. **Waning, D. L., A. P. Schmitt, G. P. Leser, and R. A. Lamb.** 2002. Roles for the cytoplasmic tails of the fusion and hemagglutinin- neuraminidase proteins in budding of the paramyxovirus simian virus 5. *J Virol* **76**:9284-97.
137. **Weingartl, H. M., Y. Berhane, J. L. Caswell, S. Loosmore, J.-C. Audonnet, J. A. Roth, and M. Czub.** 2006. Recombinant nipah virus vaccines protect pigs against challenge. *J Virol* **80**:7929-38.
138. **Williamson, M. M., P. T. Hooper, P. W. Selleck, H. A. Westbury, and R. F. Slocombe.** 2000. Experimental hendra virus infection in pregnant guinea-pigs and fruit bats (*Pteropus poliocephalus*). *J Comp Pathol* **122**:201-7.
139. **Wong, K. T., W. J. Shieh, S. Kumar, K. Norain, W. Abdullah, J. Guarner, C. S. Goldsmith, K. B. Chua, S. K. Lam, C. T. Tan, K. J. Goh, H. T. Chong, R. Jusoh, P. E. Rollin, T. G. Ksiazek, and S. R. Zaki.** 2002. Nipah virus infection: pathology and pathogenesis of an emerging paramyxoviral zoonosis. *Am J Pathol* **161**:2153-67.
140. **Wright, P. J., G. Crameri, and B. T. Eaton.** 2005. RNA synthesis during infection by Hendra virus: an examination by quantitative real-time PCR of RNA accumulation, the effect of ribavirin and the attenuation of transcription. *Arch Virol* **150**:521-32.

141. **Yao, Q., X. Hu, and R. W. Compans.** 1997. Association of the parainfluenza virus fusion and hemagglutinin-neuraminidase glycoproteins on cell surfaces. *J Virol* **71**:650-6.
142. **Yob, J. M., H. Field, A. M. Rashdi, C. Morrissy, B. van der Heide, P. Rota, A. bin Adzhar, J. White, P. Daniels, A. Jamaluddin, and T. Ksiazek.** 2001. Nipah virus infection in bats (order Chiroptera) in peninsular Malaysia. *Emerg Infect Dis* **7**:439-41.